Characterization of Methyltransferase Carbon-Oxygen Hydrogen Bonding and Sulfur-Oxygen Chalcogen Bonding with the Sulfonium of S-adenosyl-L-methionine

by

Robert J. Fick

A dissertation submitted in partial fulfillment
of the requirements for the degree of
Doctor of Philosophy
(Biological Chemistry)
in the University of Michigan
2018

Doctoral Committee:

Associate Professor Raymond C. Trievel, Chair
Associate Professor Tomasz Cierpicki
Professor Kevin J. Kubarych
Associate Professor Patrick J. O'Brien
Associate Professor Mark A. Saper

Robert J. Fick

rjfick@umich.edu

ORCID iD: 0000-0002-5979-4605

Acknowledgements

I would like to thank my advisor Dr. Raymond Trievel for his excellent guidance and patience during the course of my research. I would also like to thank all the members that have served on my thesis committee for their help and insight along the way: Dr. Tomasz Cierpicki, Dr. Kevin Kubarych, Dr. Patrick O'Brien, Dr. Mark Saper, and Dr. John Tesmer. Thanks to all who have provided their assistance and knowledge.

I would like to thank the members of the Trievel laboratory, for providing useful discussions and a great group of people to work around. I would also like to thank the undergrads who I had the pleasure to work with, for letting me teach them science and being great help in the lab. I also owe many thanks to my collaborators, for lending a hand with their expertise and greatly aiding my work, especially Dr. Steve Scheiner.

I would like to thank my family for the love and support they have provided: my parents, Orlin and Amy, for visiting often and my brother Andy, for being there to talk. Likewise, I express my thanks to Anna Ganios, for your love, support, and giving me focus on the future.

Table of Contents

List of Figures

List of Tables

Abstract

Methyltransferases use S-adenosyl-L-methionine (AdoMet) to transfer the one-carbon group to nitrogen, carbon, oxygen, and sulfur nucleophiles, among other atoms. AdoMet is the most common biological methyl donor, and the methyl group is used in numerous biological processes such as signaling, metabolism, and gene regulation. The mechanism of transfer has been determined to be a bimolecular nucleophilic substitution (S_N2) reaction, but the origin of the catalytic rate enhancement induced by methyltransferases remains a longstanding point of debate. The objective of this dissertation is to explore carbon-oxygen hydrogen bonding and sulfur-oxygen chalcogen bonding in several different families of methyltransferases to understand the importance of these interactions between active site oxygen atoms and the AdoMet sulfonium cation in substrate binding and catalysis. Carbon-oxygen hydrogen bonding was probed in two methyltransferase families, the Rossmann-like fold methyltransferase TylM1, and the reactivation domain of methionine synthase. Mutation to remove carbon-oxygen hydrogen bonding of TylM1 to the AdoMet methylene groups flanking the sulfur atom showed slight defects in both binding and catalysis. Furthermore, a second TylM1 active site residue involved in carbon-oxygen hydrogen bonding to the methyl group of AdoMet was shown to be crucial to enzyme catalysis through its role in binding and aligning both substrates. Carbon-oxygen hydrogen bonding to active site waters in methionine synthase was manipulated by mutation of active site glutamates which coordinated these waters to glutamine resulting in a loss of substrate binding and a lesser ability to discriminate substrate from product. In addition to carbon-oxygen hydrogen bonding, sulfur-oxygen chalcogen bonding between the AdoMet sulfonium cation and the active site of the lysine methyltransferase SET7/9, was found to facilitate AdoMet binding, discrimination between substrate and product, and catalysis. These

results are among the first to establish chalcogen bonding as an important interaction in enzymes. Collectively, these studies further reinforce the roles of carbon-oxygen hydrogen bonding in substrate binding and catalysis across different methyltransferase families, and identifies the significance of sulfur-oxygen chalcogen bonding as a newly discovered interaction within these enzymes.

.

Chapter 1:

Introduction

1.1 S-adenosyl-L-Methionine

S-adenosyl-L-methionine (AdoMet or SAM) is a biological substrate most often utilized as a methyl group donor, transferring its one-carbon group to a host of nucleophiles, including C, N, O, and S. AdoMet has been cited as the second most commonly used biological substrate.[1, 2] The molecule is synthesized from adenosine tri-phosphate and methionine,[3] resulting in the formation of a methyl-sulfonium that electrophilically activates the methyl group, with the remaining molecule, S-adenosyl-L-homocysteine (AdoHcy or SAH) acting as a leaving group. Though many years have passed since the detailing of the structure, AdoMet still remains a point of study in both its binding to methyltransferases and catalytic rate enhancement of up to 10^{16} caused when bound by these enzymes versus comparable reactions in solution.[4]

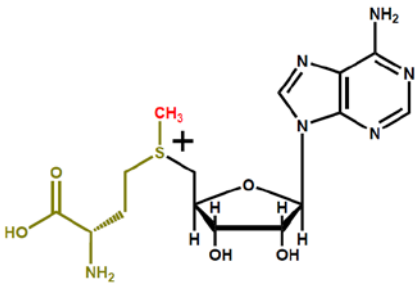

Figure 1.1: The structure of AdoMet.

The portion of the molecule from ATP is shown in black, with the rest of the molecule coming from methionine. The methyl group donated is above the sulfur atom and is shown in red.

1.2 Bonding

1.2.1 Hydrogen Bonding

The hydrogen bond is well known within the field of biology,[5-7] with early characterization of basic biological structures noting their importance. Hydrogen bonding is cited by Pauling, in his *Nature of the Chemical Bond*[8], as being first mentioned in 1912[9] in the structure of trimethylammonium hydroxide, shown then as possessing a $(CH_3)_3N$-H-OH arrangement, in which the hydrogen atom is covalently attached to the hydroxide and the additional bond to the nitrogen is weaker and is now best described as an OH•••N hydrogen bond. The transient but ubiquitous character of hydrogen bonding in water was described in 1920[10], noting that "the liquid may be made up of large aggregates of molecules, continually breaking up and reforming…" and that a hydrogen "held between 2 octets constitutes a weak "bond."" The energetics of hydrogen bonding in bulk water is well demonstrated by the differences between the boiling points of water and methane (Figure 1.2), especially when related to the trends seen among elements in the same periodic column.[8] The bond was classified as one where a hydrogen was bonded to an electronegative atom, and then was engaged with a second electronegative atom in an ionic type bond. The electronegative atoms given were fluorine, oxygen, nitrogen, and to a lesser extent, chlorine. The charge on the electronegative atom is also an important property that can increase the strength of the hydrogen bonding, with a positive charge on the atom acting to increase its electronegativity, enhancing the strength of donated hydrogen bonds.[8] The various attractive and repulsive elements of hydrogen bonding were characterized computationally in 1977[11], with electrostatics shown as the dominant component of

attraction, but charge transfer and polarization being important at closer distances to help overcome the increasing repulsion term. It was also stated that ionic species have greater electrostatic contributions, giving more flexibility in arrangement of donor and acceptor than in non-ionic hydrogen bonding.

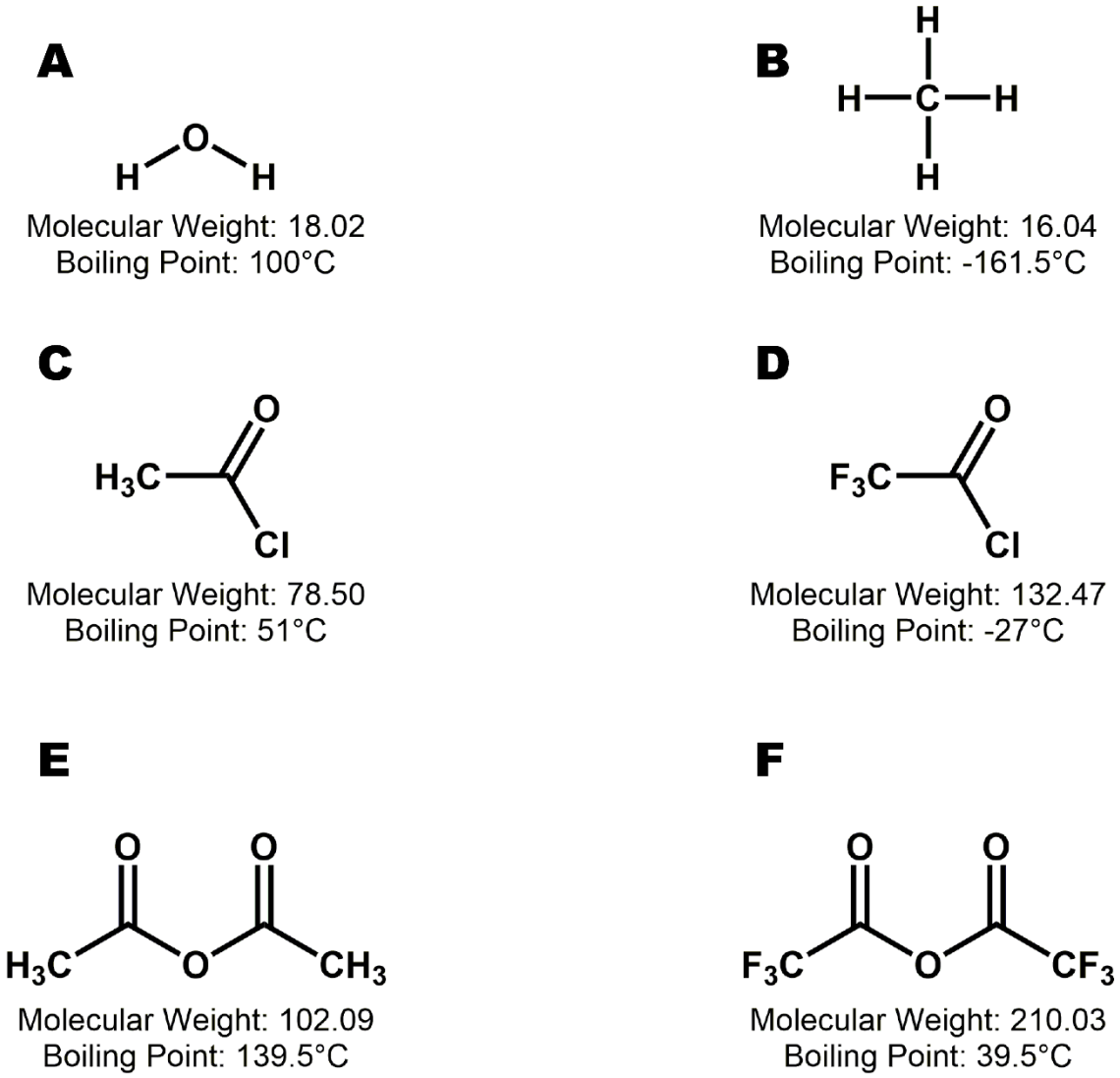

Figure 1.2: Boiling points[12] of comparative small molecules.

Water (A) and methane (B) boil at greatly different temperatures despite similar molecular mass due to the ability of water to form hydrogen bonds. This is also seen in acetyl chloride (C) vs. trifluoroacetyl chloride (D) and acetic anhydride (E) vs. trifluoroacetic anhydride (F).

1.2.2 Carbon-Oxygen (CH•••O) Hydrogen Bonding

The CH•••O hydrogen bond is analogous to a classical hydrogen bond, and Pauling notes the evidence for this is quite clear in the difference of acetic anhydride or acetyl chloride and the fluoro-derivatives of those compounds.[8] As seen in figure 1.2, the boiling points of the hydrogen-containing compounds is much higher, even though the molecular weight for these compounds is lower. The apparent difference between the two pairs of compounds is that the fluoromethyl group is not able to act as a donor for hydrogen bonds that the methyl group would be able to form with either the oxygen or chlorine atoms. This interaction shows the attractiveness of the CH•••O hydrogen bond in an electron withdrawing environment, with the acid anhydride and acid chloride polarizing the methyl C-H bond, increasing the ability to hydrogen bond.[13]

CH•••O hydrogen bonding was also observed in small molecule crystal structures of the time. Sutor, in solving structures of xanthine compounds such as caffeine, noted “short” C-O interaction distances where there were hydrogen positions determined by their positioning with respect to the sp2 hybridized carbon atom to which they were bonded.[14-16] Such an interaction was indicative of a CH•••O hydrogen bond, as the interaction distance between the carbon and oxygen atoms was closer than their combined van der Waals radii (see figure 1.3). Other groups also noted bonding characteristic of CH•••O hydrogen bonding by the overly short interactions between ethynyl hydrogens and carbonyl oxygens, with predicted H•••O distance at ~2.2 Å, based on the linear positioning of the alkyne.[17, 18] Proposed structures of the helical peptides collagen and polyglycine II possessed saw distances that would indicate CH•••O hydrogen bonding[19-21], and spectroscopic evidence in polyglycine II supported

the observation, as evidenced by a blue-shift of C-H stretches.[22-24] While the collagen structure did not prove to be correct,[25] there is clear evidence of CH•••O hydrogen bonding between chains in collagen-like structure.[26] In 1968, there was a critique of the carbon-oxygen hydrogen bonding,[27] though work did continue on the CH•••O bond both computationally[28-30] and spectroscopically.[31] The field was aided by the positional certainty of small molecule neutron structures, where the hydrogen positions are experimentally determined, to examine molecular CH•••O interactions[32] and those with water[33]. These reports spurred a return to examining the CH•••O hydrogen bond in small molecule crystal structures,[34-36] as well as nucleic acids[37] and protein structure and function.[38, 39] Computation studies of CH•••O hydrogen bonding showed that they behave similarly to normal hydrogen bonds,[13] are important energetically in protein structure,[40-43] and can be highly energetic in a charged system such as AdoMet.[44, 45] Energies for CH•••O hydrogen bonds can range from ~0.6 kcal/mol for a methane and water interaction, up to ~7 kcal/mol/bond for trimethyl sulfonium interacting with the N-methylacetamide carbonyl.[44, 46] A survey of high resolution (< 2.0 Å) AdoMet-bound structures in the Protein Data Bank found that CH•••O hydrogen bonding to the AdoMet methyl group is common across different classes of methyltransferases.[47]

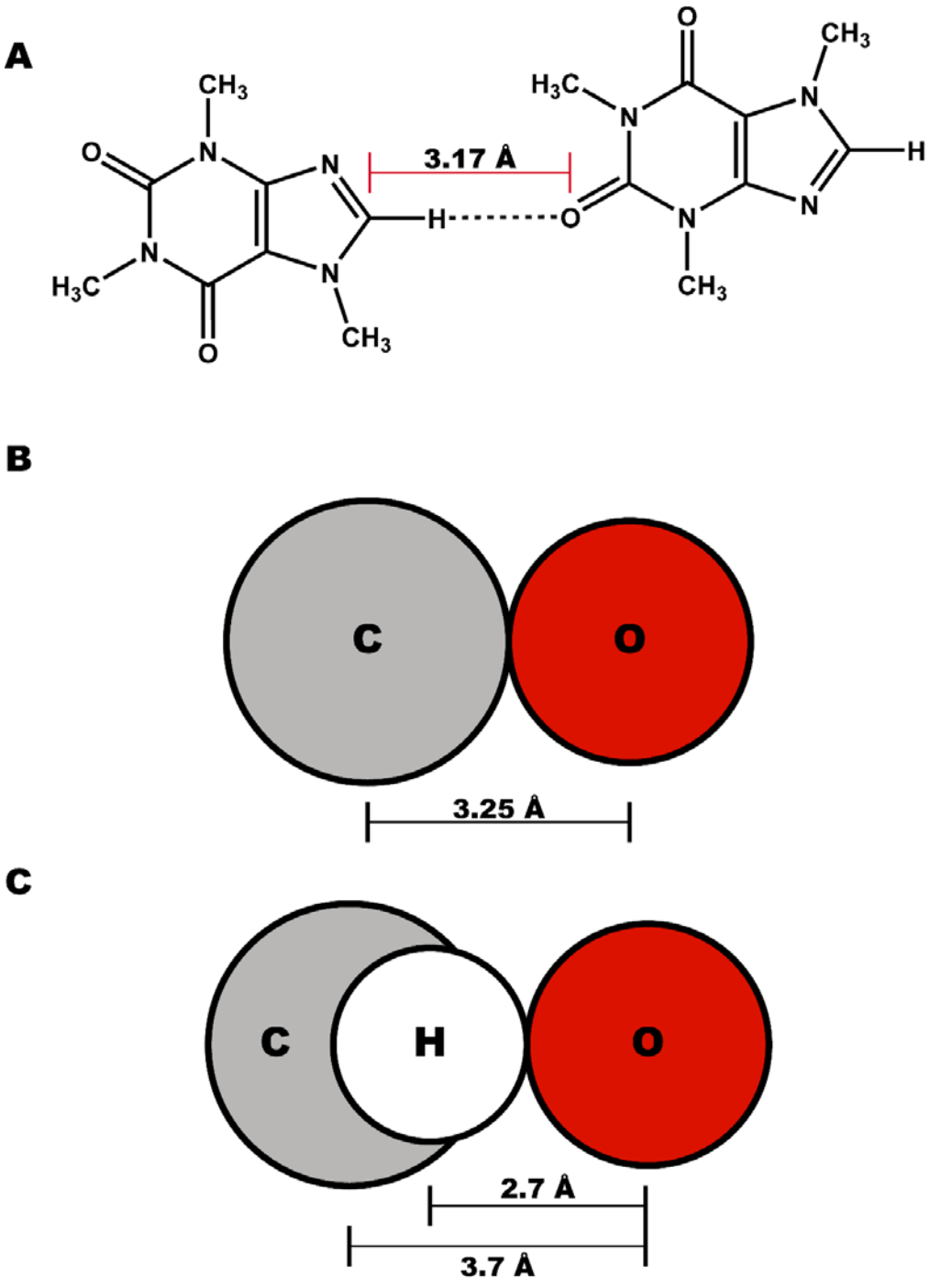

Figure 1.3: CH•••O hydrogen bonding and van der Waals radii.

The structure of caffeine with the CH•••O hydrogen bond shown (A).[14] The interaction distance is shorter than the combined van der Waals radii of oxygen and carbon (B), and much shorter than the C•••O distance with an intervening hydrogen atom (C).[32] Size of circles is roughly to scale of ~0.5 inch to 1 Å.

1.2.3 S•••O Chalcogen Bonding

A chalcogen bond is another bond that has been identified as a possible interaction that methyltransferases can have with AdoMet. Chalcogen bonding was detailed based on interactions closer than van der Waals radii with chalcogen atoms (column 16 elements: O, S, Se, etc.) in small molecule crystal structures.[48, 49] In these studies of thioethers and sulfonium systems, electron-rich nucleophiles preferentially approached the sulfur *anti* to one of the substituents (Fig 1.4). This interaction is similar to halogen bonding, where there exists a more positive 'σ-hole' where the σ* antibonding orbital is located, generally resulting in interaction angles between 160° and 180° for the electron donor, the halogen, and the covalently bonded substituent.[50, 51] The chalcogen bond also has a positive region[52], and can be a highly attractive interaction in the context of a sulfonium system.[45] The chalcogen bond may also have implications in protein folding, as there is evidence for the enrichment of oxygen atoms in close contact with sulfur atoms in methionine residues,[53-55] particularly in phospholipase A_2 where key active site residues are near to structural chalcogen bonds.[56] AdoMet synthetase contains a possible chalcogen bond to an aspartate, and upon mutation of this residue to asparagine an almost 5-fold loss in K_M for methionine is seen.[57] Chalcogen bonding is also present in small molecules, with carbonyl oxygens in amide groups forming close contacts with sulfurs,[55] and intramolecular S•••O distances in multiple drug-like molecules much shorter than the van der Waals radii of the two atoms.[58]

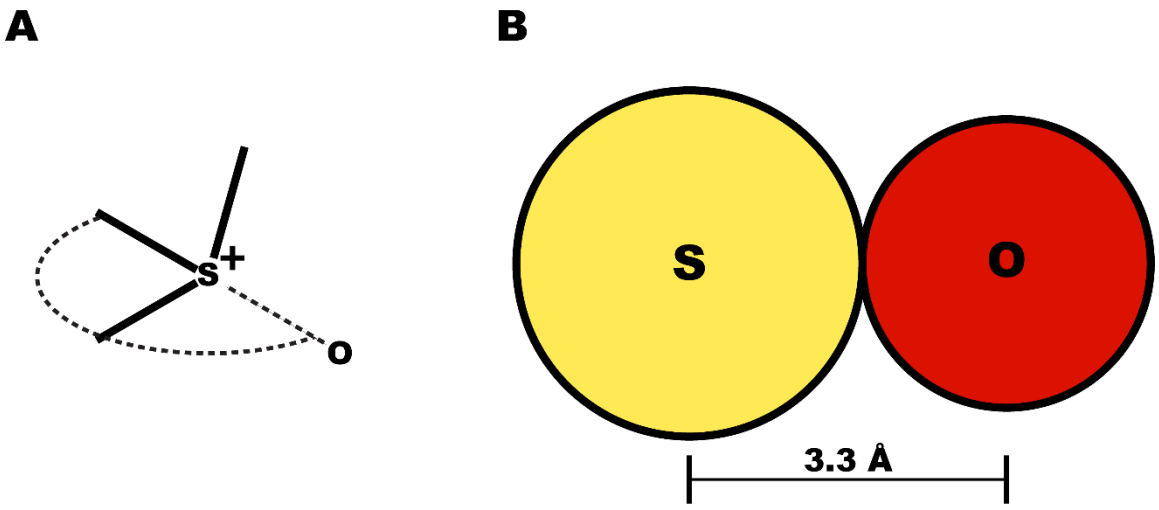

Figure 1.4: The geometry of chalcogen bonding and van der Waals radii.

The electron donor in a chalcogen bond, which is a σ*-bonding interaction, approaches from ~160°-180° in relation to one of the bonded substituents, seen represented here as an oxygen. The van der Waals interaction distance for a sulfur-oxygen chalcogen bond is 3.3 Å, shown above, a sum of 1.8 Å for the sulfur and 1.5 Å for the oxygen.[32] Size of circles is roughly to scale of ~0.5 inch to 1 Å.

1.3 Methyltransferase Classes

There are at least nine methyltransferase classes, with seven structurally characterized AdoMet-dependent methyltransferase classes bound to AdoMet or AdoHcy.[59-61] In a survey looking for methyltransferases of the human proteome, 208 genes encoding predicted methyltransferases were identified, accounting for about 0.9% of human gene products.[59] In a survey of AdoMet-bound, <2.0 Å methyltransferase structures in the Protein Data Bank, though having diverse protein folds, all structures showed evidence of CH•••O hydrogen bonding to the AdoMet methyl group (Figure 1.5).[47] There is also broad conformational freedom in binding AdoMet, with the methionyl and adenosyl arms in different conformations in relation to the central sulfonium, as seen in AdoMet from

representative methyltransferases (Figure 1.6).

1.3.1 Class I: The Rossmann-like Fold

The Rossmann-like fold methyltransferases are also referred to as the Class I methyltransferases, as this was the first fold of methyltransferases crystallized, and they remain the largest group of methyltransferases.[59] The class was first structurally characterized in 1993 with the structure of Hha I DNA cytosine methyltransferase.[62] The heavily studied catechol O-methyltransferase (COMT) followed shortly in 1994 and gave a shape to more than three and a half decades of research into the metabolism of neurotransmitters.[63,64] The common fold seen in both structures was similar to the previously characterized Rossmann fold seen in other nucleotide binding proteins, with a seventh strand added to the beta sheet.[65] The base of the sheet, along with the alpha helices that flank the sheet, form a cleft that binds AdoMet. These enzymes possess a wide variety of substrates (such as catechols,[64] RNA,[66] DNA,[67] lysine,[68] arginine,[69] histamine,[70] and thiopurine[71]), modifying carbon, oxygen, nitrogen and sulfur nucleophiles, and therefore can contain many domains outside of the catalytic core to aid in binding as well as signaling and regulation. The amount of diversity seen within the Rossman-like fold methyltransferases is demonstrated in a simple comparison of two well-studied members: COMT (~180 residues) and human DNA methyltransferase I (~1600 residues).[67] COMT is composed of the catalytic core, while DNMT1 has roughly 1100 residues used for purposes outside of catalysis.

1.3.2 Class II: The Reactivation Domain of Methionine Synthase

The second fold of methyltransferase characterized was the C-terminal reactivation domain of the larger methionine synthase enzyme. The construct was isolated through a tryptic digest of the *E. coli* enzyme, indicating a stable methyltransferase domain as part of the larger enzyme.[72] The domain is responsible for the reductive methylation of the cobalamin ring when it undergoes an oxidative side reaction once every ~2000 productive cycles,[73] regenerating the methylcobalamin necessary for the production of methionine. The fold, which contains a central anti-parallel beta sheet surrounded by helices and loops binds AdoMet on a concave face, almost appearing to cup the molecule on its surface. This presents the AdoMet with a largely open face and extended confirmation allowing the methyl to approach the central cobalt contained within the planar B12 cofactor. The enzyme is unique in its role, and as such is also unique among AdoMet-dependent methyltransferases containing this fold, with no similar methyltransferases in the human genome.[59]

1.3.3 Class III: Cobalamin-synthase Methyltransferases

The precorrin synthase methyltransferases are a small class responsible for the methylation of pyrrole rings of corrin precursors. The methyltransferases are responsible for placing eight methyl groups during the synthesis of the cobalamin ring, and there are homologues that function either in an aerobic or anaerobic context, depending on organism.[74,75] The structure of this family of methyltransferase also contains an alpha-beta-alpha motif similar to the Rossman-like fold enzymes, though the number of strands in beta sheet has been reduced to five, and the enzyme has two

of these αβα domains. The AdoMet binds in a groove between the two domains, rather than at the base of one of the sheets as in the Class I methyltransferases.[75,1]

1.3.4 Class IV: SPOUT Methyltransferases

The SPOUT methyltransferases, named for SpoU-Trmd, two members of the family, are largely tRNA modifying methyltransferases, transferring a methyl group to 2' oxygens of the ribose or nitrogen 1 of adenine and guanine rings,[76] with a known exception being the methylation of protein arginine residues.[77] The family is characterized by a Trefoil knot-type fold, with the knot being near the C-terminus of the protein and donating several residues to the active site. The AdoMet is bound to the protein in a curved manner, with the amino acid end of the molecule bending towards the top face of the ribose ring.[78]

1.3.5 Class V: SET Domain Methyltransferases

The SET methyltransferases are the second largest class of methyltransferase, and are the next best studied.[59] The methyltransferases are protein lysine methyltransferases, with most of the enzymes specific for various lysines along the histone tails (H3K4, H3K9, K3K27, H3K36, and H4K20), though non-histone lysine substrates are known.[79] They are named for the Drosophila enzymes Suppressor of variegation 3-9, Enhancer of zeste, and Trithorax. Methylation on histone lysines is important in gene regulation, with trimethylation of a lysine acting to either repress or activate transcription, depending on the site of the lysine.[80] The structure of the SET domain is composed of 9 beta strands forming 3 sheets with two of the sheets and a helix forming a pore through which the methyl group is transferred, as the other side of

the pore is the substrate pocket.[81,82] CH•••O hydrogen bonding within the methyl transfer pore has been characterized in the SET-domain methyltransferase SET7/9.[47, 83, 84] SET7/9 also exemplifies the ability to methylate non-histone substrates, methylating lysine residues on the estrogen receptor,[85] the tumor suppressor p53,[86] and the transcription factor TAF10,[87] among many other protein substrates.[88]

1.3.6 Class VI: Radical-SAM Methyltransferases

The Radical-SAM methyltransferases belong to the larger class of Radical-SAM enzymes, which make use of AdoMet in the production of the adenosyl radical produced by homolytic cleavage of the C-S bond. The characteristic fold of the Radical SAM methyltransferases is the TIM barrel fold, with the beta sheets holding the active site in the middle of the barrel.[89] The methyltransferases also contain the characteristic iron sulfur (Fe_4-S_4) cluster of the Radical SAM family, which is used in radical generation from AdoMet to form the adenosyl radical, which is used in methylation of difficult nucleophiles in this class.[90, 91] The founding member of this class was a novel chloramphenicol resistance gene (Cfr) for modifying an adenine ring in the peptide exit channel of the ribosome.[92] This modification requires the use of AdoMet for both methyl transfer as well as radical production, with the methyl being transferred to an internal cysteine residue, and the next equivalent of AdoMet generating a radical in the substrate, allowing the reaction to proceed through the formation of a better nucleophile. The transfer of the methyl group from AdoMet to the internal cysteine residue is proposed to proceed in a similar manner to known methylation reactions, with the methyl of AdoMet being aligned in a linear manner to the cysteine so that the S_N2 reaction can occur. The second enzyme of this class, RlmN, has been shown to have

dual specificity, methylating carbon 2 of adenine rings in both rRNA and tRNA in *E. coli*.[93, 94]

1.3.7 Class VII: Integral Membrane Methyltransferases

The isoprenylcysteine carboxyl methyltransferase (ICMT) and phosphatidylethanolamine N-methyltransferase (PEMT) are integral membrane proteins that represent a unique fold of methyltransferase, with the crystal structure of ICMT showing a fold largely dictated by the fact that it is an integral membrane protein.[60] The protein contains five transmembrane helices, and a sixth cytosolic helix which stacks against a cytosolic extension of helix 5. S-adenosylhomocysteine is seen bound within a pore on the cytosolic side of the transmembrane helices, enabling access to the lipid-bound substrate. The methylation of the carboxy terminus on the lipidated cysteine is a final step of processing on these prenylated proteins, and increases the ability to associate with the membrane. PEMT also acts on substrates within the membrane, converting phosphatidylethanolamine into phosphatidylcholine.[95]

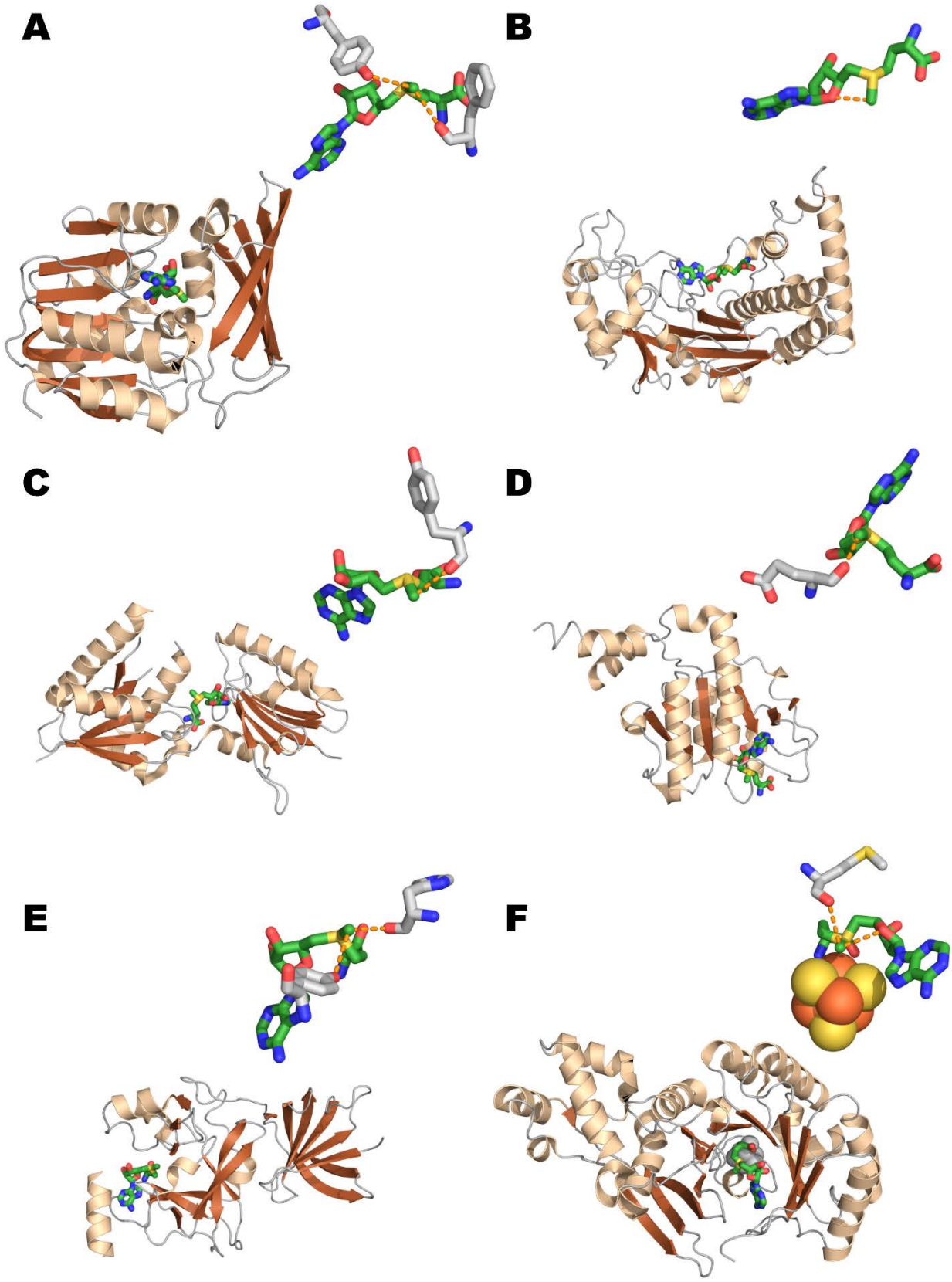
A
B
C
D
E
F

Figure 1.5: Methyltransferase Class Structures and AdoMet methyl CH•••O interactions.

Representative enzymes of methyltransferase folds shown. Active site CH•••O distances of less than 3.7 Å to the AdoMet methyl group shown as orange dashes. Class I is represented by TylM1 (A, PDB: 3PFG).[96] Class II is represented by the *E. coli* Methionine Synthase Reactivation domain (B, PDB: 1MSK).[72] Class III is represented by CobF (C, PDB: 2NPN). Class IV is represented by TrmH (D, PDB: 1V2X).[78] Class V is represented by SET7/9 (E, PDB: 1N6A).[82] Class VI is represented by RlmN, with the Iron-Sulfur cluster shown as spheres (F, PDB: 3RFA).[89]

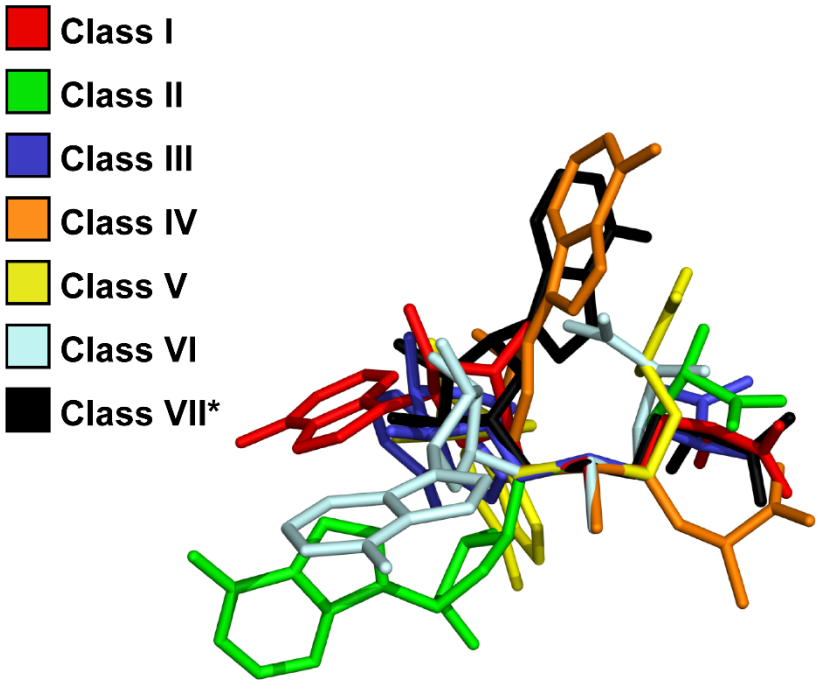

Figure 1.6: Conformations of AdoMet across Methyltransferase Classes aligned by the sulfonium.

AdoMet overlay generated from the six methyltransferases from figure 1.5, with AdoHcy from a Class VII enzyme as a representative of that class (PDB: 4A2N).[60] Though all methyltransferases need to align the C-S bond with the nucleophile for effective transfer, there is conformational freedom in how that is accomplished.

1.4 Mechanism of Methyl Transfer

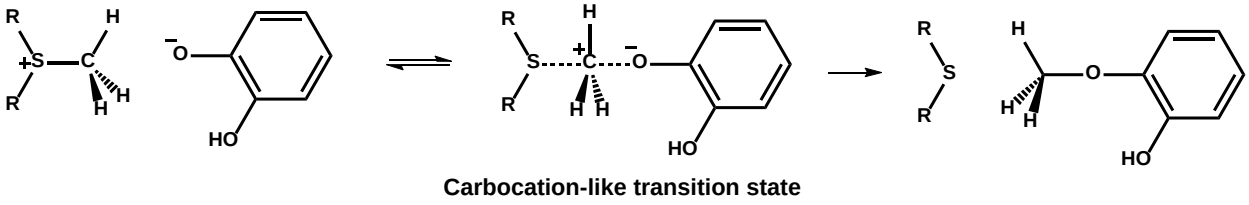

Figure 1.7: Mechanism for AdoMet methyl transfer.

The mechanism for the methylation of a catecholate (as the representative nucleophile) by AdoMet (without the methionyl and adenosyl arms shown). The reaction proceeds with the positive charge on the sulfur partially moving to the carbon as the methyl group goes through a carbocation-like transition state of the S_N2 mechanism. The transition state is roughly planar, and the transfer results in the inversion of the methyl group stereochemistry.

Characterization of COMT methylation activity demonstrated substrate preference, noting that the reaction is likely a nucleophilic attack on the methyl group of AdoMet.[64] Further work by Woodward confirmed the inversion of stereochemistry of the methyl group upon transfer by COMT, as well as the inversion of stereochemistry on N and C methyl transfers carried out by two other enzymes.[97, 98] Kinetic isotope effect studies were carried out by the Schowen group in 1979 to compare intermolecular and intramolecular methyl transfer with the catalysis of COMT.[4, 99, 100] These studies showed a large inverse kinetic isotope effect with respect to the hydrogens on the methyl group (CH_3/CD_3 = 0.83) leading to the conclusion that it is a tight transition state[101], and a large isotope effect with respect to the carbon ($^{12}C/^{13}C$ = 1.09) was interpreted as the result of a symmetrical transition state.[102] This gave rise to one of the explanations of the source of catalytic rate enhancement for methyl transfer: the compression model, in which the enzyme brings AdoMet and the nucleophile into closer proximity than would

be in solution by constraining them.[103] Though the compression model has been challenged,[104-109] it does continue to be an active point of research.[110-112] Another pair of models for methyl transfer that have been challenged[113, 114] are the entropic[115] and 'cratic'[116-118] models, which attribute catalytic enhancement to the enzyme-substrate binding energy paying entropic or other penalties that would arise for the transition state in solution. There are two other models, Bruice's Near Attack Conformers (NAC)[119, 120] and Warshel's Electrostatic Preorganization[114, 121-124] The Near Attack Conformer model is one in which the enzyme binds the substrates in a manner that favors the formation of close proximity conformations, leading to reaction. The Electrostatic Preorganization model states that the enzyme electrostatics are arranged to preferentially stabilize the transition state, leading to catalytic enhancement. Recent computational and experimental work have cited CH•••O hydrogen bonding as factor in the inverse kinetic isotope effect seen (CH_3/CD_3) for the methyl transfer.[106, 125]

1.5 Conclusion

Though CH•••O hydrogen bonding has become more accepted, the mechanism of AdoMet-dependent methyltransferases remains somewhat controversial. In this dissertation I set out to further characterize CH•••O hydrogen bonding in non-SET-domain enzymes, such as the Methionine Synthase Reactivation domain (chapter 2) and the Rossmann-like fold methyltransferase TylM1 (chapter 4). I also explore the effects that S•••O chalcogen bonding can have on binding and catalysis in bonding with the AdoMet sulfonium sulfur in SET7/9 (chapter 3). Through these aims I hope to further the understanding of the enzymatic features of AdoMet methyl transfer.

Chapter 2:

Water-Mediated Carbon-Oxygen Hydrogen Bonding Facilitates AdoMet Recognition in the Reactivation Domain of Methionine Synthase

Robert J. Fick, Mary Clay, Lucas P. Vander Lee, Steve Scheiner, Hashim Al-Hashimi, and Raymond C. Trievel

2.1 Introduction

Cobalamin-dependent Methionine Synthase, MetH, is a multi-domain protein that uses methyl-cobalamin as an intermediate to transfer the methyl group from methyl-tetrahydrofolate to homocysteine.[73, 126, 127] Three separate domains are responsible for the binding of methyl-tetrahydrofolate, homocysteine, and cobalamin for the regular catalytic cycle.[128] The enzyme transfers the methyl group from methyl-tetrahydrofolate to the cobalamin cofactor to produce methylcobalamin. The methylcobalamin is then used as the methyl donor to form methionine from homocysteine. MetH serves a vital role in one-carbon metabolism, with most homocysteine regeneration to methionine occurring through MetH catalytic activity; the activity of betaine-homocysteine methyltransferase serving as a secondary pathway that occurs in the liver and

This work is in preparation to be published under the same title

RJF purified the protein, performed the binding studies, and prepared the isotopically labeled AdoMet. RJF and LPV crystallized the protein and refined the structures. SS performed the QM analysis. MC performed the NMR experiments. RCT and RJF prepared the manuscript

kidneys.[129] The normal cycling of MetH is also the route for all methyl-tetrahydrofolate to enter the folate pool in cells.[130] A fourth domain binds S-Adenosyl-L-Methionine (AdoMet) and is involved in the reductive methylation of non-catalytic Co(II) cobalamin that is formed roughly every 2000 cycles.[73] The electron for this reaction comes from flavodoxin in *E. coli*[131] and cytochrome b_5 in *H. sapiens,*[132] and the favorable methylation of cobalamin by AdoMet drives the reaction. The reactivation domain of MetH represents a unique fold of AdoMet-dependent methyltransferase, present only in the context of the larger enzyme in S. cerevisiae and H. sapiens.[59, 61] The domain adopts an open, C-shaped conformation, with AdoMet held in a largely open active site to facilitate the necessary interaction with the planar B_{12} cofactor. This unique domain is also referred to as class II, as it was the second of the seven structurally characterized AdoMet-dependent methyltransferase classes.[1, 59]

The crystal structure of the MetH reactivation domain was first solved in 1996,[72] coming shortly after the first, Rossmann-like fold methyltransferases which were structurally characterized in 1993.[62] AdoMet also adopts a unique, extended conformation within the MetH active site, with the C-O distance between the methyl carbon and ribose furan oxygen in the 1996 structure at 3 Å. Carbon-oxygen (CH•••O) hydrogen bonding to the methyl group of AdoMet has been explored extensively in the context of the SET-domain lysine methyltransferase SET7/9.[47, 83, 84] As part of these studies, a survey of CH•••O hydrogen bonding to the AdoMet methyl was undertaken in high resolution (<2.0 Å) AdoMet-bound structures in the Protein Data Bank, in which the short, internal C-O interaction in MetH was noted.[47] These carbon-oxygen hydrogen bonds appear to be a universally conserved feature of AdoMet-dependent

methyltransferases, to facilitate binding of AdoMet over the product, S-adenosylhomocysteine (AdoHcy), as well as aligning the methyl carbon-sulfur bond to catalyze the S_N2 reaction. MetH presented an interesting case, as direct CH•••O bonding to the protein was not seen.

2.2 Structural Study

To probe the active site interactions in MetH, the protein was crystallized in complex with a variety of ligands (see Table 2.1 for crystallographic statistics). The substrate (AdoMet), product (AdoHcy), and a natural product inhibitor sinefungin were all found within the active site in a highly similar conformation. Clear density for each ligand is seen in simulated-annealing omit maps, along with several waters that are constant across the structures (Figure 2.1). The overall conformation of all the structures remains highly similar to the 1996 structure, with a RMSD of ≤ 0.32 Å for the aligned Cα atoms (Figure 2.2A). The binding cleft of MetH is acidic, with two glutamate residues, 1097 and 1128, flanking the sulfonium cation of AdoMet, though not directly engaged with it (Figure 2.2B), with the two glutamates noted in the 1996 structure for their unpaired charges. Instead, these residues interact through the structured waters in the active site, with the active site of MetH largely solvent exposed (Figure 2.2C-E). The structured waters engage in classical hydrogen bonds with the two glutamate residues, and the waters CH•••O hydrogen bond to methyl, methylene, and methyne carbons of AdoMet. The waters and glutamate positions are highly similar across all three ligands (Figure 2.2F). Glutamate 1097 binds to the waters labeled W1 and W2, with water W1 CH•••O hydrogen bonding to the AdoMet methyl (or a classical hydrogen bond to the amine of sinefungin) and C4', and water W2 CH•••O hydrogen bonding to the Cβ

carbon. Glutamate 1128 binds the waters, W3 and W4. Water W3 is able to CH•••O hydrogen bond to both the C5’ and Cβ carbons as well as forming a classical hydrogen bond with one of the ribose hydroxyls, whereas water W4 is able to CH•••O hydrogen bond to the C5’ carbon, though interactions with waters W3 and W4 are not present across all the ligands.

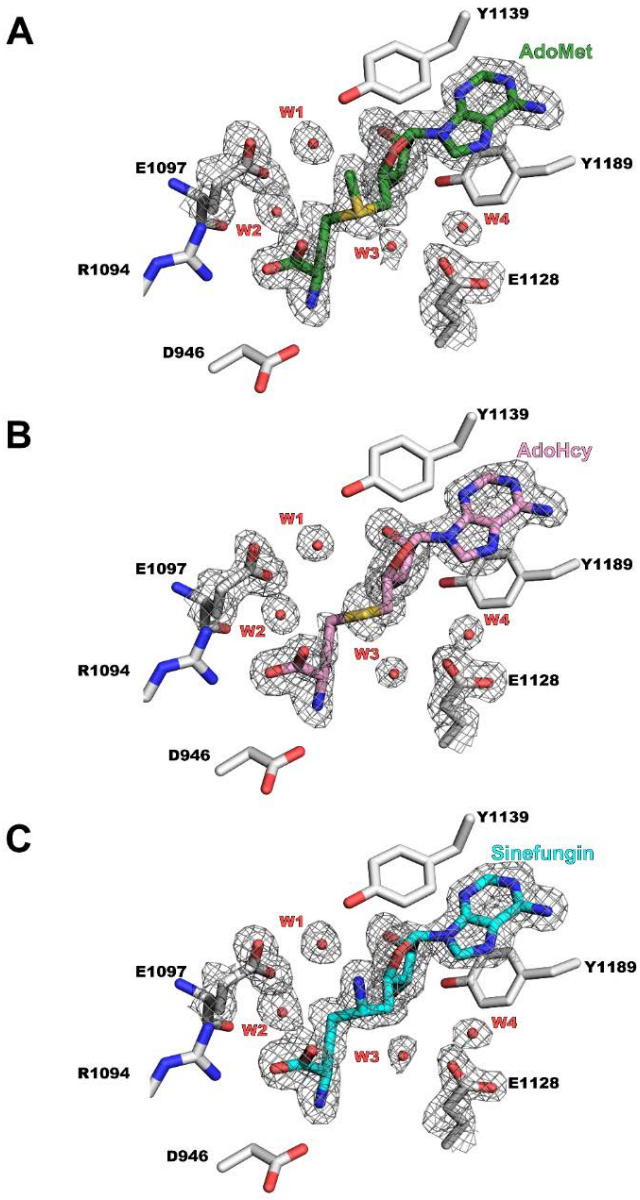

Figure 2.1: Simulated annealing F_O - F_C omit maps for AdoMet (A), AdoHcy (B), and sinefungin (C) bound to MetH.

The map is contoured at 2.0 σ. The depicted ligands as well as residues and water molecules within 5 Å of the ligands were omitted during the map calculations. For clarity, the electron density is shown for the ligands, Glu1097, Glu1128, and the waters mediating hydrogen bonding.

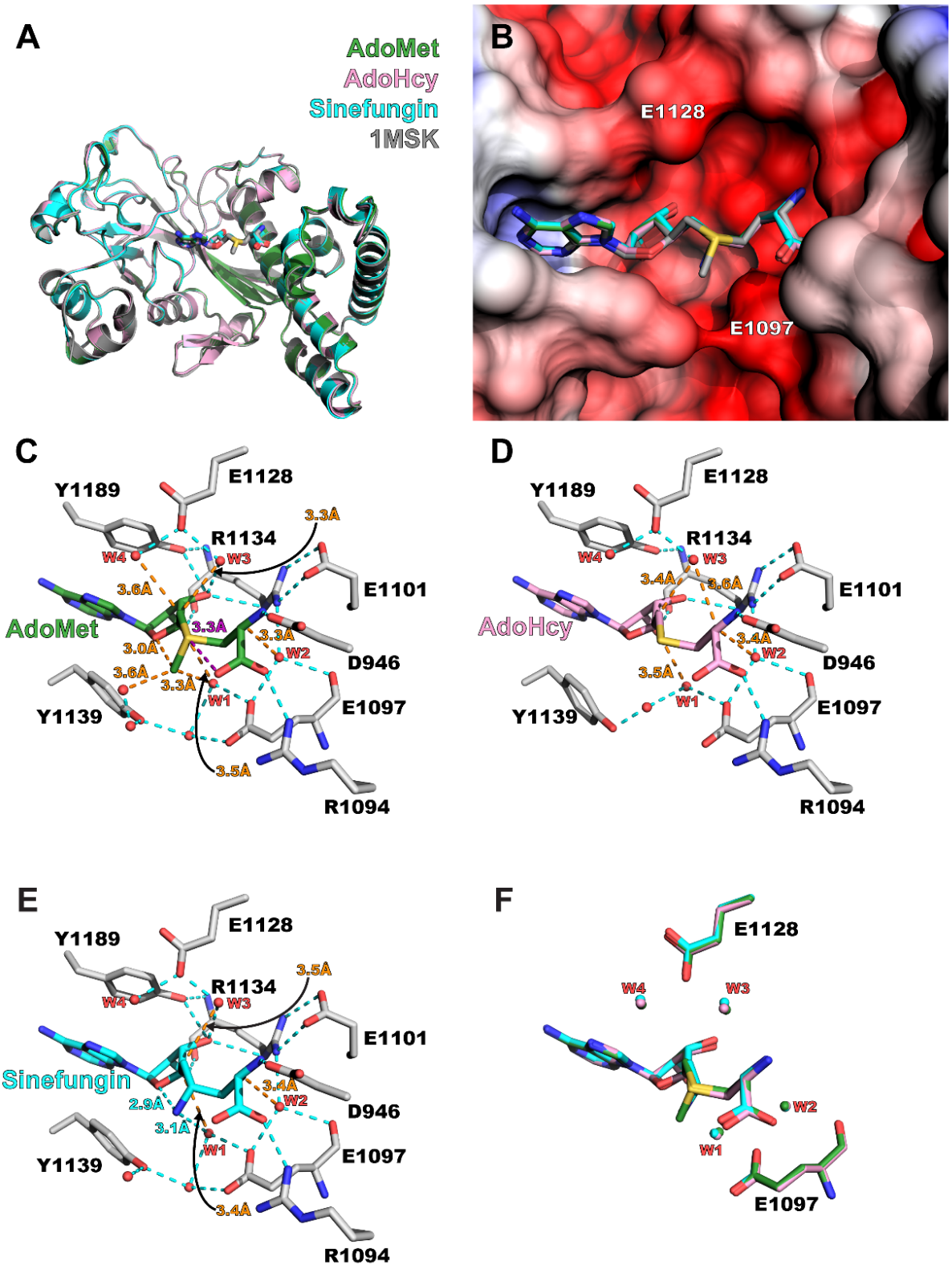
A
AdoMet
AdoHcy
Sinefungin
1MSK
B
E1128
E1097
C
Y1189
E1128
R1134
W4
W3
3.3Å
3.6Å
E1101
AdoMet
3.3Å
3.0Å
3.3Å
W2
D946
3.6Å
3.3Å
W1
E1097
Y1139
3.5Å
R1094
D
Y1189
E1128
R1134
W4
W3
3.4Å
3.6Å
E1101
AdoHcy
3.4Å
W2
D946
3.5Å
W1
E1097
Y1139
R1094
E
Y1189
E1128
R1134
W4
W3
3.5Å
E1101
Sinefungin
3.4Å
2.9Å
W2
D946
3.1Å
W1
E1097
Y1139
3.4Å
R1094
F
E1128
W4
W3
W2
W1
E1097

Figure 2.2 Structural comparisons of MetH bound to AdoMet, AdoHcy, and Sinefungin.

(A) Cartoon representation of 1MSK and MetH structures from this work superimposed by C-alpha atoms, with 1MSK shown in gray, MetH•AdoMet in green, MetH•sinefungin in cyan, and MetH•AdoHcy in pink. (B) Electrostatic render of the AdoMet bound active site, with the potential contoured between -5.0 (red) and 5.0 (blue) kT/e. The ligand superimposition from (A) is also shown, with the positions of the two glutamate residues labeled. Bonding patterns shown for the AdoMet-bound (C), AdoHcy-bound (D), and sinefungin-bound (E) structures. CH•••O hydrogen bonds shown as orange dashes, S•••O chalcogen bonds shown as purple dashes, and classical hydrogen bonds shown as cyan dashes.

	MetH•AdoMet	MetH•AdoHcy	MetH•Sinefungin
PDB Code	6BM5	6BM6	6BDY
Data Collection			
Wavelength (Å)	0.97903	0.97903	0.97903
Space group	$P2_12_12_1$	$P2_12_12_1$	$P2_12_12_1$
Cell dimensions			
a, *b*, *c* (Å)	38.10 61.67 139.92	38.23 61.66 139.95	38.35 61.58 139.88
α, β, γ (°)	90 90 90	90 90 90	90 90 90
Resolution (Å)	34.98 - 1.50 (1.53 - 1.50)	30.43 - 1.50 (1.53 - 1.50)	32.55 - 1.50 (1.53 - 1.50)
R_{merge} (%)	6.0 (23.3)	6.5 (33.1)	6.1 (28.0)
$CC_{1/2}$	(0.96)	(0.92)	(0.96)
$\langle I/\sigma I \rangle$	15.72 (4.30)	12.15 (3.10)	14.85 (4.37)
Completeness	98.5 (88.8)	98.4 (89.3)	98.5 (87.7)
Redundancy	5.4 (3.7)	4.5 (3.2)	5.9 (4.5)
Refinement			
Resolution	1.50	1.50	1.50
No. of Reflections	53030	52572	51571
R_{work}/R_{free}	0.15/0.19	0.16/0.20	0.14/0.18
No. of Atoms	3100	3078	3074
Protein	2589	2590	2605
Ligand/ion	27	26	27
Water	484	462	442
B-factors	23.44	26.29	24.34
Protein	21.44	24.54	21.95
Ligand/ion	19.1	21.83	18.79
Water	34.34	36.33	38.75
R.M.S. Deviations			
Bond lengths (Å)	0.007	0.009	0.009
Bond angles (°)	0.9	1.02	0.99
MolProbity Score			
Percentile	99%	99%	99%
Resolution Range (Å)	1.494 ± 0.25	1.504 ± 0.25	1.512 ± 0.25
Ramachandran			
Favored (%)	98.45	97.52	98.15
Allowed (%)	1.55	2.48	1.85
Outliers (%)	0	0	0

Table 2.1: Crystallographic and refinement statistics for MetH WT and mutants

2.3 NMR Spectroscopic Study

Chemical shift studies were performed on MetH with $^{13}CH_3$-methyl AdoMet in a 2D-HSQC experiment to determine the electronic environment of the AdoMet methyl group and to provide a comparison to past results. The original studies of SET7/9 paired quantum mechanical studies of NMR chemical shift of the methyl at various rotations with experimentally determined chemical shift to provide insight into the methyl rotamer position and subsequent CH•••O hydrogen bonding.[83]

MetH has a solvent exposed binding pocket, where AdoMet forms no direct interaction with active site residues. This should result in much smaller perturbations in the ^{13}C and ^{1}H chemical shifts upon binding compared to SET7/9 which forms two CH•••O between the AdoMet methyl and Y335 and H293 carbonyl groups. As shown in figure 2.3, a substantially smaller chemical shift perturbation is noted for MetH-bound AdoMet relative to the solution ^{1}H chemical shift of 2.97 ppm and ^{13}C chemical shift of 26.0 ppm previously reported.[133] Furthermore, we observe a cross peak in the SOFAST-HMQC spectra of MetH-AdoMet but not SET7/9-AdoMet. This is consistent with the exclusion of water from the SET7/9 binding pocket and solvent accessibility of the MetH binding pocket (Figure 2.4), as the SOFAST-HMQC method relies on exposure of the excited proton to many non-perturbed protons, reducing the relaxation time.[134]

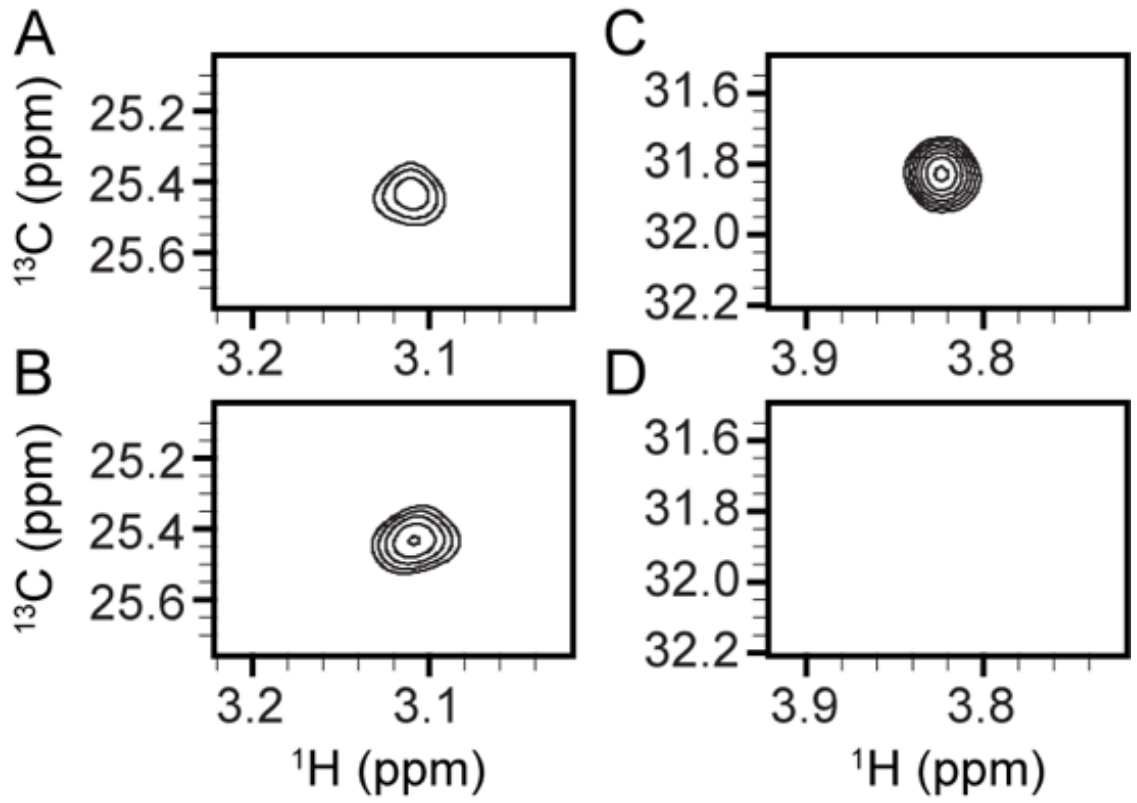

Figure 2.3: Two-dimensional NMR studies of MetH and SET7/9 with $^{13}CH_3$-methyl AdoMet

Chemical shifts of the AdoMet methyl group in MetH by HSQC (A) and SOFAST-HMQC (B). For comparison, the same chemical shift studies were performed on SET7/9, with a much greater chemical shift by HSQC (C), and an absent peak in the SOFAST-HMQC experiment (D).

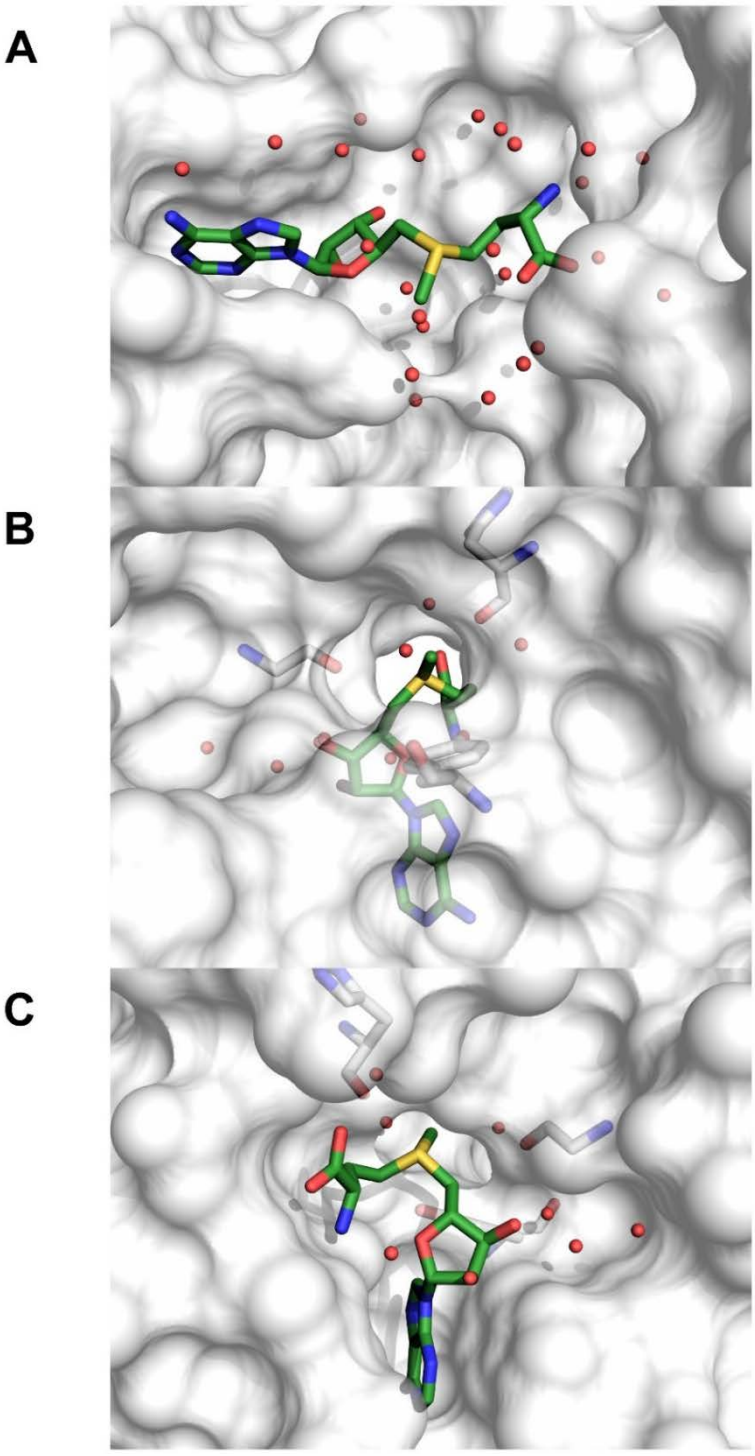

Figure 2.4: Solvent exposure of the AdoMet methyl group in MetH (A) and SET7/9 (B and C, using 4J83).

Waters within 5 Å show as spheres, and amino acids forming the methyl pore[47] in SET7/9 shown as gray sticks.

2.4 Quantum Mechanical Study and Isothermal Titration Calorimetry

Direct disruption of the CH•••O hydrogen bonding by mutagenesis was not possible in MetH due to the donors being active site waters. However, the charge of the two noted glutamate residues could be manipulated through the introduction of a glutamine mutation, conserving the hydrogen bonding potential with the neighboring waters. Mutation of glutamate to glutamine was explored both quantum mechanically with minimal model systems and by isothermal titration calorimetry with various ligands (Figure 2.5). The minimal active sites consisted of either $S(Et)_2$, representing the product AdoHcy, or $MeS^+(Et)_2$, representing the substrate AdoMet. The interaction with each glutamate was tested separately to give the clearest interpretation of the energy obtained. In both glutamate and glutamine systems, the representative ligand atoms were frozen in their respective crystallographic positions. In the glutamate structures, the waters were also frozen in their crystallographic positions, while the glutamine waters allowed to optimize in position, with the exception of water W4 in the 1128 AdoHcy model, as this water migrated to a position that would cause a steric clash with tyrosine 1189. The glutamates and glutamines were modeled as the sidechain alone, with the beta carbons being frozen, and at the 1097 position the gamma carbons were also frozen in the crystallographic positions, as the sidechain would pivot on the beta carbon to be further underneath the sulfonium and displace the waters. The glutamines were modeled in the position of the glutamates, with the amide being placed distal to the ligand atoms, such that the carbonyl would still preserve the hydrogen bonding pattern of the carboxylate.

The calculations were carried out in vacuum (dielectric =1), allowing comparison with past results conducted in the same manner. This will show the maximum change in energy, as there will be no shielding of charges.

Isothermal titration calorimetry was used as an *in vitro* measure of hydrogen bonding within MetH, utilizing various ligands to compare the effects of charge removal at points in the active site (see Appendix for data). Differences between AdoMet and AdoHcy are largely due to loss of charge on the central sulfur atom, influencing the strength of bonding to methyl and methylene hydrogen atoms by active site oxygens.[44] Sinefungin, an AdoMet natural product analog in which the sulfur and donated methyl group have been substituted for a carbon and an amine group. The trend seen between both the binding data and the energy calculations is that the substrate AdoMet more energetically binds to MetH than does the product AdoHcy (Table 2.2). The wild type has both a larger ratio of K_D's (AdoHcy/AdoMet) and larger difference in energy between the AdoMet and AdoHcy minimal systems. The ratio of K_D's in the WT enzyme is ~14.6, while either glutamate to glutamine mutation greatly drops the ratio to ~2.5-2.2. The energies mirror this trend, with the minimal active sites for glutamates having a difference of 79 and 67 kcal between AdoMet and AdoHcy, while the glutamine mutants have differences of 12 and 26, respectively. While there is a lesser energy gap between the 1128 WT and 1128 E to Q mutant for AdoMet (Table 2.2, ΔE_B [E-Q]), it is more disruptive to binding, with the K_D for AdoHcy doubling and the K_D for AdoMet increasing by about 12-fold. This is opposed to the 1097 position which has a greater difference in the calculated energies, but only a 4-fold loss of AdoMet binding, and a tighter binding of AdoHcy upon introduction of the mutation, though the calculated energy difference for

AdoMet between the wild type and glutamine mutant is much larger, as the wildtype has a greater binding energy and the mutant a lower binding energy than the respective 1128 AdoMet models. The divergence of K_D disruption and calculated energies is probably due to the interactions of 1097 and 1128 with the ligand, with 1097 largely encompassed by the interactions in the minimal model, while 1128 also interacts through a water with a ribose hydroxyl of the ligand that is not represented in the minimal model to avoid ascribing energy from that interaction to CH•••O hydrogen bonding. The charge would be expected to increase the hydrogen bonding strength to ribose hydroxyl as well,[11] causing the loss of both AdoHcy and AdoMet binding.

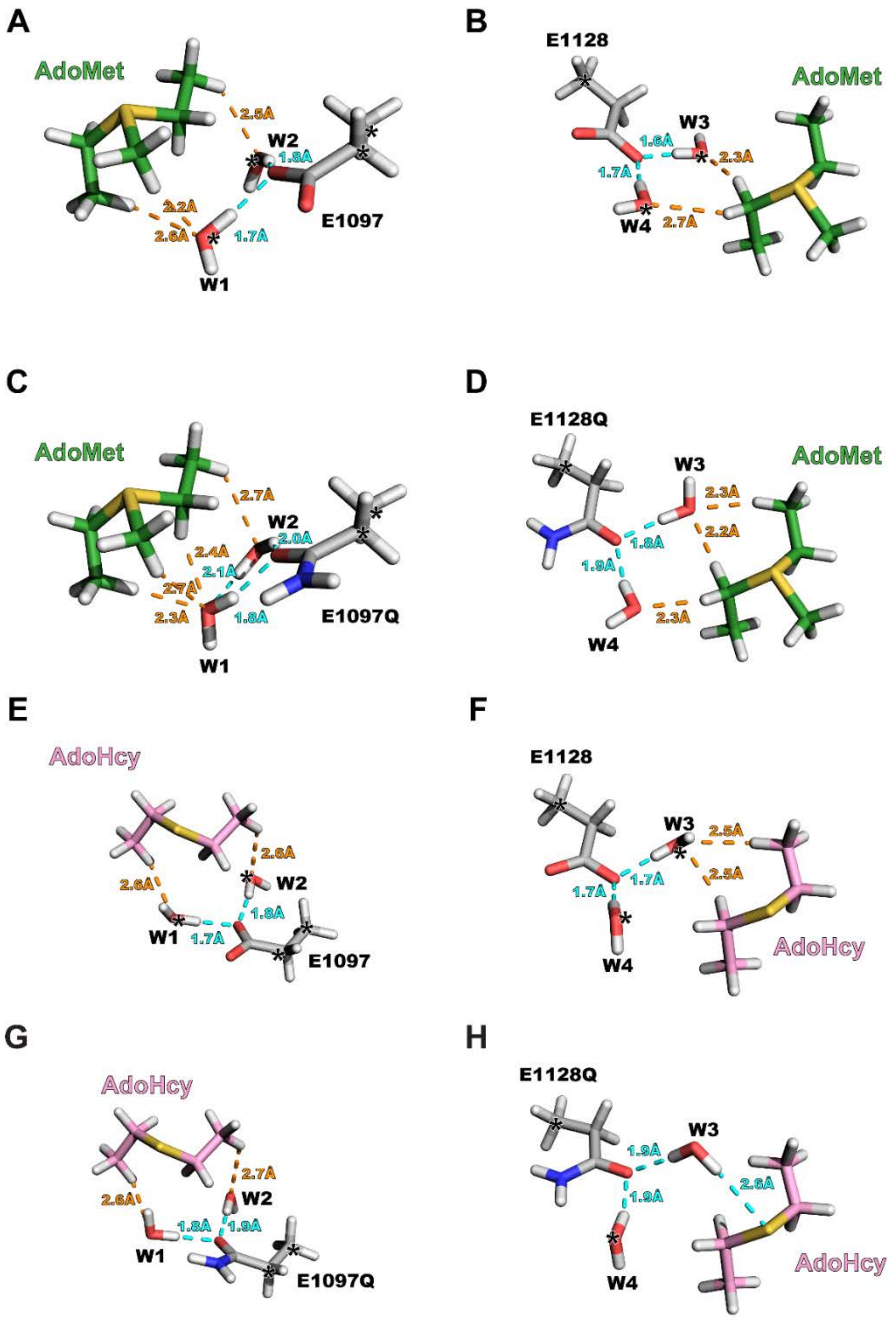

Figure 2.5: MetH quantum mechanical minimal models.

All ligand atoms (representing AdoMet and AdoHcy) were frozen, with other frozen atoms denoted by asterisks on those atoms. Models representing AdoMet (shown in green) complexed with glutamate 1097 (A), glutamate 1128 (B), glutamine 1097 (C), and glutamine 1128 (D). Models representing AdoHcy (shown in pink) complexed with glutamate 1097 (E), glutamate 1128 (F), glutamine 1097 (G), and glutamine 1128 (H).

	K_D (μM)		
	WT	**E1097Q**	**E1128Q**
AdoMet	**1.43 ± 0.05**	**6.10 ± 0.68**	**17.5 ± 1.0**
AdoHcy	**20.8 ± 0.2**	**15.0 ± 0.5**	**38.2 ± 1.0**
Sinefungin	**2.04 ± 0.07**	**17.7 ± 1.56**	**44.8 ± 2.51**
	ΔH (kcal mol^{-1})		
	WT	**E1097Q**	**E1128Q**
AdoMet	**-23.92 ± 0.10**	**-19.43 ± 0.16**	**-15.65 ± 0.09**
AdoHcy	**-15.30 ± 0.03**	**-11.95 ± 0.04**	**-11.22 ± 0.04**
Sinefungin	**-18.59 ± 0.09**	**-17.02 ± 0.17**	**-14.63 ± 0.13**

	QM binding energies (kcal mol^{-1})					
	E1097	**Q1097**	**ΔE_B [E-Q]**	**E1128**	**Q1128**	**ΔE_B [E-Q]**
$MeS^+(Et)_2$ complex energy	**87.69**	**19.19**	**68.50**	**73.41**	**29.30**	**44.11**
$S(Et)_2$ complex energy	**8.45**	**7.25**	**1.20**	**6.30**	**3.53**	**2.77**
ΔE_B [$MeS^+(Et)_2$ - $S(Et)_2$]	**79.24**	**11.94**		**67.11**	**25.77**	

Table 2.2: ITC data and QM calculated binding energies for the various ligands with MetH WT, E1097Q, and E1128Q.

Differences in energy between the glutamate and glutamine models, giving an estimation of lost interaction energy upon mutation, shown as ΔE_B [E-Q], and differences in the binding energy between the AdoMet-like model and the AdoHcy-like models, giving an estimation of the ability to selectively bind substrate over product, shown as ΔE_B [$MeS^+(Et)_2$ - $S(Et)_2$].

2.5 Discussion

MetH represents a unique fold of methyltransferase and possesses a unique method of binding to AdoMet, binding the sulfonium system exclusively through waters within the active site. MetH is also an enzyme of great metabolic importance since it is the enzyme at the center of one-carbon metabolism within the cell.[130] Though the enzyme characterized in this study was the *E. coli* enzyme, the *H. sapiens* enzyme is highly similar, with a key difference of a leucine (L1166) in the human enzyme in

position of glutamate 1128 that we explored in the *E. coli* enzyme.[135] This would be expected to decrease the substrate/product discrimination of the enzyme based on the results of the glutamine mutation at that position. The difference in the human enzyme, coupled with the binding affinities of sinefungin relative to AdoMet, causes some concern with respect to sinefungin analogs. Sinefungin has been used as a scaffold for inhibitor development,[136] but with the open active site of MetH, these compounds may be accommodated and cause inhibition of the enzyme. This in turn could disrupt the AdoMet/AdoHcy balance, which is between 2-11 fold normally,[137, 138] and cause further inhibition of the enzyme by high AdoHcy levels, with implications for global methyl flux. Screening of AdoMet-like inhibitors may be aided by study of their binding to MetH, in an effort to stem possibly cytotoxic effects.

2.6 Materials and Methods

AdoMet purification

Isotopically-labeled AdoMet was produced enzymatically using *E. coli* AdoMet synthetase (MetK)[139, 140] similar to a previously described method.[3] The sequence for MetK was used in an expression vector, pHT4 (based on pET15b, Novagen) with Tobacco etch virus (TEV) protease cleavable N-terminal His-tag to aid in purification. Rosetta 2 cells were transformed with the plasmid and over expressed overnight at 18°C in 2XYT media with ampicillin (100 µg/mL) and chloramphenicol (50 µg/mL) used throughout and 250 µM IPTG used for induction. Cultures were spun at 3800 rpm (Sorvall H6000A rotor) for 30 min. Media was decanted and each pellet was resuspended in 50 mM sodium phosphate, pH 7.0, and 500 mM sodium chloride, pooled, and aliquoted in 1L pellets and stored at -80°C.

Pellets were lysed by addition of lysozyme and HALT protease inhibitor (Roche) and rocked at 4°C. Pellet was brought up to 60 mL with Buffer A (50 mM sodium phosphate, pH 7.0, 500 mM sodium chloride, 5 mM β-mercaptoethanol) lysed by 3, 1 minute bursts of sonication in a metal beaker on ice, with at least 30 seconds between to allow the lysate to cool. Lysate was spun at 18,000 rpm (SS34 rotor) for 30 minutes, and the decantate was filtered with 0.45 µm SFCA filters before loading onto the chromatography system. The filtered decantate was purified on a 4 mL TALON column (Clontech) pre-equilibrated in Buffer A, loaded and washed with 5 column volumes of Buffer A, and eluted with a 15 column volume gradient from Buffer A to Buffer B (50 mM sodium phosphate, pH 7.0, 500 mM sodium chloride, 5 mM β-mercaptoethanol, and 300 mM imidazole). Protein containing fractions were pooled and cleaved overnight with ~1 mg of TEV protease, while dialyzing at 4°C in a 10 kDa dialysis bag against 2L of 50 mM Tris, pH 8.0, 35 mM sodium chloride, and 5 mM β-mercaptoethanol. After TEV cleavage the solution was concentrated and loaded onto gel filtration on a Superdex S200 16/60 (GE Healthcare) column in 100 mM Tris, pH 8.0, 50 mM potassium chloride. After gel filtration, protein containing fractions were pooled, concentrated, and flash frozen before storage at -80°C.

AdoMet synthesis was carried out in 10mL solutions of 100 mM Tris, pH 8.0, 50 mM potassium chloride, 30 mM magnesium chloride, 15 mM adenosine triphosphate, 10 mM methionine ($^{13}CH_3$-methyl methionine for the NMR studies), and 8% v/v β-mercaptoethanol, and ~850 µg of MetK enzyme in a variation of a previous method.[3] Reactions were rocked at room temperature for 4-16 hours before loading reaction onto a Source 15S column. AdoMet was eluted using a 15 column volume gradient from 0-

1M hydrochloric acid in milliQ water. AdoMet containing fractions pooled and brought to near dryness using a SpeedVac (Savant). Dried AdoMet stored at -20°C.

Protein expression and purification

The sequence for the E coli 897-1227 tryptic fragment that had been previously crystallized was amplified out of the supplied vector from Dr. Marcos Koutmos and inserted using BamHI and XhoI sites from the primers used to insert into a vector, pHT4 (derived from pET15b, Novagen), with a Tobacco etch virus protease (TEV) cleavable N-terminal His-tag. The protein construct contained an N-terminal extension of Gly-Ser before lysine 897 upon cleavage by TEV protease. Glutamate to glutamine mutations at position 1097 or 1128 were generated from the wild type construct using Quikchange (Agilent) mutagenesis. Protein was overexpressed using Rosetta 2 (DE3) cells in 2XYT media in an IPTG-inducible system, induced at 18°C and grown overnight. Cells were pelleted and resuspended in 50 mM sodium phosphate, pH 7.0 with 500 mM sodium chloride, aliquoted and placed in the -80°C. Cell pellets were lysed by rocking at 4°C with lysozyme and HALT protease inhibitor (Roche) followed by sonication at ~90W for 1 minute, 3-4 times, with at least 30 seconds between sonication to allow the lysate to cool. Lysate was centrifuged at 18,000 rpm (SS34 rotor) for 30 minutes. Soluble lysate was filtered with a 0.45 µm SFCA filter and loaded onto a 4 mL TALON column (Clontech) using a NGC chromatography system. The column was washed with 5 column volumes of 50mM sodium phosphate, pH 7.0, 500mM sodium chloride, and 5mM β-mercaptoethanol. The protein was eluted using a gradient with the same buffer containing 300mM imidazole. The fractions containing MetH and no major contaminants were pooled and cleaved with ~1 mg TEV protease overnight in a 10 kDa dialysis bag,

dialyzing against 2 L of 20 mM sodium phosphate, pH 8.0, 35 mM sodium chloride and 5mM β-mercaptoethanol. After cleavage, solution was passed over a small TALON column to remove uncleaved MetH and the TEV protease. The solution was concentrated to 3-6 mg/mL, brought to 5% v/v glycerol and incubated with activated charcoal (Sigma) at a ratio of 2:1 mg/mg charcoal:protein and rocked at room temperature for at least 20 minutes to remove bound AdoMet. The solution was centrifuged and filter to remove charcoal, and the protein was further concentrated and loaded onto a Superdex S200 16/60 column in 20 mM sodium phosphate, pH 8.0, 100 mM sodium chloride. Protein containing fractions were pooled, concentrated, flash frozen, and stored at -80°C until use.

Crystallization

Protein was crystallized by hanging drop vapor diffusion with a reservoir containing 27-32% PEG 6000, 60-100 mM Tris pH 7.2-7.5, with 300 mM magnesium acetate. The protein solution contained 15 mg/mL of MetH, 3 mM of AdoMet or Sinefungin, and 10 mM Tris buffer, pH 7.4, with the remaining volume made up by the addition of 10 mM EDTA. The AdoHcy was similar, with 5 mM AdoHcy and 20 mM Tris buffer, pH 7.4, with the addition of 20 mM EDTA, with twice the EDTA concentration being added due to the limited solubility of AdoHcy, resulting in the ligand stock taking a larger portion of the protein solution volume relative to AdoMet, leaving less volume for the addition of the EDTA. Crystals were cryoprotected in 34% PEG 6000, 100 mM Tris pH 7.25, 300 mM magnesium acetate and flash frozen in liquid nitrogen.

Data were collected on the MarMosaic 300 detector of the LS-CAT 21-ID-G beamline at the Advanced Photon Source of Argonne National Laboratory. HKL2000 was used to

process and scale the datasets.[141] Molecular replacement was performed using Phaser[142], with 1MSK[72] stripped of ligands, waters, and converted to poly-alanine used as the search model for the sinefungin- and AdoMet-bound structures, and mostly refined AdoMet-bound structure stripped of ligands and waters for the search model for the AdoHcy-bound structure. Coot[143] was used for model building, and Phenix[144] was used for refinement. Images for structural figures were generated using the PyMOL Molecular Graphics System, Schrödinger, LLC. Electrostatic surface was generated using the APBS plugin for PyMOL.[145]

QM calculations

Quantum mechanical binding energies were obtained by subtraction of the energies of the optimized monomers from the complex energy calculated using M06-2X/6-31+G**. The counterpoise correction method was used to correct for basis set superposition error. Positions of hydrogen atoms were optimized, while other atoms were either frozen in the crystallographic positions or allowed to optimize, as described in the text.

ITC

Isothermal titration calorimetry was performed in a VP-ITC calorimeter (Malvern instruments) for wild type MetH, and an Auto ITC-200 (Malvern instruments) for the mutant MetH proteins, with 20 mM sodium phosphate pH 8.0, 100 mM sodium chloride used as the buffer. Wild type AdoMet and sinefungin titrations were performed with 60 µM protein and 600 µM ligand, and AdoHcy titrations were performed with ~200 µM protein and 2.2 mM ligand. E1097Q and E1128Q mutant AdoMet titrations were performed with 840-870 µM protein and 9.6 mM ligand, sinefungin titrations were

performed with 830-910 µM protein and 16.2 mM ligand, and AdoHcy titrations were performed with 810-940 µM protein and 10.1-10.7 mM ligand. Titrations of the E1097Q and E1128Q mutants with sinefungin used sinefungin dissolved 20 mM sodium phosphate pH 8.0, 100 mM sodium chloride and titrated back to pH 8.0 using 210 mM hydrochloric acid in 20 mM sodium phosphate pH 8.0, 100 mM sodium chloride, to keep the ionic strength of the buffer the same. Each titration was performed once, and the curves were fitted using the Origin graphing software provided with the instrument.

Appendix: ITC titrations of MetH

Figure A.1A: ITC titration of WT MetH with AdoMet

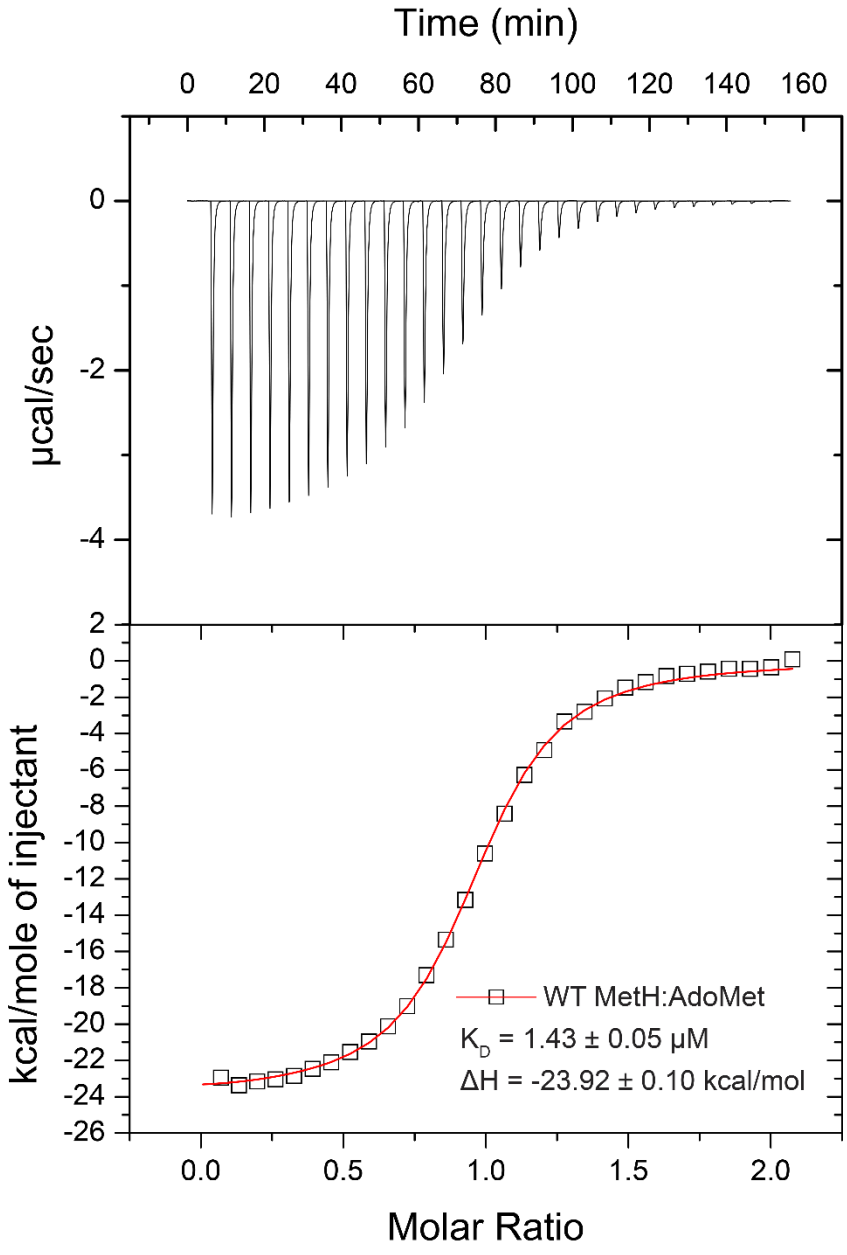

Figure A.1B: ITC titration of WT MetH with AdoHcy

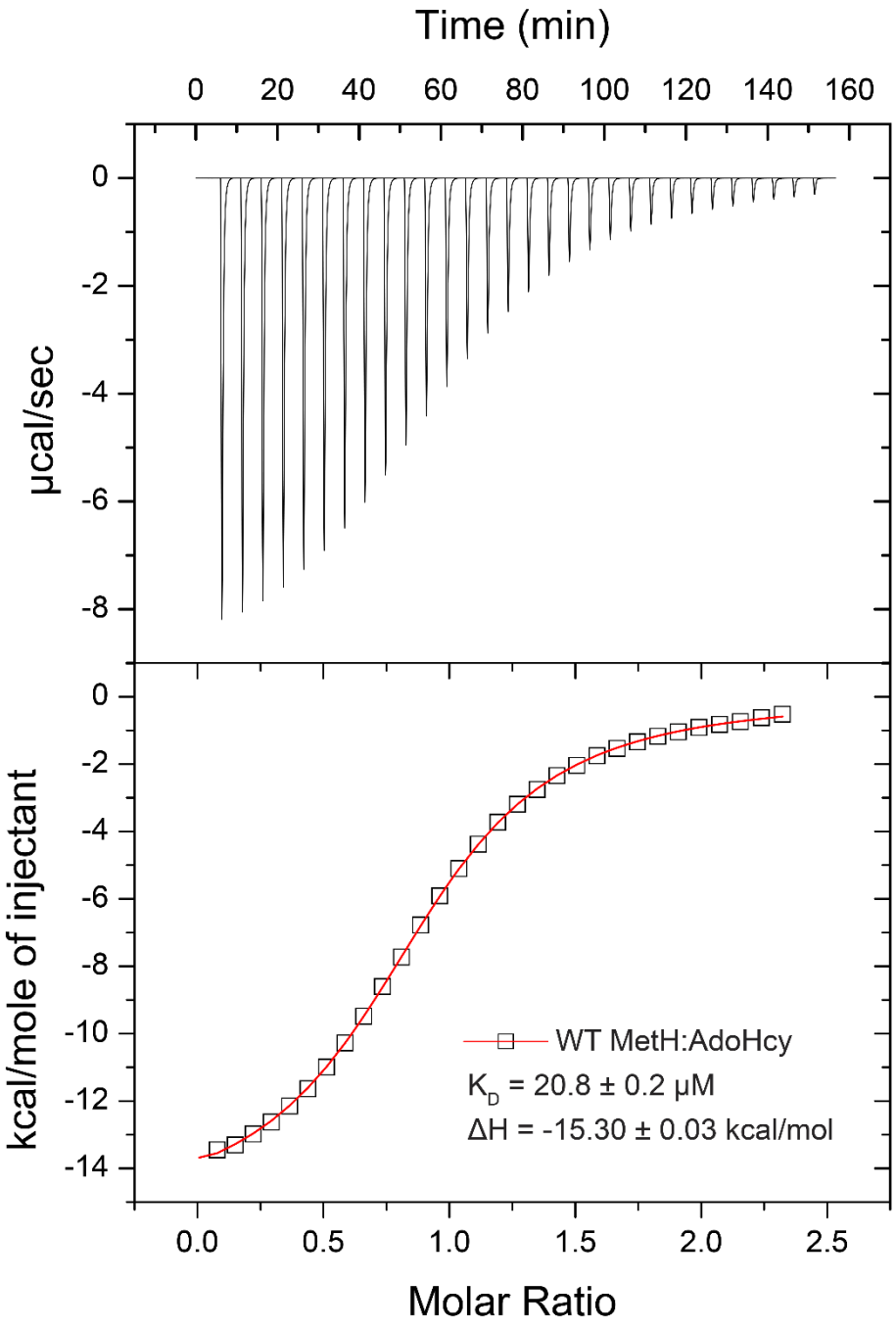

Figure A.1C: ITC titration of WT MetH with Sinefungin

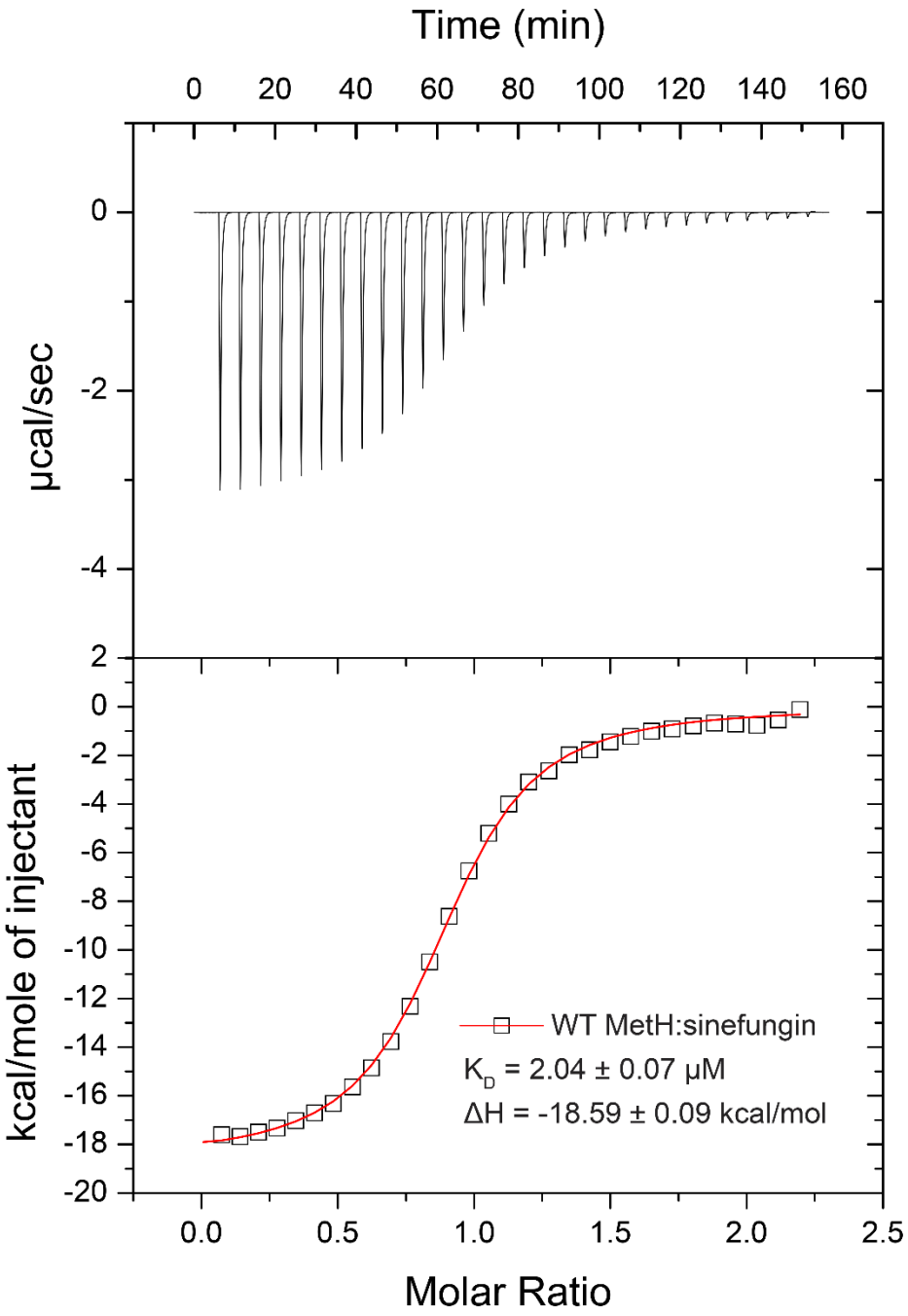

Figure A.1D: ITC titration of MetH E1097Q with AdoMet

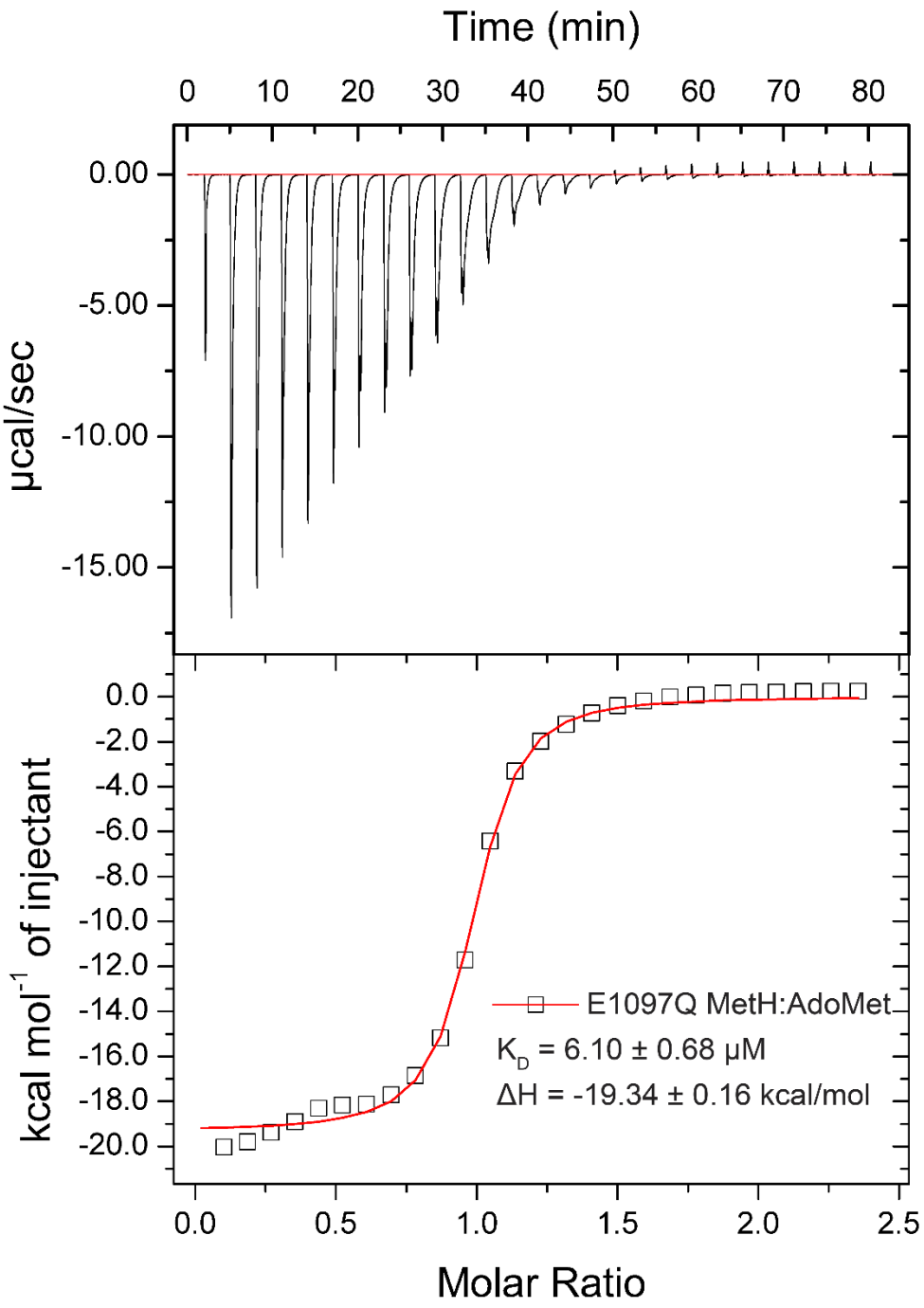

Figure A.1E: ITC titration of MetH E1097Q with AdoHcy

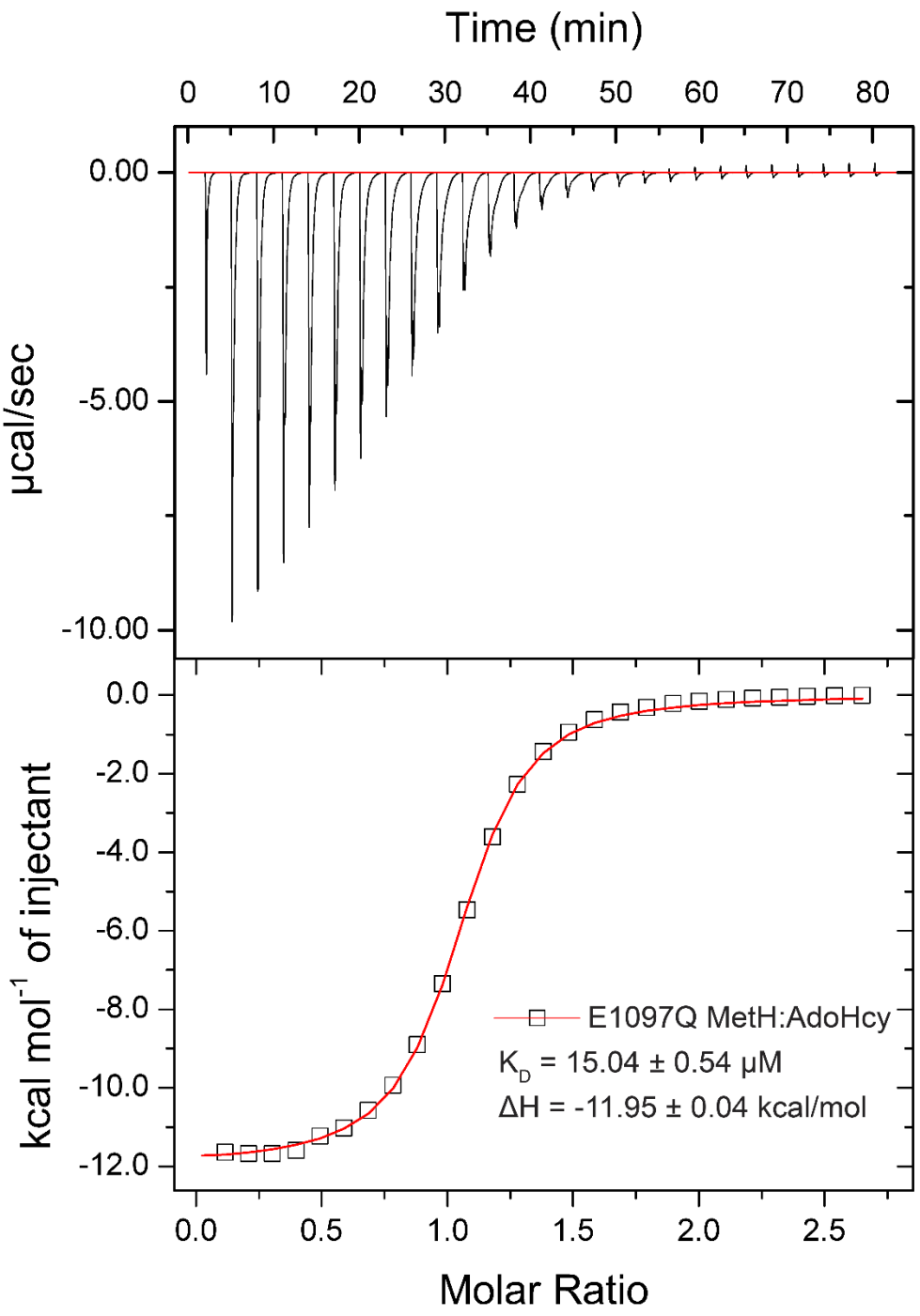

Figure A.1F: ITC titration of MetH E1097Q with Sinefungin

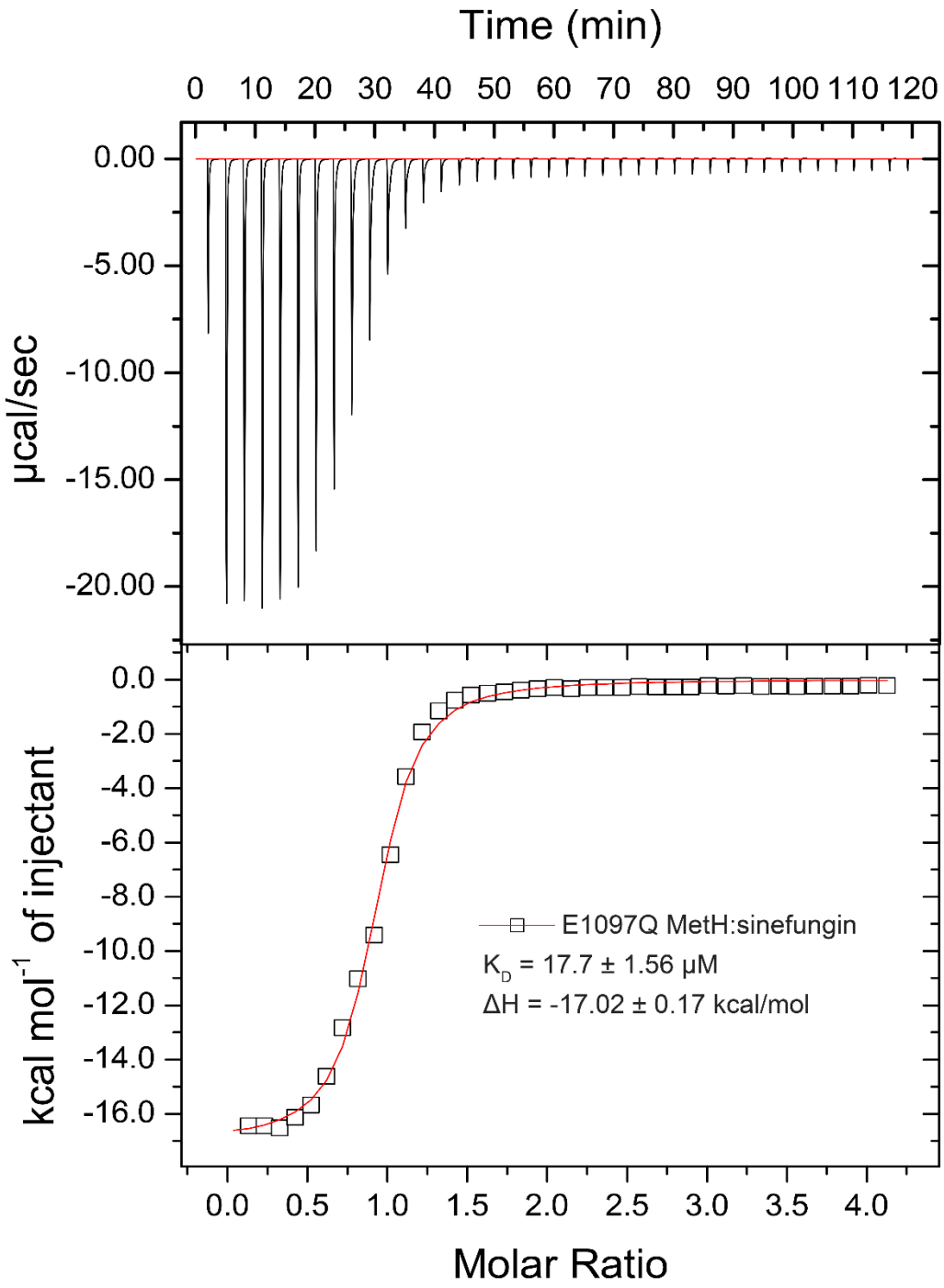

Figure A.1G: ITC titration of MetH E1128Q with AdoMet

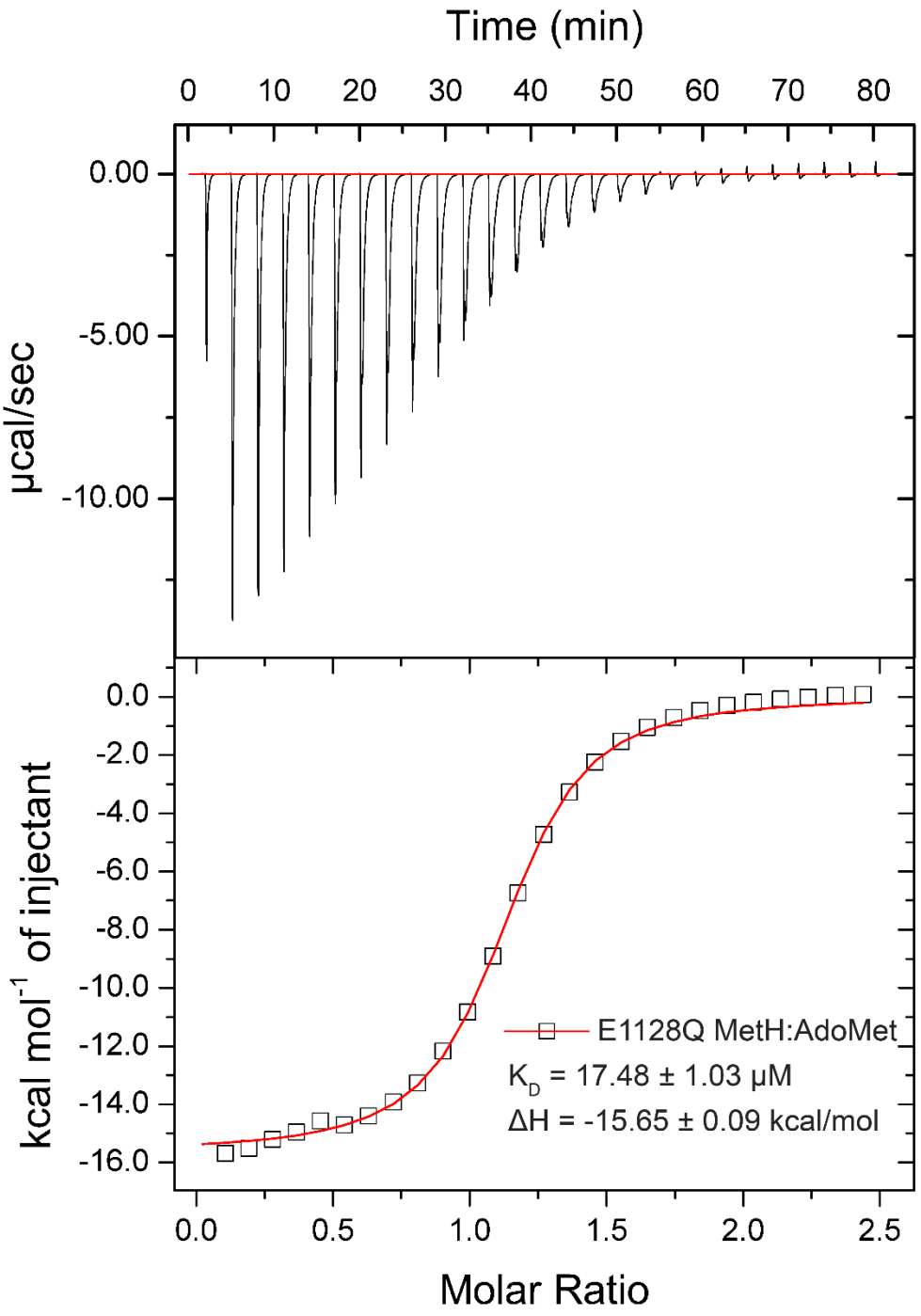

Figure A.1H: ITC titration of MetH E1128Q with AdoHcy

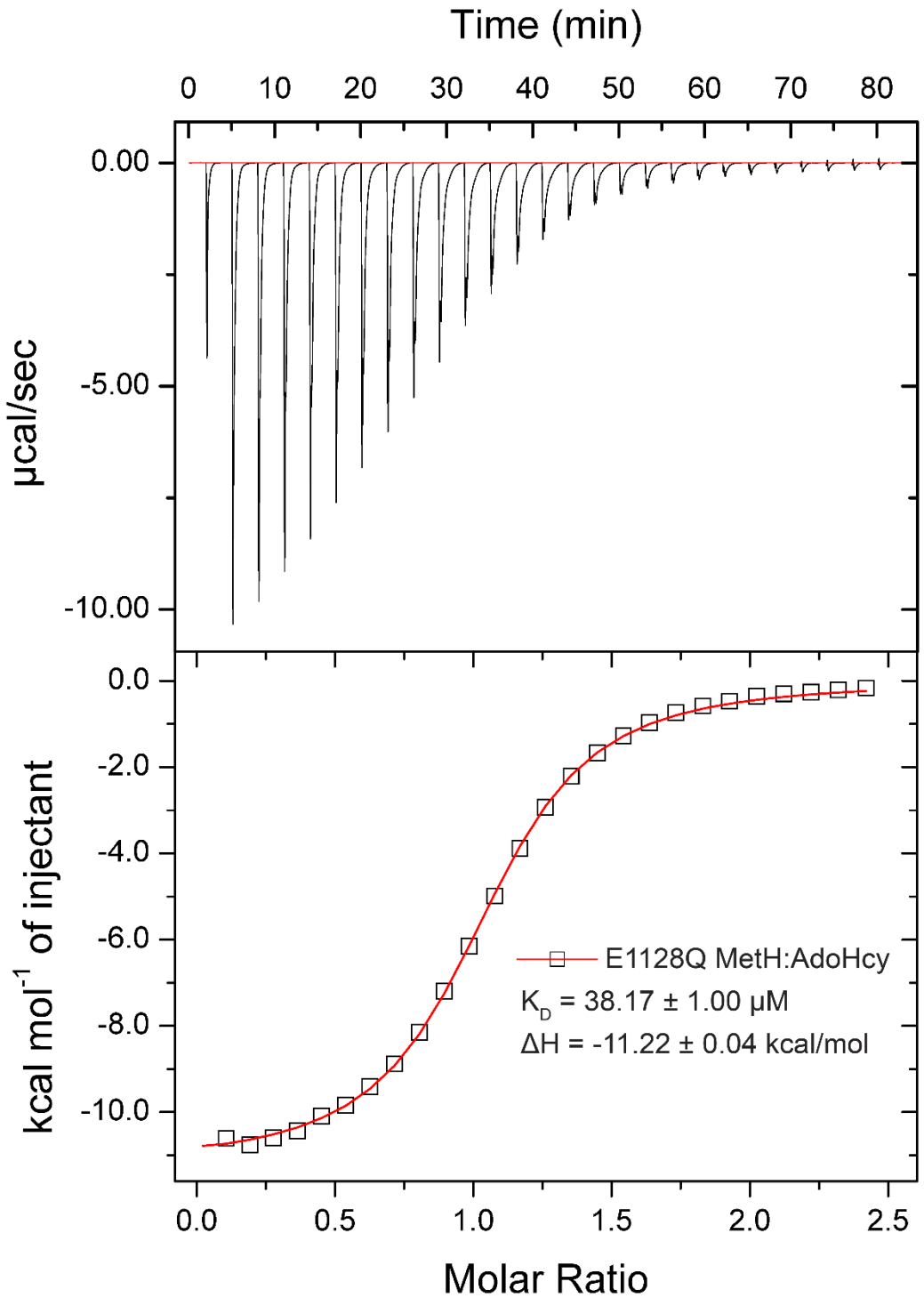

Figure A.1I: ITC titration of MetH E1128Q with Sinefungin

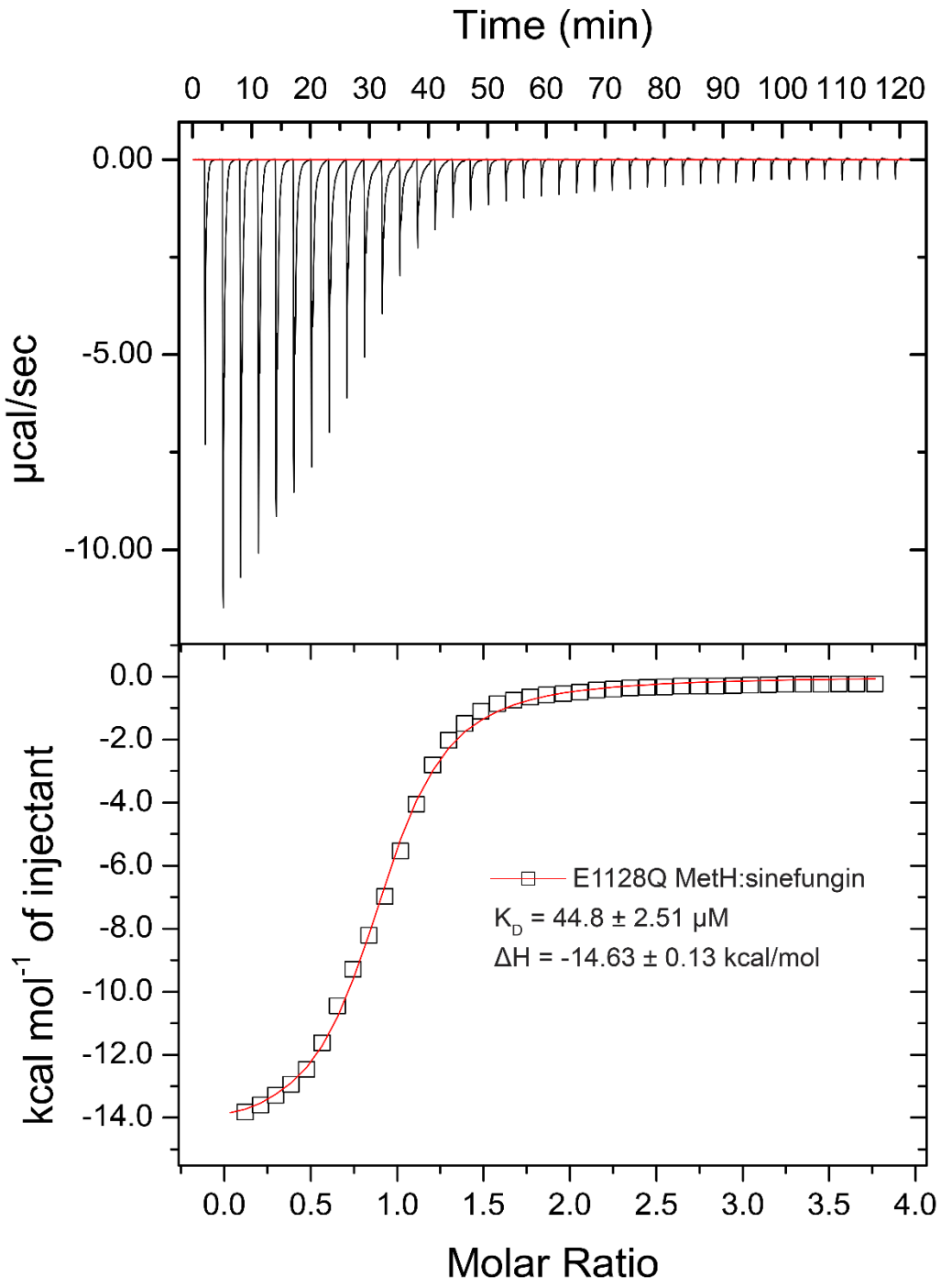

Figure A.1: Isothermal titrations and fitted isotherms of various ligands with WT MetH and the E1097Q and E1128Q mutants.

WT MetH with AdoMet (A), AdoHcy (B), and Sinefungin (C). MetH E1097Q with AdoMet (D), AdoHcy (E), and Sinefungin (F). MetH E1128Q with AdoMet (G), AdoHcy (H), and Sinefungin (I).

Chapter 3:

Sulfur−Oxygen Chalcogen Bonding Mediates AdoMet Recognition in the Lysine Methyltransferase SET7/9

Robert J. Fick, Grace M. Kroner, Binod Nepal, Roberta Magnani, Scott Horowitz, Robert L. Houtz, Steve Scheiner, and Raymond C. Trievel

3.1 Introduction

SET7/9 belongs to the SET domain class of lysine methyltransferases.[79] SET7/9 has been intensely studied by the Trievel laboratory, both in its ability to bind and catalyze methylation on peptide substrates[146, 147] and in the role of carbon-oxygen (CH•••O) hydrogen bonding in binding of S-adenosyl-L-methionine (AdoMet) and conducting catalysis of the methyl transfer reaction.[47, 83, 84] As part of the studies of CH•••O hydrogen bonding in SET7/9, CH•••O hydrogen bonding to the AdoMet methyl group was surveyed in high resolution (< 2.0 Å) AdoMet-bound methyltransferase structures.

Reproduced with permission from

ACS Chem. Biol., 2016, 11 (3), pp 748–754
DOI: 10.1021/acschembio.5b00852
Publication Date (Web): December 29, 2015

RJF performed the binding studies and differential scanning calorimetry and finished structure refinement. GMK crystallized the protein and performed initial structure refinement. BN and SS performed quantum mechanical calculations. SH made the construct and provided discussion on the manuscript. RM performed the radiometric assays. RJF and RCT prepared the manuscript.

This survey established that CH•••O hydrogen bonding to the AdoMet methyl group is not just a feature of SET7/9, but appears to be a universally conserved feature of all AdoMet-dependent methyltransferases.[47] Another interaction seen within the active site of SET7/9 is an apparent S•••O chalcogen bond, with a distance of 3.0 Å between an asparagine sidechain oxygen and the sulfonium sulfur of AdoMet. This distance is much shorter than 3.3 Å of the combined van der Waals radii of these two atoms.[32] A chalcogen bond is a σ-antibonding interaction, similar to a halogen bond,[50] in which a lone pair is able to be donated into an antibonding orbital of a chalcogen atom (elements of column 16 of the periodic table, including O, S, Se, etc.). There is evidence for these interactions in biological systems, with the relative enrichment of oxygen in contacts closer than van der Waals radii near sulfurs in methionine and cystine systems (C-S-C and C-S-S) within proteins. [53-55] The chalcogen bond also presents another possible interaction in which methyltransferases can preferentially bind AdoMet, as the interaction energy with a sulfonium is much greater than with the thioether system.[45]

3.2 Structural Study

The SET7/9 N265A mutant was produced to remove the chalcogen bond with minimal disruption to the enzyme. Before biochemical characterization of the mutant enzyme, the structure was determined to verify active site integrity. SET7/9 N265A crystal trials were set up with AdoMet and a known TAF10 substrate peptide, resulting in methyl group transfer from AdoMet to the lysine of the TAF10 and the formation of the product complex of SET7/9 N265A with S-adenosylhomocysteine (AdoHcy) and the TAF10 K189me1 peptide. The crystal diffracted to 1.55 Å (see Table 3.1), and was highly similar to the wild type enzyme with a 0.19 Å Cα RMSD for aligned atoms. The active

site showed that the loss of the chalcogen bond and other interactions formed by the asparagine sidechain caused no major change in the active site conformation or rearrangement of active site waters to occupy the location of the larger side chain (Figure 3.1). To further verify enzyme integrity, enzyme melting temperature was determined by differential scanning calorimetry (DSC, Figure 3.2). This revealed a minor decrease in melting temperature (44.3°C) relative to that of the wild type enzyme (46.6°C), owing in part to the loss of the hydrogen bond between the asparagine sidechain and the carbonyl oxygen of valine 277, among other interactions.

	SET7/9 N265A•TAF10 K189me1•AdoHcy
PDB Code	5EG2
Data Collection	
Wavelength (Å)	0.97903
Space group	$P3_221$
Cell dimensions	
a, b, c (Å)	83.20, 83.20, 95.86
α, β, γ (°)	90, 90, 120
Resolution (Å)	39.91 - 1.55 (1.59 - 1.55)
R_{merge} (%)	6.8 (90.4)
$\langle I/\sigma I \rangle$	19.49 (3.66)
Completeness	99.6 (100)
Redundancy	10.9 (10.7)
Refinement	
Resolution	1.55
No. of Reflections	56156
R_{work}/R_{free}	0.15/0.17
No. of Atoms	2282
Protein	1939
Ligand/ion	27
Water	316
B-factors	29.5
Protein	27.6
Ligand/ion	32.2
Water	41.3
R.M.S. Deviations	
Bond lengths (Å)	0.009
Bond angles (°)	1.18
MolProbity Score	
Percentile	98%
Resolution Range (Å)	1.55 ± 0.25
Ramachandran	
Favored (%)	96.8
Allowed (%)	3.2
Outliers (%)	0

Table 3.1 Crystallographic and refinement statistics for SET7/9 N265A.

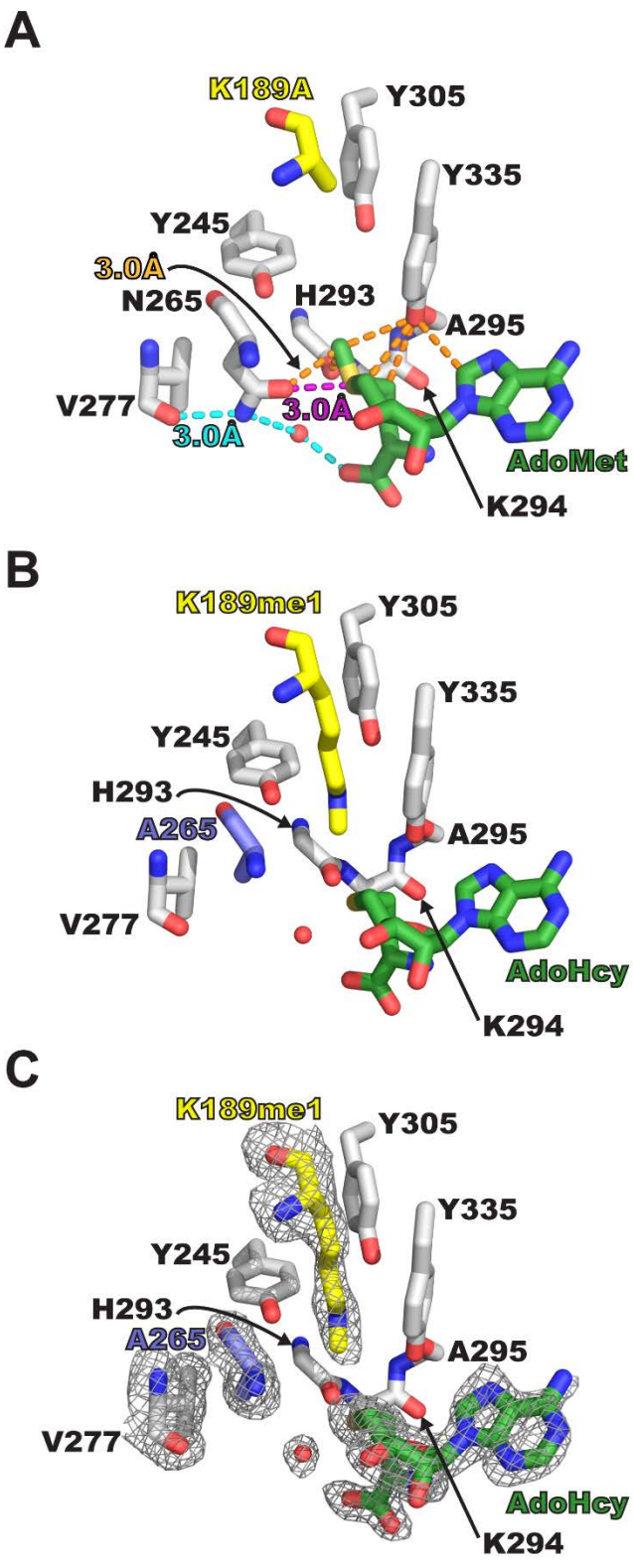
A
K189A
Y305
Y335
Y245
3.0Å
N265
H293
A295
V277
3.0Å
3.0Å
AdoMet
K294
B
K189me1
Y305
Y335
Y245
H293
A265
A295
V277
AdoHcy
K294
C
K189me1
Y305
Y335
Y245
H293
A265
A295
V277
AdoHcy
K294

Figure 3.1: The chalcogen bond in SET7/9 and the SET7/9 N265A active site.

The active site of SET7/9 WT•AdoMet•TAF10 K189A (PDB ID: 4J83)[47] showing the chalcogen bond to asparagine 265 (A). CH•••O hydrogen bonding in the SET7/9 active site is shown as orange dashes. The chalcogen bond between the asparagine sidechain carbonyl and the AdoMet sulfur is shown as purple dashes. Classical hydrogen bonding network between an active site valine backbone carbonyl, the asparagine sidechain, an active site water, and the AdoMet carboxylate shown as cyan dashes. Active site of the SET7/9 N265A•AdoHcy•TAF10 K189me1 complex with the site of the mutation shown in slate blue (B). Simulated annealing omit map (F_O - F_C) contoured at 2.0 σ (C). The map is displayed for AdoHcy, TAF10 K189me1, alanine 265, valine 277, and the water that engaged in hydrogen bonding shown in (A). No water was seen in place of the asparagine sidechain.

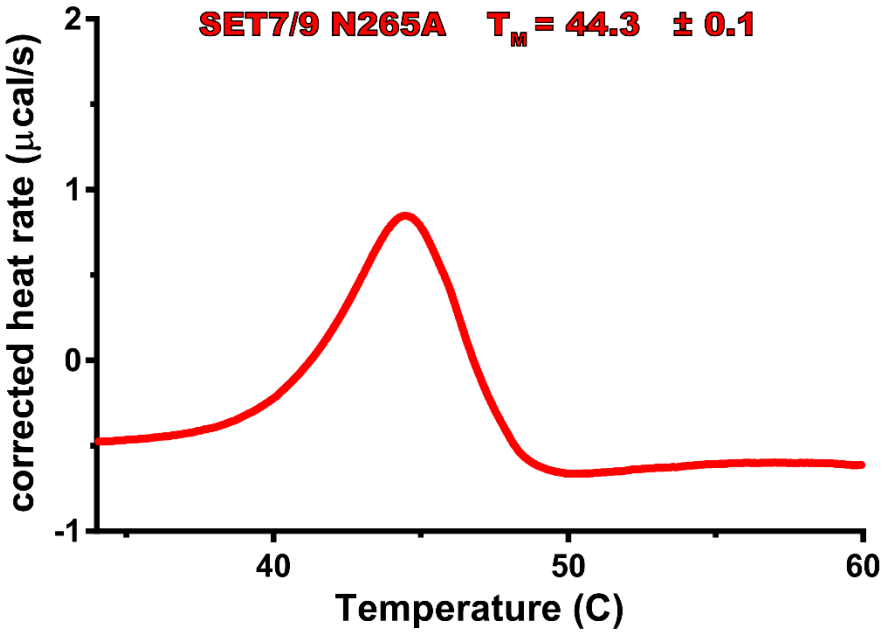

Figure 3.2: Differential Scanning Calorimetry of the SET7/9 N265A mutant.

Differential Scanning Calorimetry (DSC) was performed to confirm mutant stability. The melting temperature of 44.3°C is slightly lower than the wildtype value of 46.6°C.[47]

3.3 Biochemical and Quantum Mechanical Characterization

Binding of the mutant enzyme to the TAF10 peptide was measured to confirm a defect was not present that may complicate kinetic analysis (Figure 3.3). The binding constant was within 1.4-fold of the wild type value (Table 3.2). Binding of the enzyme to

AdoMet measured by isothermal titration calorimetry (ITC) showed an 8-fold loss in binding relative to wild type (Figure 3.4). The binding to AdoHcy was measured by an intrinsic tryptophan fluorescence assay and was found to be only disrupted around 2-fold. This represents a 4-fold loss in substrate/product discrimination. The loss of affinity for AdoMet is also seen in the radiometric activity assay run with SET7/9 N265A, with a 7-fold increase in the K_M of AdoMet and a 7-fold decrease in the catalytic rate.

Quantum mechanics was used to probe the binding energies of the interactions by determining the energies of complex formation for minimal model systems (Figure 3.5). The minimal models included N-methylacetamide (NMA) in place of the backbones of valine 277 and histidine 293. The sidechain of tyrosine 335 was modeled as a 4-methylphenol group, asparagine 265 was modeled as a propanamide, and the alanine mutation was modeled as an ethane. The water that hydrogen bonds to the asparagine sidechain was also modeled. AdoMet was modeled as diethylmethyl sulfonium, and AdoHcy was modeled as diethyl thioether. Select model atoms were frozen in their crystallographic positions to prevent deviation of the model during energy minimization. The loss of selectivity in binding AdoMet over AdoHcy is also borne out in the quantum mechanical results. The difference between the AdoMet and AdoHcy binding energies is greater in wild type than in the N265A mutant. The loss of binding energy upon mutation relative to wild type in the AdoMet-like complex is 21 kcal/mol, while the loss for the AdoHcy complex is only 10 kcal/mol, recapitulating the effect seen in charged vs uncharged chalcogen systems.[45] The loss of energy upon mutation in the quantum mechanical systems cannot be purely ascribed to the loss of a chalcogen bond, as the

AdoMet also forms a possible CH•••O hydrogen bond to the asparagine side chain (Figure 3.7B).

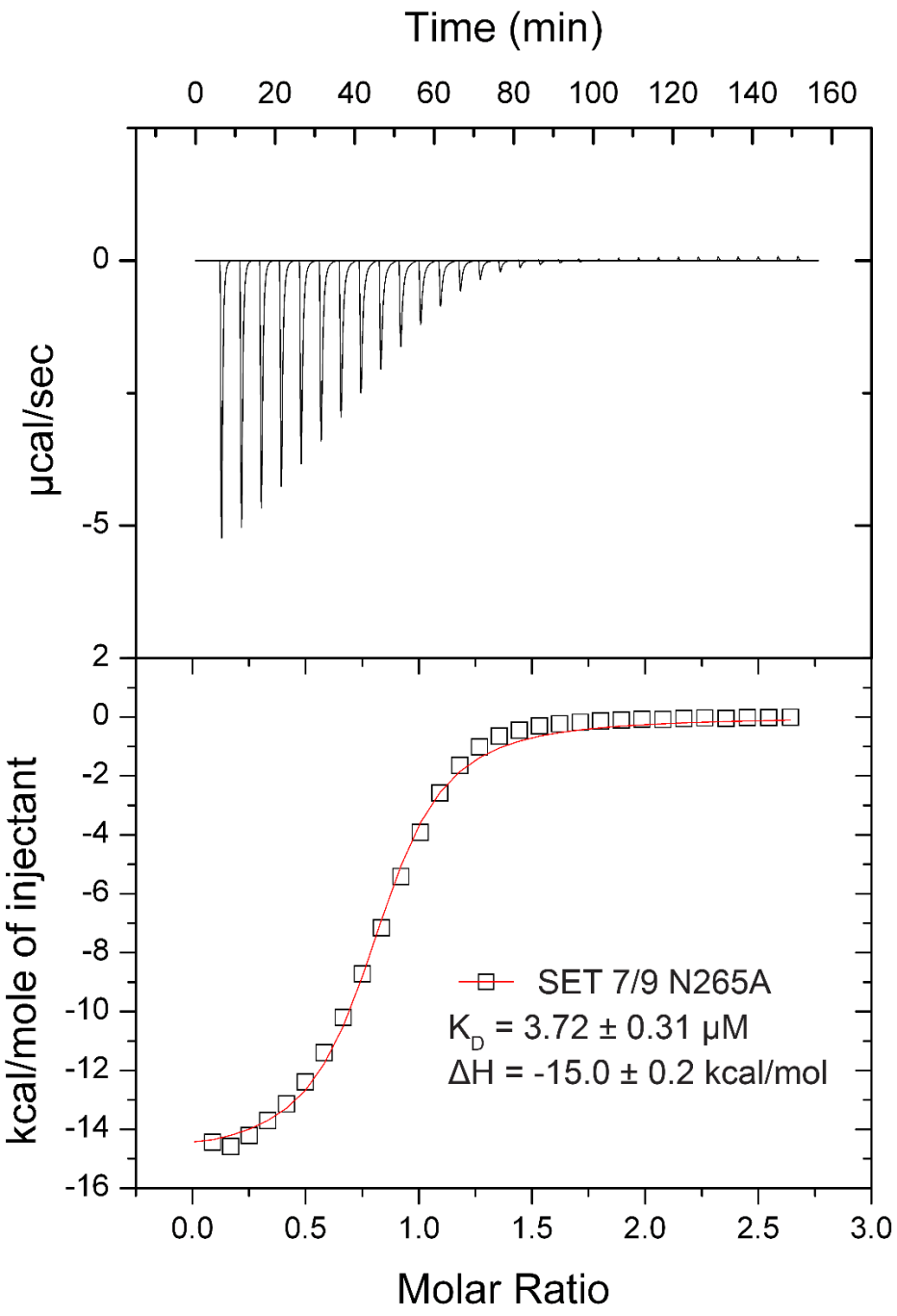

Figure 3.3: Isothermal Titration Calorimetry of SET7/9 N265A with TAF10 peptide

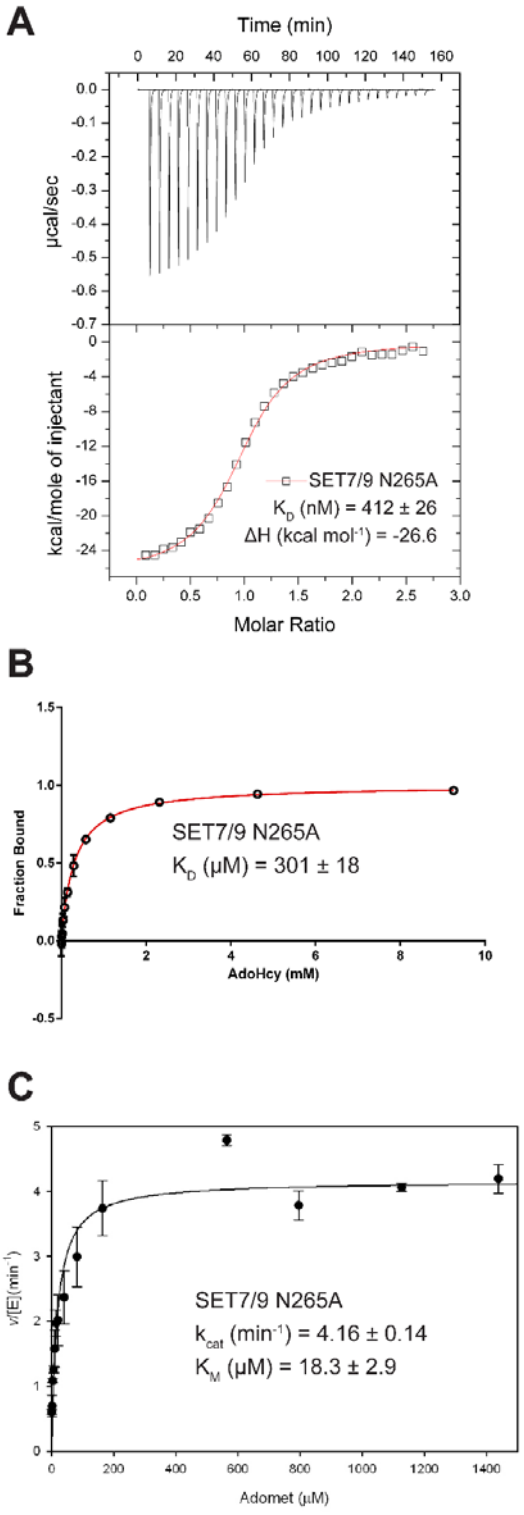

Figure 3.4: Biochemical Characterization of the SET7/9 N265A mutant.

Isothermal Titration Calorimetry of SET7/9 N265A with AdoMet (A). Intrinsic tryptophan fluorescence assay of AdoHcy binding to SET7/9 N265A (B). Radiometric assay of SET7/9 N265A with a fitted Michaelis-Menten curve.

Table 3.2: Biochemical and quantum mechanical values for SET7/9 wild type and N265A.

	K_D (μM)	
	WT	**N265A**
AdoMet	**0.053 ± 0.003**[a]	**0.41 ± 0.03**[d]
AdoHcy	**134 ± 36**[b]	**301 ± 18**[e]
TAF10	**4.9 ± 0.1**[c]	**3.7 ± 0.3**[d]
Sinefungin	**0.33 ± 0.02**[a]	**7.46 ± 0.07**[d]
	Kinetic Parameters	
k_{cat} (min^{-1})	**29.6 ± 0.9**[b]	**4.16 ± 0.14**
AdoMet K_M (μM)	**2.5 ± 0.3**[b]	**18.3 ± 2.9**
k_{cat}/K_M (μM^{-1} min^{-1})	**12 ± 1.5**[b]	**0.227 ± 0.037**
	QM binding energy (kcal mol^{-1})	
Complex energy	**WT**	**N265A**	**ΔE**
$MeS^+(Et)_2$ complex energy	**-56.48**	**-35.43**	**-21.05**
$S(Et)_2$ complex energy	**-19.61**	**-9.72**	**-9.89**
3-NH_3^+-pentane complex energy	**-72.74**	**-45.22**	**-27.52**
3-NH_2-pentane complex energy	**-29.54**	**-15.86**	**-13.68**

Wild type values were reproduced from *a:* Horowitz *et al.*[83] *b:* Horowitz *et al.*[47] and *c:* Del Rizzo *et al.*[146] Binding values were obtained by ITC *(d),* and intrinsic tryptophan fluorescence assay *(e)*. QM binding energies were obtained by subtraction of the energies of the optimized monomers from the complex energy calculated using M06-2X/6-31+G**.

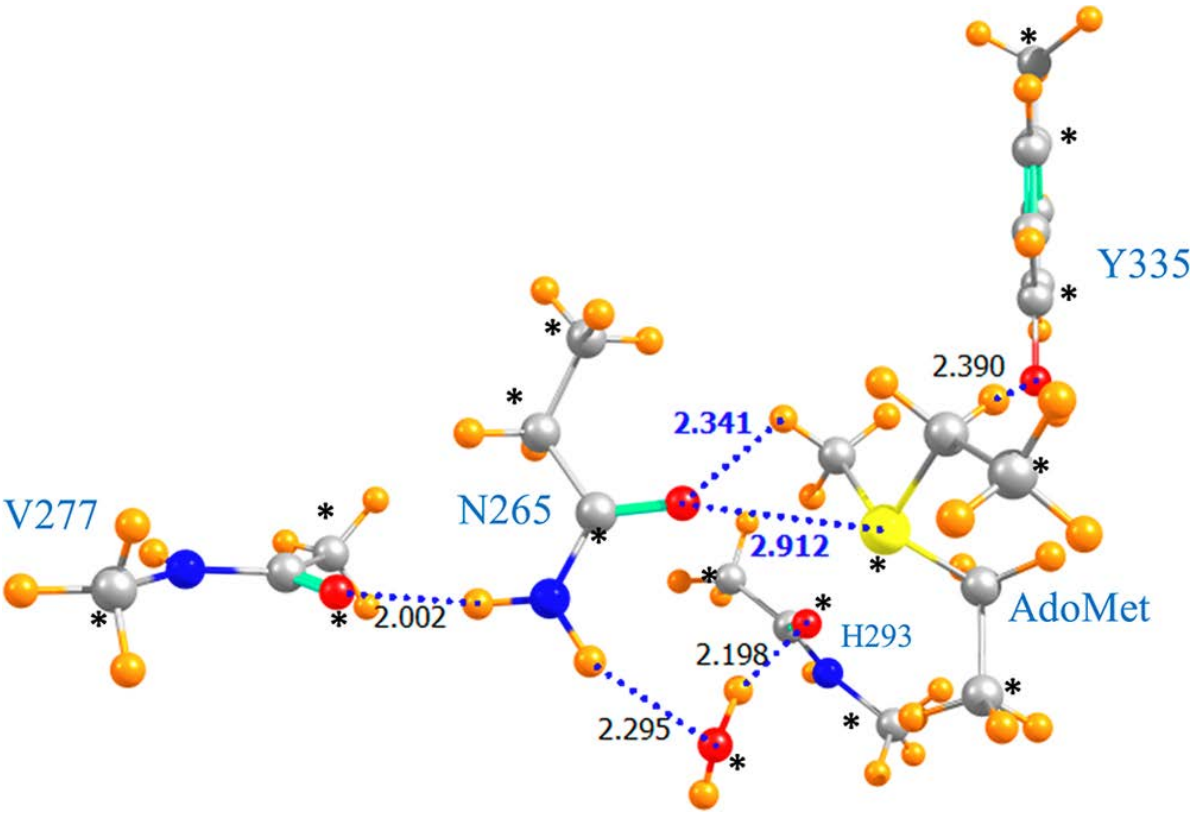

Figure 3.5: Representative system of the quantum mechanical models.

Model representative of AdoMet bound to the wild type SET7/9 active site. Distances and residues are labeled, and frozen atoms are marked with an asterisk.

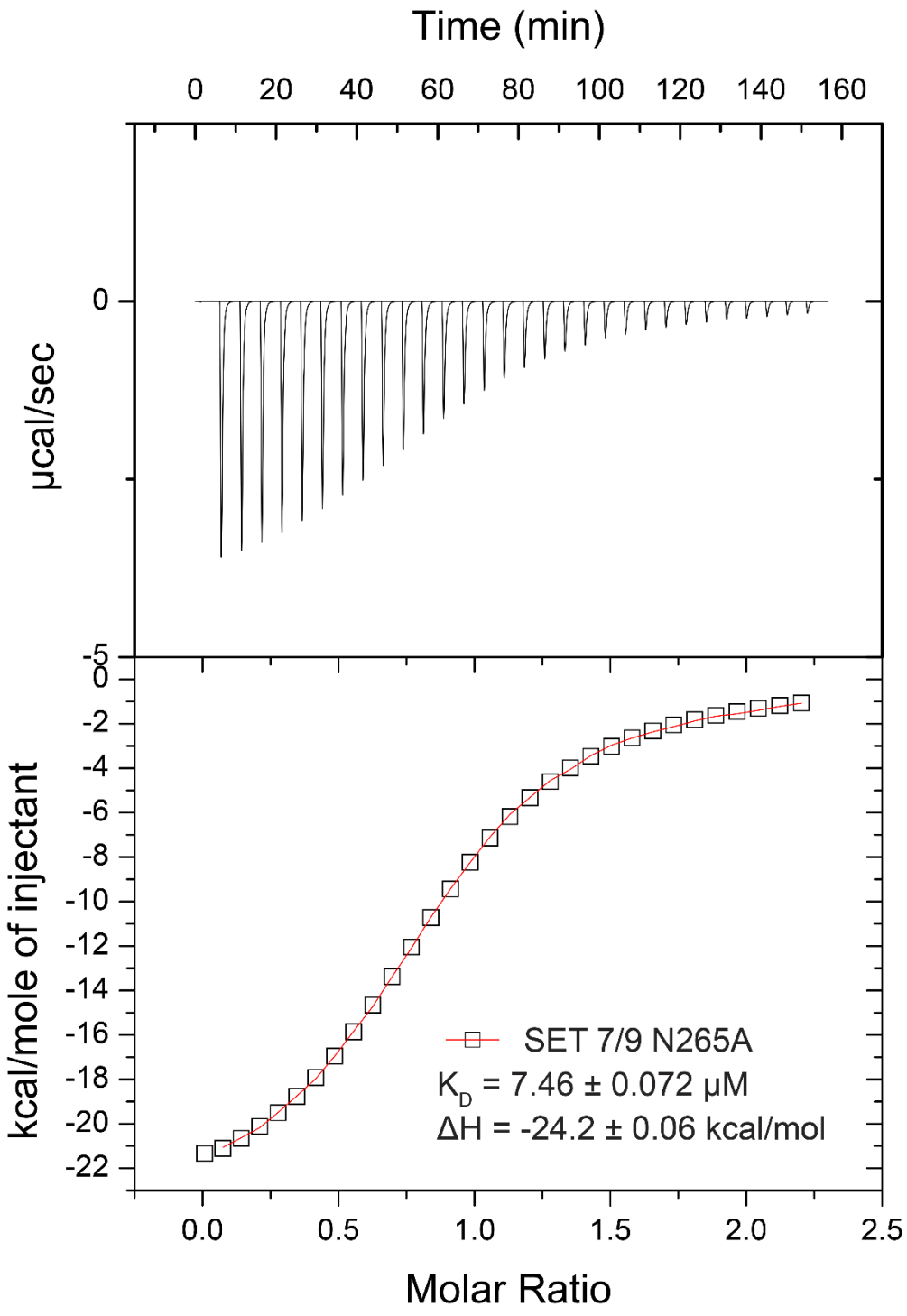

Figure 3.6: Isothermal Titration Calorimetry of SET7/9 N265A with sinefungin

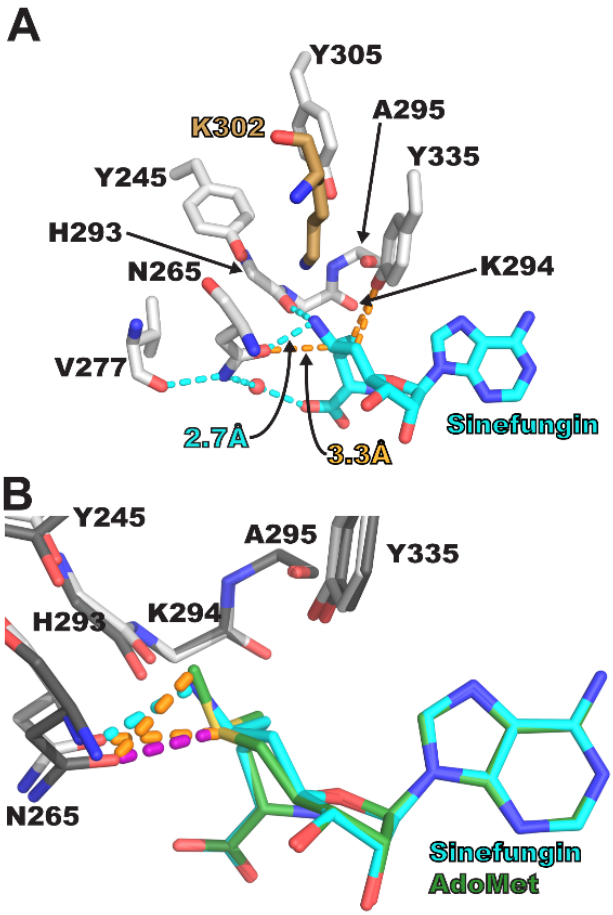

Figure 3.7: Binding of sinefungin to SET7/9.

Key interactions of sinefungin binding to SET7/9 (from 3CBP)[85] shown, with orange dashes for CH•••O hydrogen bonds, and cyan dashes for classical hydrogen bonds (A). Overlay of AdoMet (from 4J83) and sinefungin bound to asparagine 265 (B). Active site residues from the AdoMet structure shown as light gray and the residues from the sinefungin structure shown in dark gray. The chalcogen bond is shown as purple dashes.

The AdoMet analog sinefungin, in which the S^{+}-CH_3 is substituted by CH-NH_3^{+}, (Figure 3.7A) presented the opportunity to study the binding of a ligand without the ability to form a chalcogen bond. The affinity of the mutant for sinefungin was more dramatically affected than that of AdoMet, with a ~23-fold loss in binding relative to sinefungin binding to wild type SET7/9. The explanation for this phenomenon is that

sinefungin binds to the asparagine sidechain with both a CH•••O hydrogen bond and a NH•••O hydrogen bond, thereby replacing the S•••O chalcogen bond and CH•••O hydrogen bond, respectively (Figure 3.7). The crystal structure of SET7/9 bound to sinefungin even shows movement of the asparagine 265 sidechain to better form the NH•••O hydrogen bond to the amine of sinefungin. Quantum mechanical models similar to what had been used for the AdoMet and AdoHcy binding energies were used for the calculation of sinefungin binding energies. Because the protonation state of the amine group of sinefungin was not known, the models included either 3-aminopentane in the amine ($(Et)_2CHNH_2$) or ammonium ($(Et)_2CHNH_3^+$) state. The ammonium model system showed a much greater binding energy (Table 3.2) than did the amine models system, consistent with the effects of charge on hydrogen bonding.[44] The large difference seen in the ammonium system is consistent with the dramatic loss in binding to the mutant. The binding energy of the ammonium system is greater than AdoMet in both the wildtype and mutant models, indicating a possible mix of ammonium and amine states within the active site.

3.4 Discussion

The importance of the S•••O chalcogen bond within the active site of SET7/9 in binding and catalysis leads to the question of the general importance of S•••O chalcogen bonding in methyltransferases. Considering the conservation of CH•••O hydrogen bonding to the AdoMet methyl across methyltransferase classes, examination of the original set of structures used for the survey of AdoMet methyl CH•••O hydrogen bonding was undertaken. Additionally, further structures were surveyed to increase the diversity of classes. The results of this survey (Figure 3.8) indicate that chalcogen

bonding to the AdoMet sulfonium is a much more limited interaction within methyltransferase active sites, with only the Rossmann-like fold, SPOUT, and SET domain classes represented.

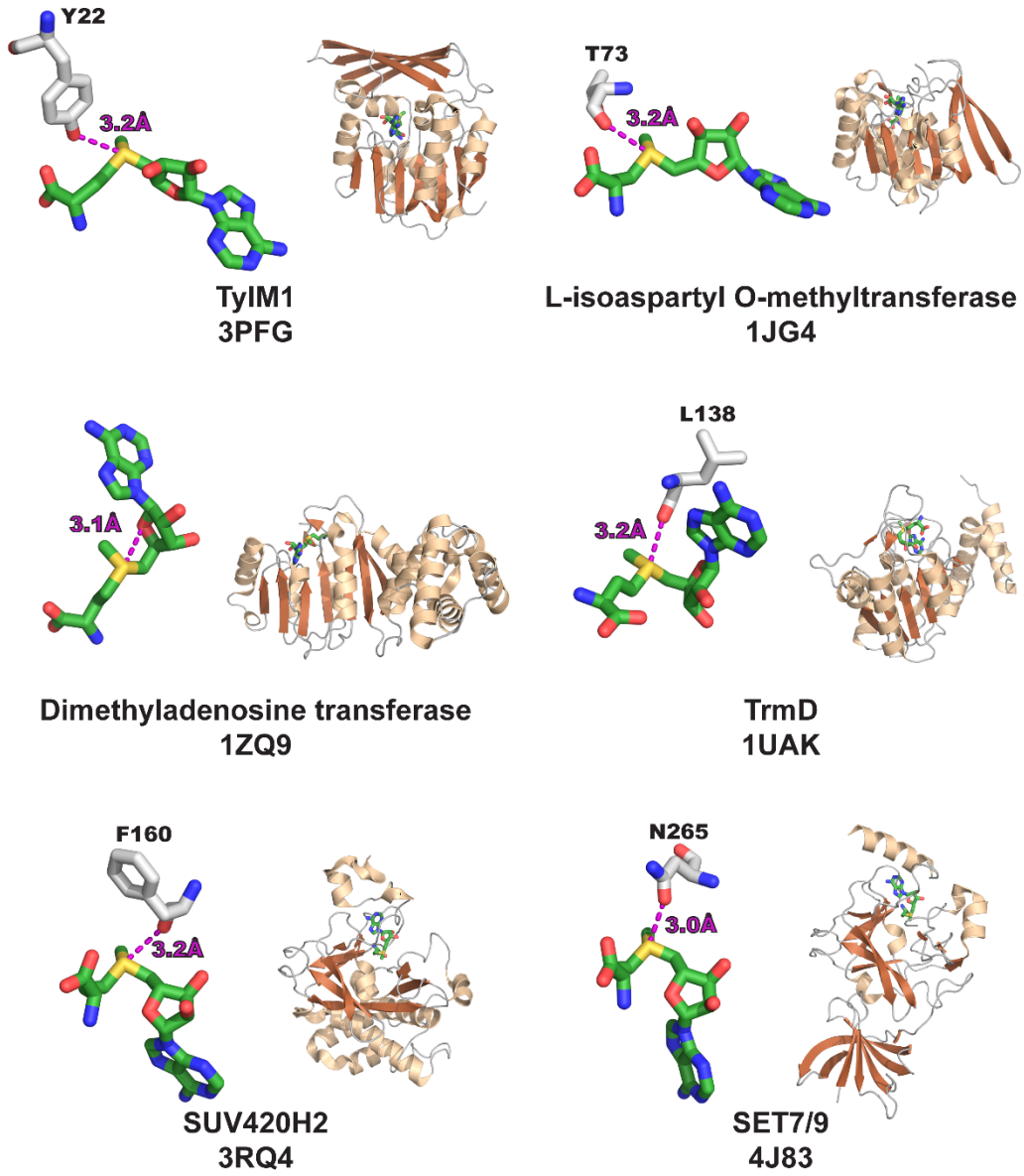

Figure 3.8: Chalcogen bonding in AdoMet-dependent methyltransferases.

Chalcogen bonds shown are < 3.3 Å and > 150°, where the angle is defined as the O•••S-C for the S-C bond anti the σ antibonding orbital. The classes represented above are the Rossmann-like fold (Class I: 3PFG, 1JG4, 1ZQ9), SPOUT (Class IV: 1UAK), and SET domain (Class V: 3RQ4, 4J83).[96, 148-150]

The interaction does not even represent a conserved feature within those classes. Though chalcogen bonding is not a conserved feature, it still has characteristics seen in CH•••O hydrogen bonding that make them important in methyltransferases. Both CH•••O hydrogen bonding and S•••O chalcogen bonding are charge-dependent in the strength of their interaction, favoring the sulfonium of the substrate AdoMet over the thioether of the product AdoHcy. The loss of the chalcogen bond also showed catalytic defects, with the stabilization of the SN_2 reaction by sulfur binding as the possible cause.

The ability of sinefungin to bind to the residue that is responsible for chalcogen bonding represents an opportunity for inhibitors to target such interactions. This is possible even if the inhibitors are lacking an atom to chalcogen bond at that position, as is the case with sinefungin. In this case, the uniqueness of chalcogen bonding presents the opportunity for selectivity in binding a methyltransferase target, as the interaction is only in select methyltransferases and not always in the same position, bonding *anti* to the ribosyl methylene in two of the methyltransferases and *anti* to the methionyl methylene in the four others surveyed.

3.5 Materials and Methods

Protein purification

The N265A SET7/9 expression vector was produced using Quikchange site-directed mutagenesis (Agilent) on the WT SET7/9 110-366 pHIS2 construct.[146, 147] The plasmid was transformed into Rosetta2 (DE3) cells and overexpressed in a manner similar to what has been previously described.[81]

The protein was purified as previously described, with the exception of adding a charcoal treatment post-TEV cleavage to remove AdoMet cofactor instead of using a denaturation and refolding step. The charcoal treatment involved concentrating the protein and adding 5% v/v glycerol, with a final protein concentration of ~5 mg/mL. Activated charcoal (Sigma) was added at a ratio of 1.5 to 2 mg per mg of protein, and the solution was rocked at room temperature for 10-20 minutes. The solution was then centrifuged to pellet the charcoal, the solution was decanted by serological pipette, filtered by 0.45 um PTFE filter, and further concentrated for loading onto the gel filtration column.

For the tryptophan fluorescence studies the protein was purified by refolding as previously described.[83]

Structure refinement

Model building using Coot[143] and refinement using Phenix[144] was continued for the partially refined structure obtained from GMK. Images for structural figures were generated using the PyMOL Molecular Graphics System, Schrödinger, LLC.

Tryptophan fluorescence binding study

The intrinsic tryptophan fluorescence assay makes use of the quenching of an internal tryptophan residue upon AdoHcy binding, as the adenine ring stacks with the tryptophan ring. The enzyme was at 1.75 µM as with previous experiments in the lab.[47] The top concentration of AdoHcy (Sigma) used was 9.26 mM, with ten additional points from 2-fold dilutions of the top concentration and also a zero point. AdoHcy inherent fluorescence was background subtracted by using AdoHcy at the same concentration in

buffer as a reference. The maximal fluorescence value for the tryptophan residue was determined by fitting a gaussian to a fluorescence scan of 320-390 nm with excitation at 280 nm. The maximal values as determined by the gaussian fit were used to fit a hyperbola, from which the K_D was determined. The AdoHcy dilution series with protein was run in triplicate on one plate. The R-squared of the fit was 0.9971. Prism (GraphPad) was used as the fitting software.

QM calculations

Quantum mechanical binding energies were obtained by subtraction of the energies of the optimized monomers from the complex energy calculated using M06-2X/6-31+G**. The counterpoise correction method was used to correct for basis set superposition error. Positions of hydrogen atoms were optimized, while other atoms were either frozen in the crystallographic positions or allowed to optimize, as seen in the minimal model system.[151]

Isothermal titration calorimetry

The AdoMet and TAF10 peptide K_D's were determined using a Microcal VP-ITC (Malvern instruments) with previously described conditions.[146] The AdoMet titration contained 6.66 µM protein in the cell and 84.8 µM AdoMet (Sigma, purified using the Source 15S, see Chapter 2.6 for details) in the syringe. The TAF10 titration was performed as previously described.[146] Curves were fitted using the Origin graphing software provided with the instrument.

Chapter 4:

Functions of CH•••O Hydrogen Bonding in the Rossmann-like fold Methyltransferase TylM1

Robert J. Fick, Brandon McDole, James B. Thoden, Hazel M. Holden, Steve Scheiner, Raymond C. Trievel

4.1 Introduction

TylM1 is a Rossmann-like fold methyltransferase that uses S-adenosyl-L-methionine (AdoMet) to N,N dimethylate a dTDP-loaded deoxyamino sugar.[152] The methylation at this position is the final step in the biosynthesis of mycaminose. Mycaminose is attached to a macrolide core along with another sugar, and the addition of a third sugar attached to different position on the macrolide forms the antibiotic, tylosin.[153] TylM1 also poses as an ideal model system representing the Rossmann-like fold methyltransferases, as the enzyme has been biochemically[153] and structurally characterized,[96] and contains residues within the active site that can be mutated to remove CH•••O hydrogen bonds to AdoMet. The Rossmann-like fold methyltransferases, also called Class I because they were the first methyltransferase

RJF purified the protein and AdoMet, performed the biochemical assays, and refined the structures. RJF and BM crystallized the proteins. JBT and HMH provided the construct, dTDP-phenol inhibitor, and dTDP-Qui*p*3N substrate. SS performed the quantum mechanical calculations.

class to be structurally characterized,[62] remain the largest and most diverse class of methyltransferases.[59, 61] This class has been a particular point of study with respect to the mechanism by which AdoMet-dependent methyltransferases conduct catalysis, specifically in the enzyme catechol O-Methyltransferase (COMT).[4, 99, 100, 111, 114]

The purpose of this study was to examine the effects of carbon-oxygen (CH•••O) hydrogen bonding in the context of a Rossmann-like fold methyltransferase. TylM1 was identified in a survey of high-resolution (<2.0 Å) AdoMet-bound structures in the PDB that examined CH•••O hydrogen bonding to the AdoMet methyl group.[47] This survey found that CH•••O hydrogen bonding was a conserved feature of AdoMet-dependent methyltransferases. The functions of these bonds were explored in the SET domain methyltransferase SET7/9, identifying binding and catalytic defects upon mutation of tyrosine 335, a key CH•••O hydrogen bonding residue to the AdoMet methyl group.[47, 84] The residues that can be mutated in TylM1 expand on these previous studies, as tyrosine 14 CH•••O hydrogen bonds to the AdoMet methyl similar to tyrosine 335 studied in SET7/9, but serine 120 bonds to the AdoMet methylene groups.

4.2 Structural Study

TylM1 wild type and mutant (Y14F, S120A, and Y14F S120A) enzymes were crystallized to determine any structural abnormalities upon mutation of the active site. A noncanonical amino acid, *para*-aminophenylalanine (pAF), was also used, similar to previous studies,[84] yielding the Y14pAF mutant. The substitution of pAF for tyrosine effectively replaces the hydroxyl of the tyrosine side chain with an amine group. The wild type enzyme diffracted to high resolution, 1.05 Å, and was very similar to the previously solved wild type structure, PDB ID: 3PFG, with a RMSD for the aligned Cα

atoms of 0.10 Å. The mutant enzymes were less similar to the wild type structures, crystallizing in different space groups than the previously reported structures, and though they were crystallized in the presence of AdoMet, the product S-adenosylhomocysteine (AdoHcy) was found within the mutant active sites (Table 4.1).[96, 154] The S120A, Y14pAF, and Y14F S120A mutants were collected to 1.3 – 1.4 Å resolution and were in the I222 space group, with the single mutants having a RMSD of 0.15-0.17 Å for the Cα atoms aligned to the double mutant, and an RMSD of 0.085 Å for the Cα atoms aligned between the two single mutants. The Y14F mutation resulted in twinned crystals, with a dataset collected after around 100 crystals had been screened. The Y14F mutant also exhibited the lowest resolution of the TylM1 datasets collected with a resolution of 1.78 Å. There were four nonequivalent monomers within the asymmetric unit which exhibit RMSD's of 0.27-0.46 Å for Cα atoms aligned to one another. Despite the differences between the TylM1 wild type and mutant structures, the active sites were largely similar. There were variations of the position of the phenol group of the dTDP-phenol inhibitor (Figure 4.1), but the AdoMet/AdoHcy and residue 14 superimpose. The histidine 123 shows variation in position in both phenylalanine mutations at the 14 site. This indicates a disruption of binding from the normal pattern within the active site. Histidine 123 has been mutated in previous studies, and both asparagine and alanine mutations at that position show binding and catalytic defects.[96] A Michaelis complex was modeled, using the AdoMet from the wild-type structure of these studies and the nucleophile substrate from 3PFH. The tyrosine at position 14 engages in a hydrogen bond to histidine 123, a CH•••O hydrogen bond to the AdoMet methyl group, and a second classical hydrogen bond to the methyl acceptor substrate

with one of the sugar hydroxyl groups. The importance of tyrosine 14 at this position is seen in the apparent disparity between the calculated binding energies and the biochemical characterizations of these enzymes.

		TylM1 WT• AdoMet• dTDP-phenol	TylM1 Y14F• AdoHcy• dTDP-phenol	TylM1 Y14paF• AdoHcy• dTDP-phenol	TylM1 S120A• AdoHcy• dTDP-phenol	TylM1 Y14F S120A• AdoMet• dTDP-phenol
Data Collection						
Wavelength (Å)		0.97903	0.97903	0.97903	0.97903	0.97903
Space group		C2	$P2_1$	I222	I222	I222
Cell dimensions						
a, *b*, *c* (Å)		88.19 41.53 85.81	73.90 92.35 80.56	64.56 91.57 93.39	64.52 91.27 93.63	64.57 90.89 93.25
α, *β*, *γ* (°)		90 120.08 90	90 106.44 90	90 90 90	90 90 90	90 90 90
Resolution (Å)		30.02-1.05 (1.07-1.05)	35.44-1.78 (1.82-1.78)	34.97-1.40 (1.43-1.40)	32.68 - 1.37 (1.40 - 1.37)	34.9 - 1.33 (1.36 - 1.33)
R_{merge} (%)		6 (n/a)	6.4 (30.9)	3.8 (57.5)	4.9 (42.3)	4.0 (95.8)
$CC_{1/2}$		(0.417)	(0.950)	(0.733)	(0.838)	(0.800)
$\langle I \rangle / \langle \sigma I \rangle$		23.72 (1.05)	44.26 (4.13)	56.87 (1.71)	44.01 (2.12)	63.94 (2.50)
Completeness		99.9 (99.7)	97.5 (80.7)	98.1 (76.0)	97.9 (77.3)	96.9 (94.8)
Redundancy		4.7 (3.0)	7.0 (4.6)	13.1 (3.4)	12.6 (3.2)	14.9 (13.2)
Refinement						
Resolution		1.05	1.78	1.40	1.37	1.33
No. of Reflections		125133	96411	53914	57235	61443
R_{work}/R_{free}		0.15/0.16	0.18/0.21	0.15/0.17	0.15/0.18	0.16/0.19
No. of Atoms		2265	8181	2125	2117	2100
Protein		1852	7167	1806	1835	1831
Ligand/ion		58	228	57	57	57
Water		351	786	260	224	212
B-factors		22.06	28.31	24.1	20.99	23.26
Protein		18.99	27.34	21.84	19.62	22.18
Ligand/ion		13.67	30.16	28.49	19.51	19.96
Water		39.68	36.62	38.64	32.62	33.5
R.M.S. Deviations						
Bond lengths (Å)		0.005	0.007	0.014	0.015	0.012
Bond angles (°)		1.2	1.15	1.49	1.61	1.47
Ramachandran						
Favored (%)		99.16	99.05	98.71	98.31	98.72
Allowed (%)		0.84	0.84	1.29	1.69	1.28
Outliers (%)		0	0.11	0	0	0

Table 4.1: Crystallographic and refinement statistics of TylM1 WT and mutants.

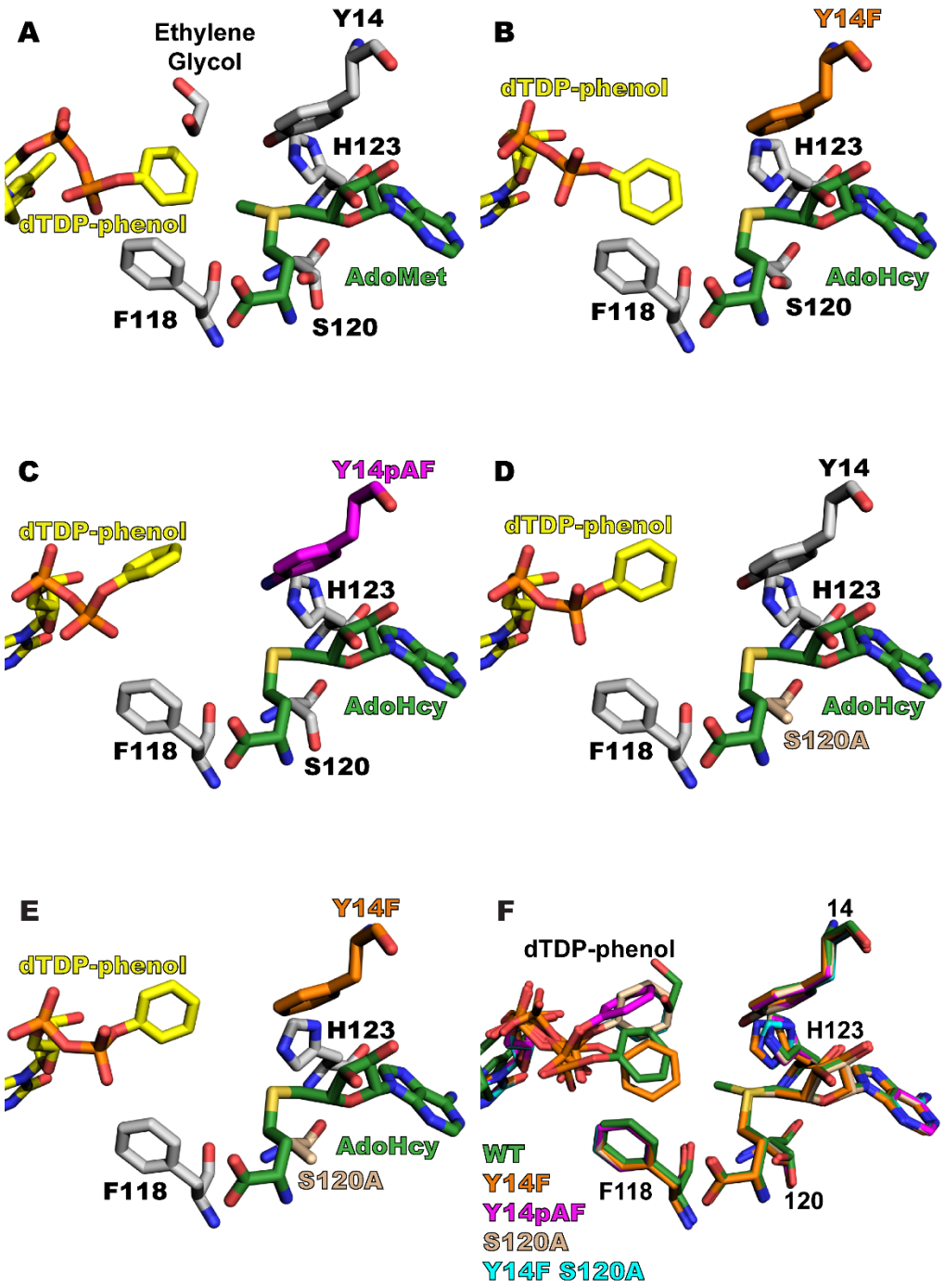

Figure 4.1: TylM1 wild-type and mutant active sites.

TylM1 wild-type (A), Y14F (B), Y14pAF (C), S120A (D), and Y14F S120A double mutant (E) shown. The relative positions of the active site residues and ligands shown from the superimposition of the Cα atoms of the protein chains (F).

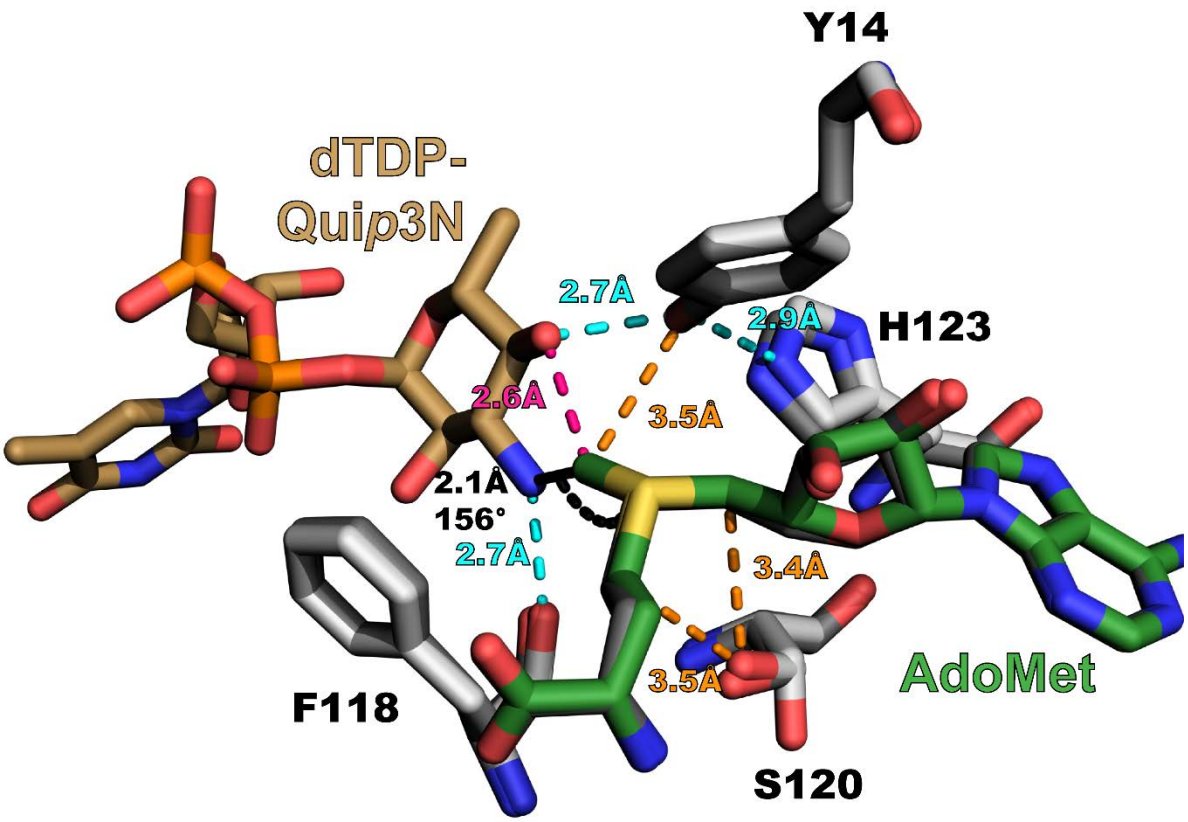

Figure 4.2: Modeled Michaelis complex of TylM1.

The wild-type structure modeled in complex with the substrate dTDP-Qui*p*3N (PDB ID: 3PFH) by alignment of the Cα atoms of both structures. Active site residues and AdoHcy from 3PFH shown in dark gray, indicating the good alignment within the active site. Select classical hydrogen bonds shown as cyan dashes, CH•••O hydrogen bonds formed by tyrosine 14 and serine 120 shown as orange dashes, alignment of the AdoMet methyl with the nitrogen nucleophile shown in black, and a possible clash within the model shown in hot pink. The possible clash, coupled with the somewhat acute angle for the reaction indicate that there may be some rearrangement upon binding of both substrates.

4.3 Quantum Mechanical Study

Quantum mechanical studies of minimal models (see Figure 4.3 for an example) were undertaken to determine the relative energy perturbations in active sites corresponding to the mutations made. Binding could not be characterized by isothermal titration calorimetry, so the binding energies of modeled active sites were used to access disruption caused by specific mutations. The position of protonation of histidine 123 could not be determined, and thus was modeled in both positions. The serine 120 to alanine mutation shows a loss of binding energy to AdoMet greater than that to AdoHcy; therefore, this results in a smaller difference of energy between the two complexes and a theoretical loss of the ability to discriminate substrate from product. This is evidence that the two CH•••O hydrogen bonds that serine 120 can form with the AdoMet methylenes (see Figure 4.2) can aid in enzyme selectivity toward its substrate. The Y14F loses binding energy about equally for AdoMet and AdoHcy when Nε2 is protonated leaving the difference in energy between the two complexes about the same. When Nδ1 is protonated, there is a much larger loss in binding energy for both ligands, but this position still has a greater energy difference between the ligands, indicating the tyrosine 14 is less discriminating in ligand preference than the serine 120. The Y14pAF shows the least defective binding energies of the mutants, with the possible compensation for loss of the CH•••O bond by the formation of the similar CH•••N hydrogen bond, which has been previously observed in calculations using this amino acid.[84] The Y14F S120A double mutant has the largest disruption of binding energy to both ligands, with the loss in binding energy similar to the combined loss in energies of the independent single mutations.

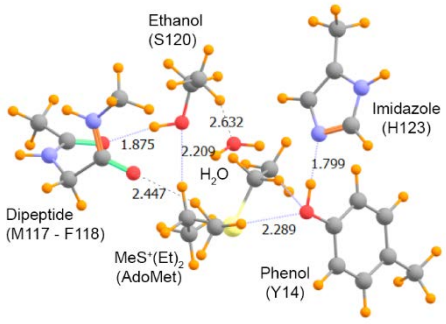

Figure 4.3: Optimized geometry of a representative TylM1 minimal active site.

Active site residues modeled as minimal functional groups to probe binding energies of AdoMet-like or AdoHcy-like molecules. In this model the Nδ1 of histidine 123 is modeled as protonated.

	H123 Nε2 protonated			H123 Nδ1 protonated		
TylM1 Complex	$MeS^+(Et)_2$	$S(Et)_2$	$[MeS^+(Et)2 - S(Et)2]$	$MeS^+(Et)_2$	$S(Et)_2$	$[MeS^+(Et)2 - S(Et)2]$
WT	-51.69	-25.56	-26.13	-65.49	-27.27	-38.22
S120A	-42.41	-21.53	-20.88	-56.74	-23.45	-33.29
Y14F	-46.74	-21.09	-25.65	-56.04	-21.74	-34.3
Y14paF	-50.81	-24.23	-26.58	-62.2	-24.94	-37.26
Y14F/S120A	-37.34	-16.12	-21.22	-46.83	-17.39	-29.44

Table 4.2: Quantum mechanical binding energies of TylM1 model complexes

4.4 Biochemical Study

To study the effects of CH•••O hydrogen bonding on catalysis in a class I methyltransferase, a continuous, coupled fluorescent assay was used. Saturating levels of the dTDP-Qui*p*3N substrate were used and k_{cat} and the K_M for AdoMet were determined. The wild type TylM1 enzyme had a k_{cat} value of 4.74 min^{-1} at pH 7.5, and a K_M of 27.3 μM for AdoMet. The catalytic value is slightly slower at pH 7.5 than the observed value of ~10 min^{-1} at pH 8.0,[96] as the more basic pH should increase the deprotonation of the amine nucleophile. The serine 120 to alanine mutation showed roughly a two-fold loss in both k_{cat} and K_M, with values of 2.9 min^{-1} and 59.3 μM. Both

the Y14F single mutant and Y14F S120A double mutant appeared catalytically inactive when used at the concentration and time of reaction for the WT and S120A enzymes (Figure 4.4). Though the binding energy loss in the computation study of minimal active sites showed little loss of energy upon mutation of tyrosine 14 to phenylalanine, the complete loss of catalytic activity in both of the enzymes containing the mutation at this site seems to indicate that the loss of binding both substrates in a coordinated manner may disrupt formation of a catalytically productive complex.

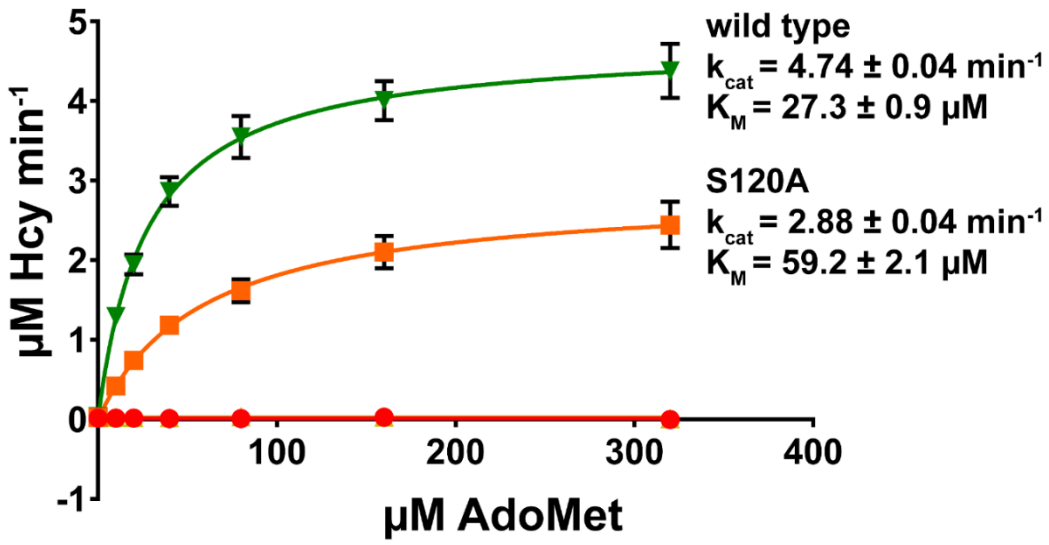

Figure 4.4: Biochemical characterization of TylM1 wild type and mutant enzymes.

Wild type TylM1 (green) and S120A (orange) show activity by the continuous assay, with fit parameters labeled to the right of the curves. The error on the values is the standard error. The Y14F and Y14F S120A mutants are not labeled but are shown in yellow and red along the baseline.

4.5 Discussion

TylM1 is a Rossmann-like fold methyltransferase, and the ease of crystallization and use in steady state assays make it an optimal enzyme to determine the effects of CH•••O hydrogen bonding in this class of methyltransferases. The serine 120 to alanine mutation shows subtle defects in AdoMet affinity and catalysis. This demonstrates the ability of methylene CH•••O interactions to influence the S_N2 reaction. The ability to kinetically characterize the effects of phenylalanine mutations at residue 14 within TylM1 was precluded by the lack of catalytic activity, possibly owing to a lack of alignment of AdoMet with the second substrate dTDP-Qui*p*3N, which also hydrogen bonds to this residue. Though the alignment of the AdoMet methyl axis and nitrogen nucleophile could be closer to 180° in the modeled Michaelis complex, indicating some active site rearrangement may be necessary, the loss of the bifurcated interaction seen with the tyrosine 14 hydroxyl group may allow more conformational freedom for the sugar moiety, similar to the positional freedom seen with the phenol ring of the inhibitor. The coupled assay will be used to determine the kinetic parameters of the Y14pAF mutant, which may restore the ability to hydrogen bond with dTDP-Qui*p*3N, but the analysis will be complicated by the ability to form CH•••N hydrogen bonds, as seen in the minimal perturbation of binding energy in the quantum mechanical calculations. Further QM calculations will be used to probe the energies of the methyl transfer reaction with model systems in the presence and absence of the tyrosine 14 sidechain, exploring whether the catalytic defect is caused by mis-alignment or a raising of the S_N2 energetic barrier.

4.6 Materials and Methods

Purification of AdoMet by CM-Sepharose Fast flow

To obtain pure AdoMet for use in kinetic assays, a lower acid protocol than the Source 15S purification (chapter 2.6) was used. This method allows the pure AdoMet to be used as a solution that consists of pooled AdoMet-containing fractions at a pH much closer to neutral than would result from the 1.0 M hydrochloric acid used in the elution gradient for the Source 15S, which is dried after pooling fractions to remove most of the hydrochloric acid, though is still highly acidic upon resolvating the dried AdoMet. A 10/30 Tricorn column was packed with CM Sepharose fast flow resin (GE Healthcare), using a carboxymethyl functionalized weak cation exchange resin in an automated update of Chirpich.[155] The column was equilibrated at a flow rate of ~2 mL/min with 900 mL of 50 mM sodium acetate buffer, pH 5.0, then 800 mL of 5 mM sodium acetate buffer, pH 5.0. The higher concentration buffer equilibrates the resin in a lesser volume, while the second buffer is the lower ionic strength that the original method used. 50 mg of AdoMet chloride dihydrochloride salt (A7007, Sigma) is dissolved in ~2.2 mL of the 5 mM sodium acetate buffer and loaded into a 2 mL loop. The AdoMet was run over the column using the 5 mM sodium acetate and washed for 1.5 column volumes and continued washing until the A255 returned to 25 mAU at around 3 CV. The AdoMet was then eluted by a step elution using 27.5mM hydrochloric acid, with fractions of 4 mL collected when the A255 was over 50 mAU. The AdoMet containing fractions were pooled and stored in at -20C until use, with the solution at pH 5 or slightly lower, as measured by pH paper, not requiring neutralization upon dilution into assay buffer as the ~pH 1 dried and dissolved AdoMet from Source 15S purification.

Purification of TylM1

The TylM1 pET31 expression vector was used as supplied by the Holden laboratory, yielding a construct with an uncleavable C-terminal His-tag.[96] For the extended expression necessary to produce fully deuterated protein in minimal media for neutron crystallography trials, the gene encoding the enzyme was moved to pET 24b using NdeI and XhoI, yielding the exact same construct within kanamycin resistant vector. This expression vector was also used to produce wild type, non-deuterated protein. The tyrosine 14 to phenylalanine, serine 120 to alanine and the Y14F S120A double mutant were introduced using Quikchange mutagenesis (Agilent). The tyrosine 14 to para-aminophenylalanine mutant utilized Quikchange mutagenesis to introduce the amber (UAG) stop codon at that position, making use of an amber stop codon suppression system used previously to introduce the unnatural amino acid, but incorporated into the pDULE2 plasmid.[84, 156] The natural proteins were all over expressed with chloramphenicol (50 µg/mL) and either ampicillin (100 µg/mL, for pET31 vectors) or kanamycin (100 µg/mL, for pET24 vectors) in 2XYT media and induced at ~0.6-1.0 OD600 with 250 µM IPTG and grown overnight at 18°C. The protein incorporating the unnatural amino acid was overexpressed utilizing the pDULE2 pAF stop codon suppression system in BL21-AI cells with ampicillin (100 µg/mL) and spectinomycin (100 µg/mL), with induction at 18°C including 250uM IPTG, 0.2% arabinose, and 1 mM of the unnatural amino acid para-aminophenylalanine. All cultures were spun down at 3800 rpm (H600A rotor) for 30 minutes, and cell pellets were resuspended in 50 mM sodium phosphate, pH 7.5, 500 mM sodium chloride. Resuspension was pooled and

aliquoted into 50 mL falcon tubes in aliquots containing roughly 1 L of cell culture and placed in the -80°C for storage.

Protein was purified by thawing the resuspended cell pellet and lysing by rocking at 4°C with lysozyme and HALT protease inhibitor cocktail (Roche). The resuspension was brought up to 60-70 mL of total volume with Buffer A (50 mM sodium phosphate, pH 7.5, 500 mM sodium chloride) before sonicating in a metal beaker 3-4 times for 1 minute at ~90 W of power, allowing at least 30 seconds between sonicating to allow cooling. Lysate was centrifuged at 18,000 rpm (in a SS34 rotor), and decantate was filtered with 0.45 μm SFCA filters before loading onto the chromatography system. The filtered decantate was loaded onto a 4 mL TALON (Clontech) column that had been pre-equilibrated in Buffer A. The column was then washed with 5 column volumes of Buffer A before a 15 column volume gradient elution from Buffer A to Buffer B (50 mM sodium phosphate, pH 7.5, 500 mM sodium chloride, 300 mM imidazole). The TylM1 containing fractions were concentrated and loaded onto gel filtration on a HiLoad 16/60 Superdex S200 column (GE Healthcare). The buffer used for gel filtration was either 20 mM sodium phosphate, pH 7-8, with 100 mM sodium chloride, or 20 mM sodium malonate, pH 7-7.6, with 100 mM sodium chloride for protein used in crystallization trials, while 20 mM Hepes, pH 7.5, with 100 mM sodium chloride was used for protein used in biochemical assays.

Crystallization

WT TylM1 was crystallized in 20% w/v PEG 5000 MME, 150 mM sodium malonate, pH 7.0, 1% v/v isopropanol, and 12 mM barium chloride. The protein solution contained 18 mg/mL TylM1, 5 mM AdoMet, and 5 mM dTDP-phenol, with the hanging drop set at 2:2

µL protein solution to well solution. Crystal was cryoprotected in 10% v/v ethylene glycol, 28% w/v PEG 5000 MME, 100 mM sodium chloride, 5 mM AdoMet, and 5 mM dTDP-phenol before flash freezing in liquid nitrogen.

Mutant TylM1 enzymes were crystallized in 23-27% w/v PEG 3350, 100 mM Hepes, pH 7.3-7.7, 4.5-5.6 mM trimethylamine hydrochloride, 20 mM sodium malonate, and 1-1.25% isopropanol v/v. Hanging drops were 4:2 µL protein:precipitant for the Y14F, S120A, and Y14F S120A mutants and 2:2 µL for Y14pAF. The protein solutions all contained 5.0 mM AdoMet and 5.0 mM dTDP-phenol, with the protein concentrations for S120A and Y14F S120A at 18 mg/mL, Y14pAF at 12 mg/mL, and Y14F at 9 mg/mL. Crystals were cryoprotected using 10% v/v ethylene glycol in solutions similar to the precipitant used, and flash frozen in liquid nitrogen.

Data were collected on LS-CAT beamlines at the Advanced Photon Source at Argonne National Laboratory. HKL2000 was used to process and scale the data sets.[141] Molecular replacement was performed using Phaser[142], using the WT TylM1•AdoMet•dTDP-phenol complex (3PFG)[96] converted to poly-alanine and with ligands and waters removed as the search model for the wild type, Y14F and Y14F S120A structures, and a partially refined WT structure with ligands and waters removed and the mutation site modeled as an alanine for the search model for the Y14pAF and S120A structures. Coot[143] was used for model building, and Phenix[144] was used for refinement. Images for structural figures were generated using the PyMOL Molecular Graphics System, Schrödinger, LLC.

QM calculations

Quantum mechanical binding energies were obtained by subtraction of the energies of the optimized monomers from the complex energy calculated using M06-2X/6-31+G**. The counterpoise correction method was used to correct for basis set superposition error. Positions of hydrogen atoms were optimized, while other atoms were frozen in their crystallographic positions.

Biochemical Assays

A continuous, coupled fluorescent assay was developed based on a previous method for a quenched coupled fluorescent assay, in which the product of methyl transfer S-adenosyl-L-homocysteine (AdoHcy or SAH) is hydrolyzed to produce adenosine and homocysteine.[157] The homocysteine then reacts with a thiol-reactive dye, producing a fluorescent readout of methyltransferase activity. The SAH Hydrolase (SAHH) construct used previously was also used in this assay, with overexpression in 2XYT with the addition of 100 µM IPTG at an OD600 of ~1 and grown at 37°C for 3 hours. The cultures were pelleted, and the pellets resuspended in 10 mL of the hydrolase was lysed by rocking with lysozyme and HALT protease inhibitor cocktail (Roche) for at least 1 hour, brought up to 60 mL with hydrolase Buffer A (50 mM sodium phosphate, pH 7.5, 500 mM sodium chloride, with 10% v/v glycerol) and sonicated 3 times for 1 minute at ~90 W, with at least 30 seconds between for cooling. Lysate was centrifuged at 18,000 rpm (SS34 rotor) for 30 minutes, and decantate was filtered with 0.45 µm SFCA filters before loading onto the chromatography system. The filtered decantate was loaded onto a 4 mL TALON column (Clontech), washed with 5 column volumes of hydrolase Buffer A, and eluted with a 15 column volume gradient to

hydrolase Buffer B (50 mM sodium phosphate, pH 7.5, 500 mM sodium chloride, 300 mM imidazole, with 10% v/v glycerol). Protein containing fractions were pooled in 10 kDa dialysis tubing and cleaved with ~1.2 mg TEV protease overnight in 2 L of 20 mM sodium phosphate, pH 8.0, 35 mM sodium chloride, and 5 mM beta-mercaptoethanol. Cleavage solution was passed over a small TALON column (~1.5 mL, Clontech) to remove uncleaved protein and TEV protease before concentrating to load onto gel filtration on a HiLoad 16/60 Superdex S200 column (GE Healthcare). The gel filtration buffer used was 20 mM Hepes, pH 7.5, 100 mM sodium chloride. Protein containing fractions were pooled, aliquoted, and flash frozen in liquid nitrogen before storage in the -80°C freezer.

ThioGlo (HC 9080, Berry and Associates) was used as the thiol-reactive dye over CME (HC 9097, Berry and Associates) even though CME has a greater fluorescent yield as CME exhibited an increasing background signal with time that was also dependent on AdoMet concentration. The assay was performed in 100 mM Hepes (neutralized with sodium hydroxide), pH 7.5 as the buffer in black ProxiPlate-384 F Plus plates (PerkinElmer) with a final volume of 16 µL per well. The calibration curve was 0-10 µM L-homocysteine (69453, Sigma-Aldrich) with SAHH present at the concentration used in the enzyme mix. Before initiation, the 384-well plate with 8 µL per well of either 2X calibration curve or 2X enzyme mix was incubated at 37°C for at least 5 minutes, with the 2X AdoMet and ThioGlo solutions incubated in tubes. The assay was initiated with the addition of 8 µL of the AdoMet and ThioGlo solution by multichannel pipette, with ThioGlo at a final concentration of 25 µM. The pipette was a single-dispensing 20 µL multichannel, with a slight mixing performed by pipetting up and down the combined

well solution upon addition. Fresh tips were used for every dispensing. The coupling enzyme, SAHH, was verified to not be rate limiting when used at 5 µM. Enzyme linearity was checked between 0 and 100 nM and points of 60, 80, and 100 nM showed good linearity (see Figure 4.5). Each point was run in quadruplicate, and the fluorescence was read on a Pherastar plate reader (BMG Labtech) using a 390 nm filter for excitation and a 505 nm filter for emission.

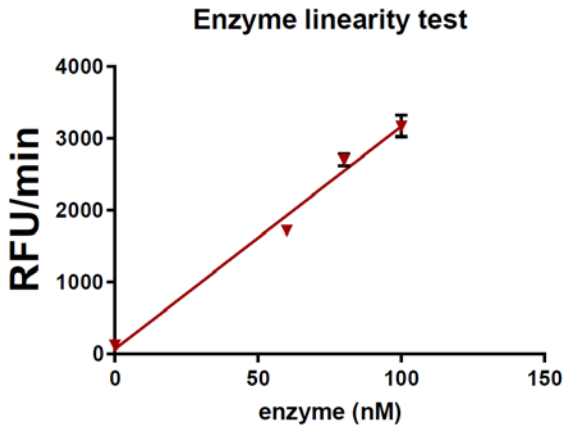

Figure 4.5: Linearity of methyltransferase active as a function of WT TylM1 concentration.

TylM1 was used at 70 nM in further assays. The K_M of dTDP-Qui*p*3N was determined with wild type TylM1 and 1 mM AdoMet (Figure 4.6), and greater than 6-fold K_M (150 µM) was used in the determination of the K_M of AdoMet and the k_{cat} value. Data was converted to concentration homocysteine produced using the initial slope and background of the calibration curve. Fluorescence was read every 45 seconds, and datapoints for 5.25 minutes were used to obtain the rate of homocysteine production, which was used to generate the points for the Michaelis-Menten curve to determine the K_M of AdoMet and the k_{cat} value for all enzymes. Prism software (Graphpad) was used to obtain all fits.

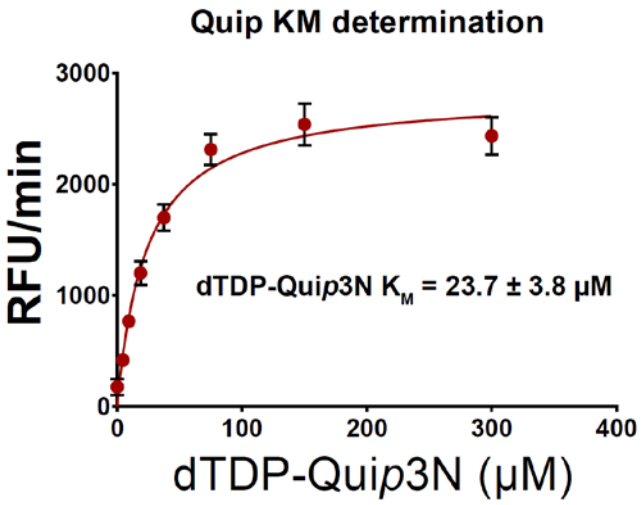

Figure 4.6: K_M determination of dTDP-Qui*p*3N with wild type TylM1.

Chapter 5:

Conclusions and Future Directions

5.1 Conclusions

Carbon-oxygen hydrogen (CH•••O) bonds and sulfur-oxygen (S•••O) chalcogen bonds to the S-adenosyl-L-methionine (AdoMet) sulfonium have been shown by these studies to be important features in binding and catalysis by AdoMet-dependent methyltransferases. These studies expand on previous work to show the importance of CH•••O hydrogen bonding to the methylene groups of AdoMet, which are also positioned proximal to the positively charged sulfur atom, similar to the methyl group. These positions are also able to engage in strong CH•••O hydrogen bonds, as the charge of the system has an influence on all three carbons connected to the sulfur.[44] The slight catalytic defects seen within TylM1 indicate that they may help align the S_N2 reaction in some methyltransferases.

The ability of waters to engage in CH•••O hydrogen bonding had been demonstrated in a study of neutron structures, in which the hydrogen positions are experimentally determined.[33] CH•••O hydrogen bonding to MetH showed the ability of waters to engage in CH•••O hydrogen bonds with strong implications for binding AdoMet by this enzyme. MetH seemed to show no CH•••O hydrogen bonding to the protein, making it an outlier of the previous survey of AdoMet-bound methyltransferases.[47] The active site of MetH is largely solvent exposed, and may

require some conformational changes to allow the methyl group to be transferred to the cobalamin cofactor.[158, 159] This necessity to interface with a planar nucleophile dictates that the active site must be more open, making waters ideal, as they can rearrange more readily than sidechains, which are limited by the polypeptide. In this type of CH•••O hydrogen bond, there are still key protein sidechains, glutamates in the case of MetH, that act to polarize the waters and potentiate the interaction. In this sense, the glutamates may be thought of as facilitating these CH•••O hydrogen bonds as second shell interaction (*i.e.* not directly bonding), as the removal of the charge at those positions by mutation to glutamines greatly disrupts AdoMet binding, consistent with the removal of bonding seen in the study of other methyltransferases in this dissertation.

Chalcogen bonding was found to play an important role in SET7/9, yet these interactions are not conserved across all AdoMet-dependent methyltransferases. This presents the opportunity for further study as to the differences between methyltransferases in which chalcogen bonds are present or absent. Study of a tyrosine within the glycine N-methyltransferase active site, which forms a chalcogen bond between the side chain hydroxyl group and the sulfur atom of AdoMet, also showed disruption of binding and catalysis upon mutation.[110] This suggests an important role for chalcogen bonding in methyltransferases when this interaction is present.

5.2 Future Directions

TylM1, with high resolution crystal structures already solved by X-ray diffraction (Figure 5.1A), presents a unique opportunity to experimentally determine the methyl rotamer position, and therefore the geometries of the hydrogen bonds formed. To make use of the high resolution data already obtained, the Trievel laboratory has entered into

collaboration with the laboratory of Dr. Ho Leung Ng at Kansas State University. Dr. Ng is developing the HyPO method (Hydrogen atom Prediction and Observation). The method makes use of low level electron density within the maps, using three-fold averaging around the methyl group axis to determine the most probable position of the hydrogens in rotation. As the method is developed, there is hope that it can be applied to medium resolution electron density maps, allowing better determination of CH•••O distances and interaction angles through experimental placement of hydrogen positions within methyltransferase active sites, rather than the current inference based on C•••O distance.

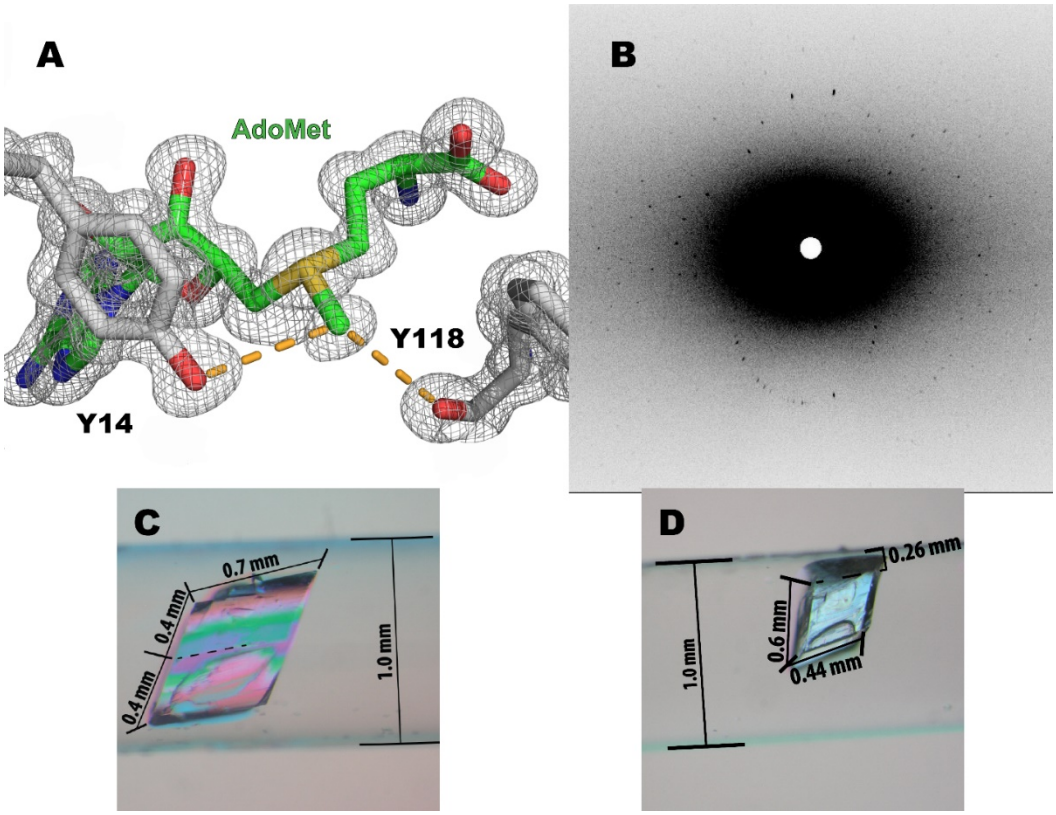

Figure 5.1: Structural determination of hydrogen positions in TylM1.

Rendering of $2F_O$-F_C density for AdoMet, tyrosine 14, and phenylalanine 118, with the map contoured at 1.5 sigma (A). A 1 hour test diffraction (B) on the IMAGINE detector at Oak Ridge National Laboratory of a hydrogenated TylM1 crystal (C) mounted in a 1mm quartz capillary tube. A perdeuterated crystal of TylM1 (D), showing the smaller size and poorer morphology.

Another method for the structural determination of hydrogens in TylM1 is the use of neutron crystallography. Neutron crystallography has been very important in the study of CH•••O hydrogen bonding,[32, 33] as neutrons readily diffract off hydrogen atoms, yielding experimental information on the atomic positions. Crystal trials with TylM1 hydrogenated protein was able to produce very large crystals, which were back-soaked into perdeuterated precipitant solution and diffracted to about 6 Å in an initial test shot (Figure 5.1B,C). To decrease the incoherent scatter from ^{1}H, and therefore background noise in the diffraction patterns, perdeuterated protein was overexpressed at Oak Ridge National Laboratory using a fermenter to get maximal growth out of a minimal media system utilizing feeding of perdeuterated glycerol. The perdeuterated protein was purified in hydrogenated buffers before exchange upon the final concentration of the protein before aliquoting and flash freezing. Initial crystal trials yielded large crystals, though the morphology was not as good as the hydrogenated protein (Figure 5.1D). The use of neutron crystallography represents a continuing point of the TylM1 work presented in this dissertation.

Catechol O-Methyltransferase could act as a model system to explore many interactions important in methyltransferases and continue the work of this dissertation. Catechol O-Methyltransferase has acted as the foremost methyltransferase in which the origin of catalytic rate enhancement has been debated.[100, 114] There have been multiple structures deposited in the Protein Data Bank,[63, 160] allowing use of crystallographic coordinates for the creation of minimal model systems to be used in computational studies. There are active site CH•••O hydrogen bonds (Figure 5.2), though they do not represent sites accessible to bond disruption by removal of the oxygen acceptor through

mutation, as two of the hydrogen bond acceptors are backbone carbonyls, and the third is a nitro group on the inhibitor, important in the inhibitor structure. Further study of chalcogen bonding in COMT presents a great opportunity. The active site of COMT has a sulfur-sulfur chalcogen bond, in which the sulfur of a methionine sidechain is *anti* the methionyl methylene, acting as the electron donor, and is 0.3 Å shorter than the van der Waals distance for such an interaction. Mutation to canonical amino acids such as alanine, leucine, or isoleucine could be used to disrupt this interaction, though may not represent ideal substitutions due to the much smaller size of the side chain or the introduction of branching. Introduction of the noncanonical amino acid norleucine (Nle), which is an isostere of methionine in which the sulfur is replaced by a methylene carbon, could be used to form a less disruptive mutation of the COMT active site, with the use of a methionine or leucine auxotroph to introduce the noncanonical amino acid at that position.[161] Exploration of the Met40Nle could further establish chalcogen bonding as an important interaction in the binding of AdoMet, either through binding studies by isothermal titration calorimetry to obtain the binding constant or the apparent affinity of the Michaelis constant (K_M) obtained from kinetic assays. The effect on catalysis seen upon loss of the chalcogen bond may also provide information influential to the debate of the near attack conformation (NAC)[119] versus the electrostatic preorganization[114] with respect to the origin of the catalytic rate enhancement of COMT. The electrostatic preorganization model states that there is a preferential stabilization of the transition state, leading to catalysis, while the near attack conformation has been interpreted as the biasing of alignment of the substrates to a productive conformation by the binding of the reactant state. A large catalytic defect in the mutant may be favorably

explained by the near attack conformation, as the bond should be much stronger in the reactant state, which contains a sulfonium sulfur, than in the transition state, in which the sulfur is progressing towards the neutrality seen in the product S-adenosylhomocysteine.

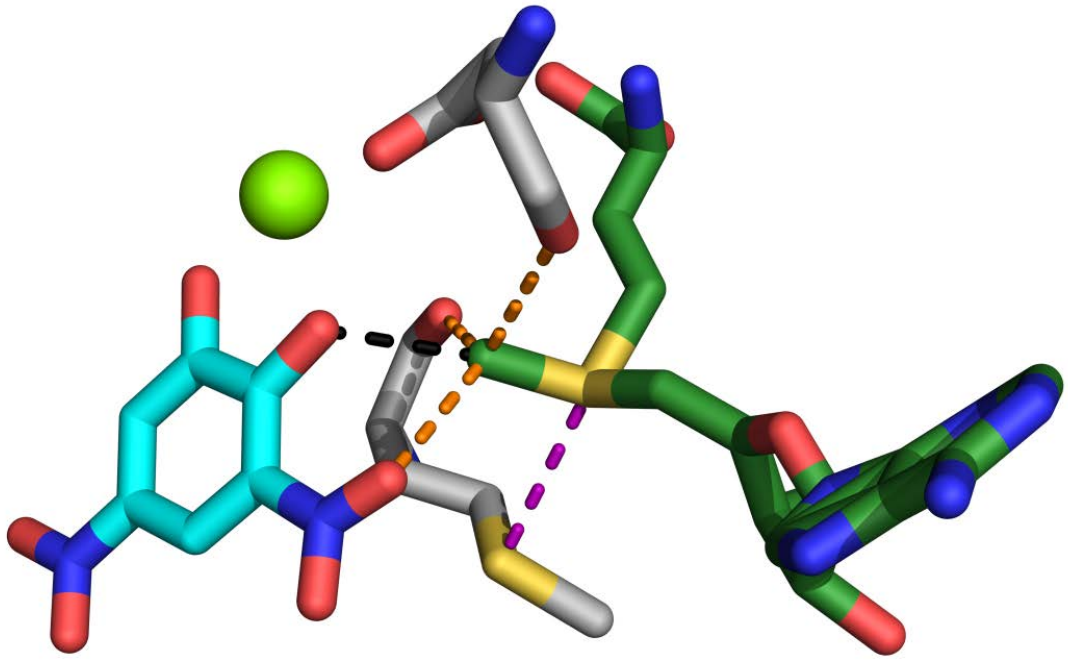

Figure 5.2: Active site interactions in catechol O-methyltransferase.

The active site of catechol O-methyltransferase (from 1VID)[63] showing AdoMet (forest green), the dinitrocatechol inhibitor (cyan), the magnesium ion (green, shown as a sphere), and two active site residues methionine 40 and aspartate 141. CH•••O hydrogen bonds shown as orange dashes, an S•••S chalcogen bond shown as purple dashes (3.3 Å, combined van der Waals radii of 3.6 Å), and a C•••O tetrel bond shown as black dashes (2.6 Å, combined van der Waal radii of 3.25).

The tetrel bond represents a new bonding interaction to probe in methyltransferases and is seen in the COMT active site when bound to AdoMet and an inhibitor dinitrocatechol. A tetrel bond is similar to the chalcogen and halogen bonds in

that it is a σ-antibonding interaction except with column 14 elements (C, Si, etc.). Similar to the chalcogen bond, it is increased in strength in a charged, sulfonium system, relative to an uncharged system,[45] and it may represent the formation of a state like a pre-transition state, though the inhibitor bound does not allow catalysis. The energy of the tetrel interaction in COMT will be studied quantum mechanically, as disruption of this interaction chemically may not be feasible, due to multiple interactions that the inhibitor oxygen and AdoMet methyl form. Substitution for other inhibitors, such as the drug tolcapone, to change the strength of the interaction may also present challenges, as tolcapone has been cited as a poor substrate,[162] with the possibility of turnover complicating any crystallographic or binding studies. SET7/9 may represent a more feasible system to study the tetrel interaction seen in COMT through the introduction of a TAF10 peptide capable of forming such a bond without reaction. The synthetic incorporation of 6-hydroxynorleucine, effectively substituting the lysine ε-amine group for a hydroxyl group, should present a nonreactive isostere that can be used in binding, crystallographic, and computational studies in the well-studied SET7/9 model system.

Though they have been studied for approaching 60 years,[64] AdoMet-dependent methyltransferases continue to be a field open to further research. This dissertation explored CH•••O hydrogen bonding to the methyl and methylene carbons of AdoMet, and an S•••O chalcogen bond to the sulfonium sulfur, and further study of these interactions will hopefully yield trends useful in understanding and classifying active site interactions in these enzymes. Expansion of study of the AdoMet-dependent methyltransferases to tetrel bonding and other interactions should bring the field ever

closer to an understanding as to how methyltransferases use their active sites to facilitate the transfer of the methyl group of AdoMet.

References

1. Schubert, H. L.; Blumenthal, R. M.; Cheng, X., Many paths to methyltransfer: a chronicle of convergence. *Trends Biochem Sci* **2003,** *28* (6), 329-35.

2. Cantoni, G. L., Biological Methylation - Selected Aspects. *Annual Review of Biochemistry* **1975,** *44*, 435-451.

3. Park, J.; Tai, J. Z.; Roessner, C. A.; Scott, A. I., Enzymatic synthesis of S-adenosyl-L-methionine on the preparative scale. *Bioorganic & Medicinal Chemistry* **1996,** *4* (12), 2179-2185.

4. Mihel, I.; Knipe, J. O.; Coward, J. K.; Schowen, R. L., Alpha-Deuterium Isotope Effects and Transition-State Structure in an Intra-Molecular Model System for Methyl-Transfer Enzymes. *Journal of the American Chemical Society* **1979,** *101* (15), 4349-4351.

5. Pauling, L.; Corey, R. B.; Branson, H. R., The Structure of Proteins - 2 Hydrogen-Bonded Helical Configurations of the Polypeptide Chain. *Proceedings of the National Academy of Sciences of the United States of America* **1951,** *37* (4), 205-211.

6. Pauling, L.; Corey, R. B., 2 Rippled-Sheet Configurations of Polypeptide Chains, And A Note About The Pleated Sheets. *Proceedings of the National Academy of Sciences of the United States of America* **1953,** *39* (4), 253-256.

7. Watson, J. D.; Crick, F. H. C., Molecular Structure Of Nucleic Acids - A Structure For Deoxyribose Nucleic Acid. *Nature* **1953,** *171* (4356), 737-738.

8. Pauling, L., *The Nature of the Chemical Bond and the Structure of Molecules and Crystals: An Introduction to Modern Structural Chemistry*. Cornell University Press: 1960.

9. Moore, T. S.; Winmill, T. F., The state of amines an aqueous solution. *Journal of the Chemical Society* **1912,** *101*, 1635-1676.

10. Latimer, W. M.; Rodebush, W. H., Polarity and ionization from the standpoint of the Lewis theory of valence. *Journal of the American Chemical Society* **1920,** *42*, 1419-1433.

11. Umeyama, H.; Morokuma, K., Origin Of Hydrogen-Bonding - Energy Decomposition Study. *Journal of the American Chemical Society* **1977,** *99* (5), 1316-1332.

12. CRC Handbook of Chemistry and Physics. 98th Edition (Internet Version 2018) ed.; Rumble, J. R., Ed. CRC Press/Taylor & Francis, Boca Raton, FL.

13. Gu, Y. L.; Kar, T.; Scheiner, S., Fundamental properties of the CH•••O interaction: Is it a true hydrogen bond? *Journal of the American Chemical Society* **1999,** *121* (40), 9411-9422.

14. Sutor, D. J., The Structures Of The Pyrmidines And Purines .7. The Crystal Structure Of Caffeine. *Acta Crystallographica* **1958,** *11* (7), 453-458.

15. Sutor, D. J., C-H ... O Hydrogen Bond In Crystals. *Nature* **1962,** *195* (4836), 68-69.
16. Sutor, D. J., Evidence For Existence Of C-H ... O Hydrogen Bonds In Crystals. *Journal of the Chemical Society* **1963,** (FEB), 1105-1110.

17. Ferguson, G.; Tyrrell, J., C-H O Hydrogen Bonding. *Chemical Communications* **1965,** (10), 195-197.

18. Ferguson, G.; Islam, K. M. S., C-H...O Hydrogen Bonding .2. Crystal And Molecular Structure Of O-Chlorobenzoylacetylene. *Journal of the Chemical Society B-Physical Organic* **1966,** (7), 593-600.

19. Ramachandran, G. N.; Sasisekharan, V., Refinement Of Structure Of Collagen. *Biochimica Et Biophysica Acta* **1965,** *109* (1), 314-316.

20. Ramachandran, G. N.; Sasisekharan, V.; Ramakrishnan, C., Molecular Structure Of Polyglycine 2. *Biochimica Et Biophysica Acta* **1966,** *112* (1), 168-170.

21. Ramachandran, G. N.; Ramakrishnan, C.; Venkatachalam, C. M., Structure of Polyglycine II with Direct and Inverted Chains. In *Conformation of Biopolymers*, Academic Press: 1967; pp 429-438.

22. Krimm, S., Antiparallelism Of Chains In Polyglycine 2. *Nature* **1966,** *212* (5069), 1482-1483.

23. Krimm, S., Hydrogen Bonding Of C-H...O=C In Proteins. *Science* **1967,** *158* (3800), 530-531.

24. Krimm, S.; Kuroiwa, K., Low Temperature Infrared Spectra Of Polyglycines And C-H...O=C Hydrogen Bonding In Polyglycine 2. *Biopolymers* **1968,** *6* (3), 401-407.

25. Fraser, R. D. B.; Macrae, T. P.; Suzuki, E., Chain Conformation In The Collagen Molecule. *Journal of Molecular Biology* **1979,** *129* (3), 463-481.

26. Bella, J.; Berman, H. M., Crystallographic evidence for C-alpha-H•••O=C hydrogen bonds in a collagen triple helix. *Journal of Molecular Biology* **1996,** *264* (4), 734-742.

27. Donohue, Structural Chemistry and Molecular Biology. Rich, A.; Davidson, N. R., Eds. W. H. Freeman: 1968; pp 444-465.

28. Olympia, P. L., Some theoretical aspects of C-H•••O bonding. *Chemical Physics Letters* **1970,** *5* (9), 593-596.

29. Talberg, H. J.; Ottersen, T., C-H...O Hydrogen-Bond - Ab-Initio Study Of Nitrosomethane And Its Hydrogen-Bonded Dimer. *Journal of Molecular Structure* **1975,** *29* (2), 225-231.

30. Kollman, P.; McKelvey, J.; Johansson, A.; Rothenberg, S., Theoretical Studies Of Hydrogen-Bonded Dimers - Complexes Involving HF, H2O, NH3, HCL, H2S, PH3, HCN, HNC,

HCP, CH2NH, H2CS, H2CO, CH4, CF3H, C2H2, C2H4, C6H6, F-, AND H3O+. *Journal of the American Chemical Society* **1975,** *97* (5), 955-965.

31. Harmon, K. M.; Gennick, I.; Madeira, S. L., Hydrogen-Bonding .4. Correlation Of Infrared Spectral Properties With C-H Triple Bond X Hydrogen-Bonding And Crystal Habit In Tetramethylammonium Ion Salts. *Journal of Physical Chemistry* **1974,** *78* (25), 2585-2591.

32. Taylor, R.; Kennard, O., Crystallographic Evidence For The Existence Of C-H...O, C-H...N, AND C-H...C1 Hydrogen-Bonds. *Journal of the American Chemical Society* **1982,** *104* (19), 5063-5070.

33. Steiner, T.; Saenger, W., Role Of C-H...O Hydrogen-Bonds In The Coordination Of Water-Molecules - Analysis Of Neutron-Diffraction Data. *Journal of the American Chemical Society* **1993,** *115* (11), 4540-4547.

34. Desiraju, G. R., The C-H...O Hydrogen-Bond In Crystals - What Is It. *Accounts of Chemical Research* **1991,** *24* (10), 290-296.

35. Desiraju, G. R., The C-H•••O hydrogen bond: Structural implications and supramolecular design. *Accounts of Chemical Research* **1996,** *29* (9), 441-449.

36. Desiraju, G. R., C-H•••O and other weak hydrogen bonds. From crystal engineering to virtual screening. *Chemical Communications* **2005,** (24), 2995-3001.

37. Wahl, M. C.; Sundaralingam, M., C-H•••O hydrogen bonding in biology. *Trends in Biochemical Sciences* **1997,** *22* (3), 97-102.

38. Derewenda, Z. S.; Derewenda, U.; Kobos, P. M., (HIS)C-Epsilon-H...O=C Hydrogen-Bond In The Active-Sites Of Serine Hydrolases. *Journal of Molecular Biology* **1994,** *241* (1), 83-93.

39. Derewenda, Z. S.; Lee, L.; Derewenda, U., The Occurrence Of C-H•••O Hydrogen-Bonds In Proteins. *Journal of Molecular Biology* **1995,** *252* (2), 248-262.

40. Scheiner, S.; Kar, T.; Gu, Y. L., Strength of the (CH)-H-alpha••O hydrogen bond of amino acid residues. *Journal of Biological Chemistry* **2001,** *276* (13), 9832-9837.

41. Scheiner, S.; Kar, T., Effect of solvent upon CH•••O hydrogen bonds with implications for protein folding. *Journal of Physical Chemistry B* **2005,** *109* (8), 3681-3689.

42. Scheiner, S., Relative strengths of NH••O and CH••O hydrogen bonds between polypeptide chain segments. *Journal of Physical Chemistry B* **2005,** *109* (33), 16132-16141.

43. Scheiner, S., Weak H-bonds. Comparisons of CH•••O to NH•••O in proteins and PH•••N to direct P•••N interactions. *Physical Chemistry Chemical Physics* **2011,** *13* (31), 13860-13872.

44. Adhikari, U.; Scheiner, S., Magnitude and Mechanism of Charge Enhancement of CH••O Hydrogen Bonds. *Journal of Physical Chemistry A* **2013,** *117* (40), 10551-10562.

45. Scheiner, S., Comparison of CH•••O, SH•••O, Chalcogen, and Tetrel Bonds Formed by Neutral and Cationic Sulfur-Containing Compounds. *Journal of Physical Chemistry A* **2015,** *119* (34), 9189-9199.

46. Novoa, J. J.; Tarron, B.; Whangbo, M. H.; Williams, J. M., Interaction Energies Associated With Short Intermolecular Contacts Of C-H Bonds - Abinitio Computational Study Of The C-H...O Contact Interaction In CH4...OH2. *Journal of Chemical Physics* **1991,** *95* (7), 5179-5186.

47. Horowitz, S.; Dirk, L. M. A.; Yesselman, J. D.; Nimtz, J. S.; Adhikari, U.; Mehl, R. A.; Scheiner, S.; Houtz, R. L.; Al-Hashimi, H. M.; Trievel, R. C., Conservation and Functional Importance of Carbon-Oxygen Hydrogen Bonding in Ado Met-Dependent Methyltransferases. *Journal of the American Chemical Society* **2013,** *135* (41), 15536-15548.

48. Britton, D.; Dunitz, J. D., Directional Preferences Of Approach Of Nucleophiles To Sulfonium Ions. *Helvetica Chimica Acta* **1980,** *63* (4), 1068-1073.

49. Rosenfield, R. E.; Parthasarathy, R.; Dunitz, J. D., Directional Preferences Of Nonbonded Atomic Contacts With Divalent Sulfur .1. Electrophiles And Nucleophiles. *Journal of the American Chemical Society* **1977,** *99* (14), 4860-4862.

50. Politzer, P.; Lane, P.; Concha, M. C.; Ma, Y.; Murray, J. S., An overview of halogen bonding. *Journal of Molecular Modeling* **2007,** *13* (2), 305-311.

51. Politzer, P.; Murray, J. S.; Concha, M. C., sigma-hole bonding between like atoms; a fallacy of atomic charges. *Journal of Molecular Modeling* **2008,** *14* (8), 659-665.

52. Scheiner, S., On the properties of X•••N noncovalent interactions for first-, second-, and third-row X atoms. *Journal of Chemical Physics* **2011,** *134* (16).

53. Iwaoka, M.; Takemoto, S.; Okada, M.; Tomoda, S., Statistical characterization of nonbonded S•••O interactions in proteins. *Chemistry Letters* **2001,** (2), 132-133.

54. Iwaoka, M.; Babe, N., Mining And Structural Characterization Of S•••X Chalcogen Bonds In Protein Database. *Phosphorus Sulfur and Silicon and the Related Elements* **2015,** *190* (8), 1257-1264.

55. Iwaoka, M.; Takemoto, S.; Tomoda, S., Statistical and theoretical investigations on the directionality of nonbonded (SO)-O-... interactions. Implications for molecular design and protein engineering. *Journal of the American Chemical Society* **2002,** *124* (35), 10613-10620.

56. Iwaoka, M.; Isozumi, N., *BIOPHYSICS* **2006,** *2*, 23-34.

57. Taylor, J. C.; Markham, G. D., The bifunctional active site of S-adenosylmethionine synthetase - Roles of the active site aspartates. *Journal of Biological Chemistry* **1999,** *274* (46), 32909-32914.

58. Beno, B. R.; Yeung, K.-S.; Bartberger, M. D.; Pennington, L. D.; Meanwell, N. A., A Survey of the Role of Noncovalent Sulfur Interactions in Drug Design. *Journal of Medicinal Chemistry* **2015,** *58* (11), 4383-4438.

59. Petrossian, T. C.; Clarke, S. G., Uncovering the Human Methyltransferasome. *Molecular & Cellular Proteomics* **2011,** *10* (1), 12.

60. Yang, J.; Kulkarni, K.; Manolaridis, I.; Zhang, Z. G.; Dodd, R. B.; Mas-Droux, C.; Barford, D., Mechanism of Isoprenylcysteine Carboxyl Methylation from the Crystal Structure of the Integral Membrane Methyltransferase ICMT. *Molecular Cell* **2011,** *44* (6), 997-1004.

61. Petrossian, T.; Clarke, S., Bioinformatic identification of novel methyltransferases. *Epigenomics* **2009,** *1* (1), 163-175.

62. Cheng, X.; Kumar, S.; Posfai, J.; Pflugrath, J. W.; Roberts, R. J., Crystal structure of the HhaI DNA methyltransferase complexed with S-adenosyl-L-methionine. *Cell* **1993,** *74* (2), 299-307.

63. Vidgren, J.; Svensson, L. A.; Liljas, A., Crystal structure of catechol O-methyltransferase. *Nature* **1994,** *368* (6469), 354-8.

64. Axelrod, J.; Tomchick, R., Enzymatic O-Methylation Of Epinephrine And Other Catechols. *Journal of Biological Chemistry* **1958,** *233* (3), 702-705.

65. Rossmann, M. G.; Moras, D.; Olsen, K. W., Chemical And Biological Evolution Of A Nucleotide-Binding Protein. *Nature* **1974,** *250* (5463), 194-199.

66. Suzuki, Y.; Noma, A.; Suzuki, T.; Ishitani, R.; Nureki, O., Structural basis of tRNA modification with CO2 fixation and methylation by wybutosine synthesizing enzyme TYW4. *Nucleic Acids Research* **2009,** *37* (9), 2910-2925.

67. Zhang, Z. M.; Liu, S.; Lin, K.; Luo, Y. F.; Perry, J. J.; Wang, Y. S.; Song, J. K., Crystal Structure of Human DNA Methyltransferase 1. *Journal of Molecular Biology* **2015,** *427* (15), 2520-2531.

68. Richon, V. M.; Johnston, D.; Sneeringer, C. J.; Jin, L.; Majer, C. R.; Elliston, K.; Jerva, L. F.; Scott, M. P.; Copeland, R. A., Chemogenetic Analysis of Human Protein Methyltransferases. *Chemical Biology & Drug Design* **2011,** *78* (2), 199-210.

69. Gui, S. Y.; Wooderchak, W. L.; Daly, M. P.; Porter, P. J.; Johnson, S. J.; Hevel, J. M., Investigation of the Molecular Origins of Protein-arginine Methyltransferase I (PRMT1) Product Specificity Reveals a Role for Two Conserved Methionine Residues. *Journal of Biological Chemistry* **2011,** *286* (33), 29118-29126.

70. Horton, J. R.; Sawada, K.; Nishibori, M.; Zhang, X.; Cheng, X. D., Two polymorphic forms of human histamine methyltransferase: Structural, thermal and kinetic comparisons. *Structure* **2001,** *9* (9), 837-849.

71. Wu, H.; Horton, J. R.; Battaile, K.; Allali-Hassani, A.; Martin, F.; Zeng, H.; Loppnau, P.; Vedadi, M.; Bochkarev, A.; Plotnikov, A. N.; Cheng, X. D., Structural basis of allele variation of human thiopurine-S-methyltransferase. *Proteins-Structure Function and Bioinformatics* **2007,** *67* (1), 198-208.

72. Dixon, M.; Huang, S.; Matthews, R.; Ludwig, M., The structure of the C-terminal domain of methionine synthase: Presenting S-adenosylmethionine for reductive methylation of B-12. *Structure* **1996,** *4* (11), 1263-1275.

73. Drummond, J. T.; Huang, S.; Blumenthal, R. M.; Matthews, R. G., Assignment Of Enzymatic Function To Specific Protein Regions Of Cobalamin-Dependent Methionine Synthase From Escherichia-Coli. *Biochemistry* **1993,** *32* (36), 9290-9295.

74. Scott, A. I., The Discovery Of Natures Pathway To Vitamin-B-12 - A 25-Year Odyssey. *Tetrahedron* **1994,** *50* (47), 13315-13333.

75. Schubert, H. L.; Wilson, K. S.; Raux, E.; Woodcock, S. C.; Warren, M. J., The X-ray structure of a cobalamin biosynthetic enzyme, cobalt-precorrin-4 methyltransferase. *Nature Structural Biology* **1998,** *5* (7), 585-592.

76. Hori, H., Transfer RNA methyltransferases with a SpoU-TrmD (SPOUT) fold and their modified nucleosides in tRNA. *Biomolecules* **2017,** *7* (1).

77. Young, B. D.; Weiss, D. I.; Zurita-Lopez, C. I.; Webb, K. J.; Clarke, S. G.; McBride, A. E., Identification of Methylated Proteins in the Yeast Small Ribosomal Subunit: A Role for SPOUT Methyltransferases in Protein Arginine Methylation. *Biochemistry* **2012,** *51* (25), 5091-5104.

78. Nureki, O.; Watanabe, K.; Fukai, S.; Ishii, R.; Endo, Y.; Hori, H.; Yokoyama, S., Deep knot structure for construction of active site and cofactor binding site of tRNA modification enzyme. *Structure* **2004,** *12* (4), 593-602.

79. Herz, H. M.; Garruss, A.; Shilatifard, A., SET for life biochemical activities and biological functions of SET domain-containing proteins. *Trends in Biochemical Sciences* **2013,** *38* (12), 621-639.

80. Mosammaparast, N.; Shi, Y., Reversal of Histone Methylation: Biochemical and Molecular Mechanisms of Histone Demethylases. *Annual Review of Biochemistry, Vol 79* **2010,** *79*, 155-179.

81. Trievel, R. C.; Beach, B. M.; Dirk, L. M. A.; Houtz, R. L.; Hurley, J. H., Structure and catalytic mechanism of a SET domain protein methyltransferase. *Cell* **2002,** *111* (1), 91-103.

82. Kwon, T.; Chang, J. H.; Kwak, E.; Lee, C. W.; Joachimiak, A.; Kim, Y. C.; Lee, J. W.; Cho, Y. J., Mechanism of histone lysine methyl transfer revealed by the structure of SET7/9-AdoMet. *Embo Journal* **2003,** *22* (2), 292-303.

83. Horowitz, S.; Yesselman, J. D.; Al-Hashimi, H. M.; Trievel, R. C., Direct Evidence for Methyl Group Coordination by Carbon-Oxygen Hydrogen Bonds in the Lysine Methyltransferase SET7/9. *Journal of Biological Chemistry* **2011,** *286* (21), 18658-18663.

84. Horowitz, S.; Adhikari, U.; Dirk, L. M. A.; Del Rizzo, P. A.; Mehl, R. A.; Houtz, R. L.; Al-Hashimi, H. M.; Scheiner, S.; Trievel, R. C., Manipulating Unconventional CH-Based Hydrogen Bonding in a Methyltransferase via Noncanonical Amino Acid Mutagenesis. *ACS Chemical Biology* **2014,** *9* (8), 1692-1697.

85. Subramanian, K.; Jia, D.; Kapoor-Vazirani, P.; Powell, D. R.; Collins, R. E.; Sharma, D.; Peng, J. M.; Cheng, X. D.; Vertino, P. M., Regulation of estrogen receptor alpha by the SET7 lysine methyltransferase. *Molecular Cell* **2008,** *30* (3), 336-347.

86. Chuikov, S.; Kurash, J. K.; Wilson, J. R.; Xiao, B.; Justin, N.; Ivanov, G. S.; McKinney, K.; Tempst, P.; Prives, C.; Gamblin, S. J.; Barlev, N. A.; Reinberg, D., Regulation of p53 activity through lysine methylation. *Nature* **2004,** *432* (7015), 353-360.

87. Kouskouti, A.; Scheer, E.; Staub, A.; Tora, L.; Talianidis, I., Gene-specific modulation of TAF10 function by SET9-mediated methylation. *Molecular Cell* **2004,** *14* (2), 175-182.

88. Del Rizzo, P. A.; Trievel, R. C., Substrate and product specificities of SET domain methyltransferases. *Epigenetics* **2011,** *6* (9), 1059-1067.

89. Boal, A. K.; Grove, T. L.; McLaughlin, M. I.; Yennawar, N. H.; Booker, S. J.; Rosenzweig, A. C., Structural Basis for Methyl Transfer by a Radical SAM Enzyme. *Science* **2011,** *332* (6033), 1089-1092.

90. Grove, T. L.; Benner, J. S.; Radle, M. I.; Ahlum, J. H.; Landgraf, B. J.; Krebs, C.; Booker, S. J., A Radically Different Mechanism for S-Adenosylmethionine-Dependent Methyltransferases. *Science* **2011,** *332* (6029), 604-607.

91. Vey, J. L.; Drennan, C. L., Structural Insights into Radical Generation by the Radical SAM Superfamily. *Chemical Reviews* **2011,** *111* (4), 2487-2506.

92. Kehrenberg, C.; Schwarz, S.; Jacobsen, L.; Hansen, L. H.; Vester, B., A new mechanism for chloramphenicol, florfenicol and clindamycin resistance: methylation of 23S ribosomal RNA at A2503. *Molecular Microbiology* **2005,** *57* (4), 1064-1073.

93. Fujimori, D. G., Radical SAM-mediated methylation reactions. *Current Opinion in Chemical Biology* **2013,** *17* (4), 597-604.

94. Benitez-Paez, A.; Villarroya, M.; Armengod, M. E., The Escherichia coli RlmN methyltransferase is a dual-specificity enzyme that modifies both rRNA and tRNA and controls translational accuracy. *Rna-a Publication of the Rna Society* **2012,** *18* (10), 1783-1795.

95. Cui, Z.; Vance, J. E.; Chen, M. H.; Voelker, D. R.; Vance, D. E., Cloning And Expression Of A Novel Phosphatidylethanolamine N-Methyltransferase - A Specific Biochemical And Cytological Marker For A Unique Membrane-Fraction In Rat-Liver. *Journal of Biological Chemistry* **1993,** *268* (22), 16655-16663.

96. Carney, A. E.; Holden, H. M., Molecular Architecture of TylM1 from Streptomyces fradiae: An N,N-Dimethyltransferase Involved in the Production of dTDP-D-mycaminose. *Biochemistry* **2011,** *50* (5), 780-787.

97. Woodard, R. W.; Tsai, M. D.; Floss, H. G.; Crooks, P. A.; Coward, J. K., Stereochemical Course Of The Transmethylation Catalyzed By Catechol O-Methyltransferase. *Journal of Biological Chemistry* **1980,** *255* (19), 9124-9127.

98. Woodard, R. W.; Mascaro, L.; Horhammer, R.; Eisenstein, S.; Floss, H. G., Stereochemistry Of Indolmycin Biosynthesis - Steric Course Of C-Methylation And N-Methylation Reactions. *Journal of the American Chemical Society* **1980,** *102* (20), 6314-6318.

99. Gray, C. H.; Coward, J. K.; Schowen, K. B.; Schowen, R. L., Alpha-Deuterium And C-13 Isotope Effects For A Simple, Inter-Molecular Sulfur-To-Oxygen Methyl-Transfer Reaction - Transition-State Structures And Isotope Effects In Transmethylation And Transalkylation. *Journal of the American Chemical Society* **1979,** *101* (15), 4351-4358.

100. Hegazi, M. F.; Borchardt, R. T.; Schowen, R. L., Alpha-Deuterium And C-13 Isotope Effects For Methyl Transfer Catalyzed By Catechol O-Methyltransferase - S_N2-Like Transition-State. *Journal of the American Chemical Society* **1979,** *101* (15), 4359-4365.

101. Hartshor.Sr; Shiner, V. J., Calculation Of H/D, C-12/C-13, And C-12/C-14 Fractionation Factors From Valence Force Fields Derived For A Series Of Simple Organic-Molecules. *Journal of the American Chemical Society* **1972,** *94* (26), 9002-9012.

102. Sims, L. B.; Wilson, J. C.; Crook, S. W.; Fry, A.; Reppond, K. D.; Netherto.Lt, Variations Of Heavy-Atom Kinetic Isotope-Effects In S_N2 Displacement Reactions. *Journal of the American Chemical Society* **1972,** *94* (4), 1364-1365.

103. Rodgers, J.; Femec, D. A.; Schowen, R. L., Isotopic Mapping Of Transition-State Structural Features Associated With Enzymic Catalysis Of Methyl Transfer. *Journal of the American Chemical Society* **1982,** *104* (12), 3263-3268.

104. Williams, I. H., Catalysis: transition-state molecular recognition? *Beilstein Journal of Organic Chemistry* **2010,** *6*, 1026-1034.

105. Moliner, V.; Williams, I. H., Influence of compression upon kinetic isotope effects for S(N)2 methyl transfer: A computational reappraisal. *Journal of the American Chemical Society* **2000,** *122* (44), 10895-10902.

106. Wilson, P. B.; Williams, I. H., Influence of Equatorial CHO Interactions on Secondary Kinetic Isotope Effects for Methyl Transfer. *Angewandte Chemie-International Edition* **2016,** *55* (9), 3192-3195.

107. Soriano, A.; Castillo, R.; Christov, C.; Andres, J.; Moliner, V.; Tunon, I., Catalysis in glycine N-methyltransferase: Testing the electrostatic stabilization and compression hypothesis. *Biochemistry* **2006,** *45* (50), 14917-14925.

108. Kanaan, N.; Pernia, J. J. R.; Williams, I. H., QM/MM simulations for methyl transfer in solution and catalysed by COMT: ensemble-averaging of kinetic isotope effects. *Chemical Communications* **2008,** (46), 6114-6116.

109. Ruggiero, G. D.; Williams, I. H.; Roca, M.; Moliner, V.; Tunon, I., QM/MM determination of kinetic isotope effects for COMT-catalyzed methyl transfer does not support compression hypothesis. *Journal of the American Chemical Society* **2004,** *126* (28), 8634-8635.

110. Zhang, J. Y.; Klinman, J. P., Convergent Mechanistic Features between the Structurally Diverse N- and O-Methyltransferases: Glycine N-Methyltransferase and Catechol O-Methyltransferase. *Journal of the American Chemical Society* **2016,** *138* (29), 9158-9165.

111. Zhang, J. Y.; Klinman, J. P., Enzymatic Methyl Transfer: Role of an Active Site Residue in Generating Active Site Compaction That Correlates with Catalytic Efficiency. *Journal of the American Chemical Society* **2011,** *133* (43), 17134-17137.

112. Zhang, J. Y.; Kulik, H. J.; Martinez, T. J.; Klinman, J. P., Mediation of donor-acceptor distance in an enzymatic methyl transfer reaction. *Proceedings of the National Academy of Sciences of the United States of America* **2015,** *112* (26), 7954-7959.

113. Roca, M.; Marti, S.; Andres, J.; Moliner, V.; Tunon, I.; Bertran, J.; Williams, I. H., Theoretical modeling of enzyme catalytic power: Analysis of "cratic" and electrostatic factors in catechol O-methyltransferase. *Journal of the American Chemical Society* **2003,** *125* (25), 7726-7737.

114. Lameira, J.; Bora, R. P.; Chu, Z. T.; Warshel, A., Methyltransferases do not work by compression, cratic, or desolvation effects, but by electrostatic preorganization. *Proteins-Structure Function and Bioinformatics* **2015,** *83* (2), 318-330.

115. Page, M. I.; Jencks, W. P., Entropic Contributions To Rate Accelerations In Enzymic And Intramolecular Reactions And Chelate Effect. *Proceedings of the National Academy of Sciences of the United States of America* **1971,** *68* (8), 1678-1683.

116. Stanton, R. V.; Perakyla, M.; Bakowies, D.; Kollman, P. A., Combined ab initio and free energy calculations to study reactions in enzymes and solution: Amide hydrolysis in trypsin and aqueous solution. *Journal of the American Chemical Society* **1998,** *120* (14), 3448-3457.

117. Kollman, P. A.; Kuhn, B.; Donini, O.; Perakyla, M.; Stanton, R.; Bakowies, D., Elucidating the nature of enzyme catalysis utilizing a new twist on an old methodology: Quantum mechanical - Free energy calculations on chemical reactions in enzymes and in aqueous solution. *Accounts of Chemical Research* **2001,** *34* (1), 72-79.

118. Kuhn, B.; Kollman, P. A., QM-FE and molecular dynamics calculations on catechol O-methyltransferase: Free energy of activation in the enzyme and in aqueous solution and regioselectivity of the enzyme-catalyzed reaction. *Journal of the American Chemical Society* **2000,** *122* (11), 2586-2596.

119. Lau, E. Y.; Bruice, T. C., Importance of correlated motions in forming highly reactive near attack conformations in catechol O-methyltransferase. *Journal of the American Chemical Society* **1998,** *120* (48), 12387-12394.

120. Bruice, T. C., A view at the millennium: The efficiency of enzymatic catalysis. *Accounts of Chemical Research* **2002,** *35* (3), 139-148.

121. Strajbl, M.; Shurki, A.; Kato, M.; Warshel, A., Apparent NAC effect in chorismate mutase reflects electrostatic transition state stabilization. *Journal of the American Chemical Society* **2003,** *125* (34), 10228-10237.

122. Warshel, A., Energetics Of Enzyme Catalysis. *Proceedings of the National Academy of Sciences of the United States of America* **1978,** *75* (11), 5250-5254.

123. Warshel, A.; Aqvist, J.; Creighton, S., Enzymes Work By Solvation Substitution Rather Than By Desolvation. *Proceedings of the National Academy of Sciences of the United States of America* **1989,** *86* (15), 5820-5824.

124. Shurki, A.; Strajbl, M.; Villa, J.; Warshel, A., How much do enzymes really gain by restraining their reacting fragments? *Journal of the American Chemical Society* **2002,** *124* (15), 4097-4107.

125. Linscott, J. A.; Kapilashrami, K.; Wang, Z.; Senevirathne, C.; Bothwell, I. R.; Blum, G.; Luo, M. K., Kinetic isotope effects reveal early transition state of protein lysine methyltransferase SET8. *Proceedings of the National Academy of Sciences of the United States of America* **2016,** *113* (52), E8369-E8378.

126. Drummond, J. T.; Loo, R. R. O.; Matthews, R. G., Electrospray Mass-Spectrometric Analysis Of The Domains Of A Large Enzyme - Observation Of The Occupied Cobalamin-Binding Domain And Redefinition Of The Carboxyl-Terminus Of Methionine Synthase. *Biochemistry* **1993,** *32* (36), 9282-9289.

127. Banerjee, R. V.; Frasca, V.; Ballou, D. P.; Matthews, R. G., Participation Of Cob(I)alamin In The Reaction Catalyzed By Methionine Synthase From Escherichia-Coli - A Steady-State And Rapid Reaction Kinetic-Analysis. *Biochemistry* **1990,** *29* (50), 11101-11109.

128. Jarrett, J. T.; Huang, S.; Matthews, R. G., Methionine synthase exists in two distinct conformations that differ in reactivity toward methyltetrahydrofolate, adenosylmethionine, and flavodoxin. *Biochemistry* **1998,** *37* (16), 5372-5382.

129. Finkelstein, J. D., Pathways and regulation of homocysteine metabolism in mammals. *Seminars in Thrombosis and Hemostasis* **2000,** *26* (3), 219-225.

130. Banerjee, R. V.; Matthews, R. G., Cobalamin-Dependent Methionine Synthase. *Faseb Journal* **1990,** *4* (5), 1450-1459.

131. Fujii, K.; Huenneke.Fm, Activation Of Methionine Synthetase By A Reduced Triphosphopyridine Nucleotide-Dependent Flavoprotein System. *Journal of Biological Chemistry* **1974,** *249* (21), 6745-6753.

132. Chen, Z. Q.; Banerjee, R., Purification of soluble cytochrome b(5) as a component of the reductive activation of porcine methionine synthase. *Journal of Biological Chemistry* **1998,** *273* (40), 26248-26255.

133. Seeger, K.; Lein, S.; Reuter, G.; Berger, S., Saturation transfer difference measurements with SU(VAR)3-9 and S-adenosyl-L-methionine. *Biochemistry* **2005,** *44* (16), 6208-6213.

134. Schanda, P.; Kupce, E.; Brutscher, B., SOFAST-HMQC experiments for recording two-dimensional heteronuclear correlation spectra of proteins within a few seconds. *Journal of Biomolecular NMR* **2005,** *33* (4), 199-211.

135. Wolthers, K. R.; Toogood, H. S.; Jowitt, T. A.; Marshall, K. R.; Leys, D.; Scrutton, N. S., Crystal structure and solution characterization of the activation domain of human methionine synthase. *Febs Journal* **2007,** *274* (3), 738-750.

136. Zheng, W. H.; Ibanez, G.; Wu, H.; Blum, G.; Zeng, H.; Dong, A. P.; Li, F. L.; Hajian, T.; Allali-Hassani, A.; Amaya, M. F.; Siarheyeva, A.; Yu, W. Y.; Brown, P. J.; Schapira, M.; Vedadi, M.; Min, J. R.; Luo, M. K., Sinefungin Derivatives as Inhibitors and Structure Probes of Protein Lysine Methyltransferase SETD2. *Journal of the American Chemical Society* **2012,** *134* (43), 18004-18014.

137. Smith, D. E. C.; Hornstra, J. M.; Kok, R. M.; Blom, H. J.; Smulders, Y. M., Folic acid supplementation does not reduce intracellular homocysteine, and may disturb intracellular one-carbon metabolism. *Clinical Chemistry and Laboratory Medicine* **2013,** *51* (8), 1643-1650.

138. Caudill, M. A.; Wang, J. C.; Melnyk, S.; Pogribny, I. P.; Jernigan, S.; Collins, M. D.; Santos-Guzman, J.; Swendseid, M. E.; Cogger, E. A.; James, S. J., Intracellular S-adenosylhomocysteine concentrations predict global DNA hypomethylation in tissues of methyl-deficient cystathionine beta-synthase heterozygous mice. *Journal of Nutrition* **2001,** *131* (11), 2811-2818.

139. Boyle, S. M.; Markham, G. D.; Hafner, E. W.; Wright, J. M.; Tabor, H.; Tabor, C. W., Expression Of The Cloned Genes Encoding The Putrescine Biosynthetic-Enzymes And Methionine Adenosyltransferase Of Escherichia-Coli (SpeA, SpeB, SpeC and MetK). *Gene* **1984,** *30* (1-3), 129-136.

140. Markham, G. D.; Deparasis, J.; Gatmaitan, J., The Sequence Of MetK, The Structural Gene For S-Adenosylmethionine Synthetase In Escherichia-Coli. *Journal of Biological Chemistry* **1984,** *259* (23), 4505-4507.

141. Otwinowski, Z.; Minor, W., Processing of X-ray diffraction data collected in oscillation mode. *Macromolecular Crystallography, Pt A* **1997,** *276*, 307-326.

142. McCoy, A. J.; Grosse-Kunstleve, R. W.; Adams, P. D.; Winn, M. D.; Storoni, L. C.; Read, R. J., Phaser crystallographic software. *Journal of Applied Crystallography* **2007,** *40*, 658-674.

143. Emsley, P.; Lohkamp, B.; Scott, W. G.; Cowtan, K., Features and development of Coot. *Acta Crystallographica Section D-Biological Crystallography* **2010,** *66*, 486-501.

144. Adams, P. D.; Afonine, P. V.; Bunkoczi, G.; Chen, V. B.; Davis, I. W.; Echols, N.; Headd, J. J.; Hung, L. W.; Kapral, G. J.; Grosse-Kunstleve, R. W.; McCoy, A. J.; Moriarty, N. W.; Oeffner, R.; Read, R. J.; Richardson, D. C.; Richardson, J. S.; Terwilliger, T. C.; Zwart, P. H., PHENIX: a comprehensive Python-based system for macromolecular structure solution. *Acta Crystallographica Section D-Biological Crystallography* **2010,** *66*, 213-221.

145. Baker, N. A.; Sept, D.; Joseph, S.; Holst, M. J.; McCammon, J. A., Electrostatics of nanosystems: Application to microtubules and the ribosome. *Proceedings of the National Academy of Sciences of the United States of America* **2001,** *98* (18), 10037-10041.

146. Del Rizzo, P. A.; Couture, J. F.; Dirk, L. M. A.; Strunk, B. S.; Roiko, M. S.; Brunzelle, J. S.; Houtz, R. L.; Trievel, R. C., SET7/9 Catalytic Mutants Reveal the Role of Active Site Water Molecules in Lysine Multiple Methylation. *Journal of Biological Chemistry* **2010,** *285* (41), 31849-31858.

147. Couture, J. F.; Collazo, E.; Hauk, G.; Trievel, R. C., Structural basis for the methylation site specificity of SET7/9. *Nature Structural & Molecular Biology* **2006,** *13* (2), 140-146.

148. Griffith, S. C.; Sawaya, M. R.; Boutz, D. R.; Thapar, N.; Katz, J. E.; Clarke, S.; Yeates, T. O., Crystal structure of a protein repair methyltransferase from Pyrococcus furiosus with its L-isoaspartyl peptide substrate. *Journal of Molecular Biology* **2001,** *313* (5), 1103-1116.

149. Ahn, H. J.; Kim, H. W.; Yoon, H. J.; Lee, B. I.; Suh, S. W.; Yang, J. K., Crystal structure of tRNA(m(1)G37)methyltransferase: insights into tRNA recognition. *Embo Journal* **2003,** *22* (11), 2593-2603.

150. Wu, H.; Siarheyeva, A.; Zeng, H.; Lam, R.; Dong, A. P.; Wu, X. H.; Li, Y. J.; Schapira, M.; Vedadi, M.; Min, J., Crystal structures of the human histone H4K20 methyltransferases SUV420H1 and SUV420H2. *Febs Letters* **2013,** *587* (23), 3859-3868.

151. Fick, R. J.; Kroner, G. M.; Nepal, B.; Magnani, R.; Horowitz, S.; Houtz, R. L.; Scheiner, S.; Trievel, R. C., Sulfur-Oxygen Chalcogen Bonding Mediates AdoMet Recognition in the Lysine Methyltransferase SET7/9. *Acs Chemical Biology* **2016,** *11* (3), 748-754.

152. Gandecha, A. R.; Large, S. L.; Cundliffe, E., Analysis of four tylosin biosynthetic genes from the tylLM region of the Streptomyces fradiae genome. *Gene* **1997,** *184* (2), 197-203.

153. Chen, H. W.; Yamase, H.; Murakami, K.; Chang, C. W.; Zhao, L. S.; Zhao, Z. B.; Liu, H. W., Expression, purification, and characterization of two N,N-dimethyltransferases, TylM1 and DesVI, involved in the biosynthesis of mycaminose and desosamine. *Biochemistry* **2002,** *41* (29), 9165-9183.

154. Thoden, J. B.; Holden, H. M., Production of a Novel N-Monomethylated Dideoxysugar. *Biochemistry* **2014,** *53* (7), 1105-1107.

155. Chirpich, T. P.; Zappia, V.; Costilow, R. N.; Barker, H. A., Lysine 2,3-Aminomutase - Purification And Properties Of A Pyridoxal Phosphate And S-Adenosylmethionine-Activated Enzyme. *Journal of Biological Chemistry* **1970,** *245* (7), 1778-1789.

156. Peeler, J. C.; Mehl, R. A., Site-Specific Incorporation of Unnatural Amino Acids as Probes for Protein Conformational Changes. In *Unnatural Amino Acids: Methods and Protocols*, Pollegioni, L.; Servi, S., Eds. Humana Press Inc: Totowa, 2012; Vol. 794, pp 125-134.

157. Collazo, E.; Couture, J. F.; Bulfer, S.; Trievel, R. C., A coupled fluorescent assay for histone methyltransferases. *Analytical Biochemistry* **2005,** *342* (1), 86-92.

158. Datta, S.; Koutmos, M.; Pattridge, K. A.; Ludwig, M. L.; Matthews, R. G., A disulfide-stabilized conformer of methionine synthase reveals an unexpected role for the histidine ligand of the cobalamin cofactor. *Proceedings of the National Academy of Sciences of the United States of America* **2008,** *105* (11), 4115-4120.

159. Koutmos, M.; Datta, S.; Pattridge, K. A.; Smith, J. L.; Matthews, R. G., Insights into the reactivation of cobalamin-dependent methionine synthase. *Proceedings of the National Academy of Sciences of the United States of America* **2009,** *106* (44), 18527-18532.

160. Ehler, A.; Benz, J.; Schlatter, D.; Rudolph, M. G., Mapping the conformational space accessible to catechol-O-methyltransferase. *Acta Crystallographica Section D-Biological Crystallography* **2014,** *70*, 2163-2174.

161. Voloshchuk, N.; Montclare, J. K., Incorporation of unnatural amino acids for synthetic biology. *Molecular Biosystems* **2010,** *6* (1), 65-80.

162. Robinson, R. G.; Smith, S. M.; Wolkenberg, S. E.; Kandebo, M.; Yao, L. H.; Gibson, C. R.; Harrison, S. T.; Polsky-Fisher, S.; Barrow, J. C.; Manley, P. J.; Mulhearn, J. J.; Nanda, K. K.; Schubert, J. W.; Trotter, B. W.; Zhao, Z. J.; Sanders, J. M.; Smith, R. F.; McLoughlin, D.; Sharma, S.; Hall, D. L.; Walker, T. L.; Kershner, J. L.; Bhandari, N.; Hutson, P. H.; Sachs, N. A., Characterization of Non-Nitrocatechol Pan and Isoform Specific Catechol-O-methyltransferase Inhibitors and Substrates. *Acs Chemical Neuroscience* **2012,** *3* (2), 129-140.